



UNIVERSITÀ
DEGLI STUDI
DI PADOVA

UNIVERSITA' DEGLI STUDI DI PADOVA

Dipartimento di Ingegneria Industriale DII

Corso di Laurea Magistrale in Ingegneria Energetica

Improvement of a PCM-based thermal energy storage system

Relatore:

Prof. Angelo Zarrella

Correlatori:

Prof. Michele Bottarelli

Ing. Giuseppe Emmi

Laureando: Giacon Luca

Matricola: 2022583

Anno Accademico 2022/2023

Index

ABSTRACT	4
Goals of the experiment	6
1. Introduction on PCM	7
1.1 Basics on phase change	8
1.2 Fields of application	9
1.3 Classification and properties	10
1.4 Main problems	12
1.4.1 Thermal conductivity	13
1.4.2 Stability	13
1.4.3 Subcooling	14
2. Overall setup	15
2.1 Description of the heat exchanger	15
2.2 Recirculation circuit	16
2.3 Acquisition system	19
2.4 Thermo Scientific bath/circulator	21
3. Choices for the experiment	24
3.1 Material: the PCM	24
3.2 Temperature sensors	25
3.3 Design of thermocouple supports	25
4. characterisation of the HE with water and thermocouples calibration	28
4.1 Calibration of the thermocouples	28
4.2 Characterisation with water	29
4.3 Powers and energies	33
5. characterisation with PCM	38
5.1 Reference test in solidification	39
5.2 Reference test in melting	53
5.3 Power comparison: solidification VS melting	59
6. ϵ-NTU characterisation	61
7. small scale tests with graphene	62
7.1 type of graphene	62
7.2 Test explanation and conductivity enhancement results	63

8. Enhancement of performance with 1.5 % of graphene	69
8.1 Solidification	70
8.2 Enhanced VS reference comparison	70
8.3 Melting	75
8.4 Enhanced VS reference comparison	78
9. Enhancement of performance with 3% of graphene	85
9.1 Solidification	86
9.2 Melting	91
10. Graphene 3% enhanced VS water	93
10.1 Solidification	93
10.2 Melting	96
Appendix - COMSOL simulation	99
Conclusions	103
Acknowledgements	105
BIBLIOGRAFY	106

abstract

Nowadays phase change materials are encountering more and more interest in the scientific community mainly thanks to the fact that they can store a huge amount of heat per unit of volume respect to the traditional sensible storage materials. In fact, the use of PCMs is one of the best ways to store thermal energy. The peculiarity of those materials is that they store and release heat at a constant temperature during their phase change.

The present work aims to study and characterize the thermal performance of a PCM-based latent heat exchanger (HE). The HE is composed by two coaxial cylinders in plexiglass (PVC) closed with PVC panels on both sides in which a smooth steel coil is present. The coil is immersed in the PCM which is a commercial paraffin with a melting point of 28 °C. To melt and solidify the PCM, hot and cold water respectively flows inside the coil.

The purpose is to explore the melting and solidification process by monitoring the temperature in the HE with multiple thermocouples placed at different heights and different radial distances from the centre of the HE to the outer wall. Measurements are taken with thermocouple type T connected to instrumentations which collect all the measurements. In that way it is possible to create curves of temperature in which is possible to see when the melting and the solidification occur, the respective temperatures and other possible phenomena like for example the subcooling, which is a typical problem with most of PCMs.

Knowing temperatures and the flow rate of water flowing into the coil throughout the process is possible to calculate the power of the HE and so the energies to characterize the whole system.

After studied the system with the pure paraffin, tests with different percentage in mass of graphene oxide are carried out to see how the increase of the thermal conductivity enhance the overall performance of the heat exchanger and so compare also the PCM-based system with the same system filled with water which can be considered the reference for thermal storages nowadays.

Nomenclature

<i>PCM</i>	phase change material
<i>HE</i>	heat exchanger
<i>LHS</i>	latent heat storage
<i>TC</i>	thermocouple
<i>ref</i>	reference (pure PCM case)
λ	thermal conductivity, W/(m K)
<i>cp</i>	specific heat capacity at constant pressure, J/(kg °K)
ρ	density
<i>T</i>	temperature, °C
Δh	phase change enthalpy (or melting enthalpy or heat of fusion), J/kg
\dot{m}	mass flow rate of water [l/h]
<i>A</i>	surface area of the coil [m ²]
ϵ	Efficiency of the heat exchanger

Goals of the experiment

The goal of the present work is to make a heat exchanger functional and study its behaviour in operation with phase change materials (PCMs). To make it operational an entire setup had to be built. There is a need for:

- an acquisition system for data collecting of temperature and flow rate
- a water circuit for the hot and cold water flowing inside the coil
- an external recirculation circuit for the melted PCM to have homogeneous properties and good mixing inside the HE (avoiding stratification in the liquid phase)

To collect temperatures as a first step, one had to think how to build the supports for the TC and where place them inside the HE.

For the construction of the two circuits (the one for the hot and cold water which will flow inside the coil, and the external one for the recirculation of the PCM) different setups with different elements (like valves, flow meters...) were considered and an attempt was made to end up to the best configuration for our purposes. These configurations will be discussed later.

The TCs are calibrated to have the most possible accurate measurement and so reference tests are performed at prefixed boundary conditions. In that way a first characterisation of the system could be done.

The reference tests with paraffin are performed after determining precise boundary conditions that will then be maintained for all the following tests.

When the characterisation of the HE with the pure paraffin is done and the energy balance is closed, it was possible to think of enhancing the performance of the HE by adding graphene at different mass percentages to see how the improving of the thermal conductivity of the PCM will influence the overall behaviour of the system.

Chapter 1.

Introduction on PCM

PCM stand for *Phase Change Material*. As the name implies, these materials change their phase at a fixed constant temperature called *melting temperature*. Depending on the application, on the market is possible to find PCMs with a melting temperature that goes from less than -100 °C to more than 800 °C.

Because of the temperature being almost constant in the phase transition, the heat storages obtained using these materials are called *latent heat storages* (LHS). Latent heat storages have a higher storage density respect to sensible heat storage; in fact, PCM can store 5 to 14 times more energy in the same volume than sensible storage materials (like concrete, woods, glass, steel...) and have a lower temperature difference in the phase change transition. For these reasons latent heat storage is considered one of the most efficient ways to store thermal energy.

By the way, sensible heat storage is still the most common way to store energy. In this case the energy is transferred to the storage material and leads to an increase in its temperature.

The sensible stored heat can be calculated as:

$$\Delta Q = m \cdot c_p \cdot \Delta T$$

Where: **m** = mass of the storage material [kg]

c_p = specific heat capacity [kJ/(kg K)]

ΔT = temperature increase of the storage material [K]

1.1 basics on phase change

As briefly mentioned above, PCMs are materials that undergo phase transition at a prefixed temperature. The most common used PCMs undergo the solid-liquid phase transition (known as melting-solidification transformation) mainly because it's the easiest transformation to manage. Materials are chosen depending on their melting temperature, which in turn depends on the application considered. During the transformation from solid to liquid, the material absorbs energy from the surrounding (or from a hot source) while remaining at constant temperature. During the transition from liquid to solid, the opposite happens and the PCM release the energy absorbed before. This energy is called *latent heat of fusion*.

In the following pictures we can see the standard heating curve of a material that bring a solid to a superheated vapor.

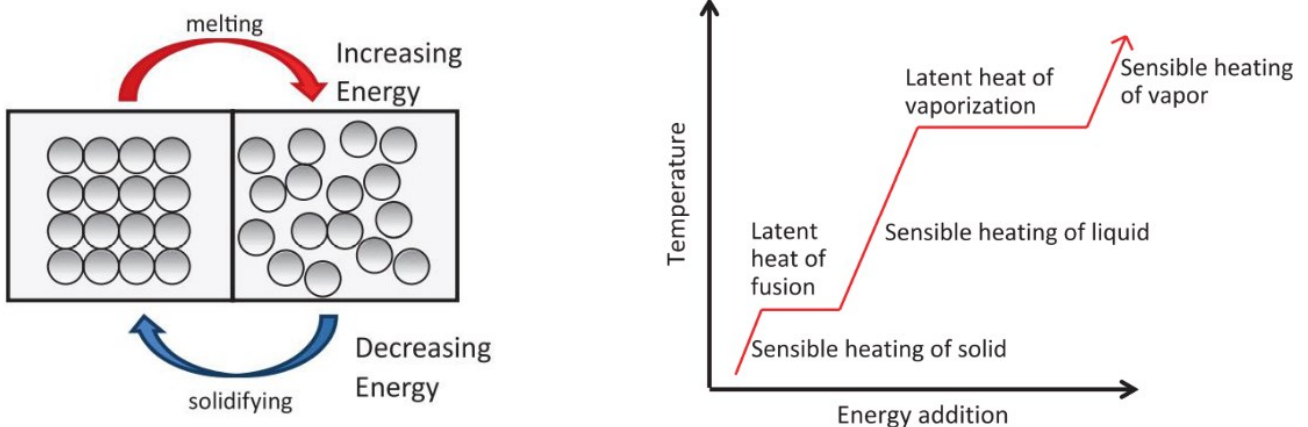


Fig. 1.1 - melting/solidification process and standard heating curve [6]

PCMs materials as already said, works mainly with the latent heat of fusion but exist also PCMs that works with the latent heat of vaporization. The transformation from liquid to vapor is usually a higher energy process. The reason why the latter is rarely used is because passing from liquid to vapor the volume of the material increase extremely (while the volume change in melting/solidification is usually less than 10% [2]) so big boilers and more support equipment are needed, making all the system very expensive becoming not convenient from an economic point of view.

In solidification process, we initially have all the PCM in the liquid state and it start to solidify driven by the conduction between the cold surface (the steel coil in our case) and the liquid PCM. Since solidification start, the solid front moves always by conduction between the solid front and the liquid PCM while the convection is very limited.

During melting, the process is quite different.

As in literature is widely demonstrated, the melting process happens due to conduction and convection. In fact, when the PCM start to melt due to the contact between the solid PCM and the hot surface, its density decreases and due to buoyancy, it tends to rise inside the container and so convection phenomena occur, increasing the melting rate.

So, we expect to see in our experiment that in cooling conditions, the solidification start locally on the coil's surface when the hot PCM is directly in contact with the cold coil and then propagate radially towards the inner and the outer parts of the cylinder. While in melting we supposed to have the first liquid that forms in contact with the coil and then when it finds a "path" it starts to rise (due to the lower density) and reach the top of the HE. So, more and more liquid accumulates on the top during the process showing an horizontal front of liquid that move downwards.

1.2 fields of application

In recent time PCMs materials receive more and more attention because their use can be extended in a lot of fields of application thanks to their wide range of temperature. For example, one of the first applications was in boxes and containers for food, beverage, and medicine transport. PCM can be used also in clothing to maintain the optimal body temperature (which is about 36-37 °C).

One of the most interesting and common application nowadays is in heating and cooling of buildings both for temperature control and for heat/cold storage. PCM is directly used into

the envelope as building material and it has the capability to store a lot thermal energy per unit volume compared to others building materials, as is shown in the following table:

material	Cp per mass [kJ/(kg K)]	ρ [kg/m ³]	Cp per volume [MJ/(m ³ K)]	Q/V for $\Delta T = 4 \text{ }^\circ\text{K}$ [MJ/m ³]
EPS	1.2	16	0.02	0.08
Mineral wool	0.8	200	0.16	0.64
Cork	1.8	150	0.27	1.08
Gypsum	0.8	800	0.64	2.56
Wood	1.5	700	1.05	4.20
Concrete	0.84	1600	1.34	5.38
Sandstone	0.7	2300	1.61	6.44
Brick	1	1800	1.80	7.20
PCM: peak values	≥ 75	800	≥ 60	
PCM: 22 °C to 26 °C				130

Tab. 1.1 - properties comparison of different materials [2]

Another interesting comparison is done in the following picture which shows the equivalent layer thickness in cm needed to store the same amount of heat as in 1cm of PCM.

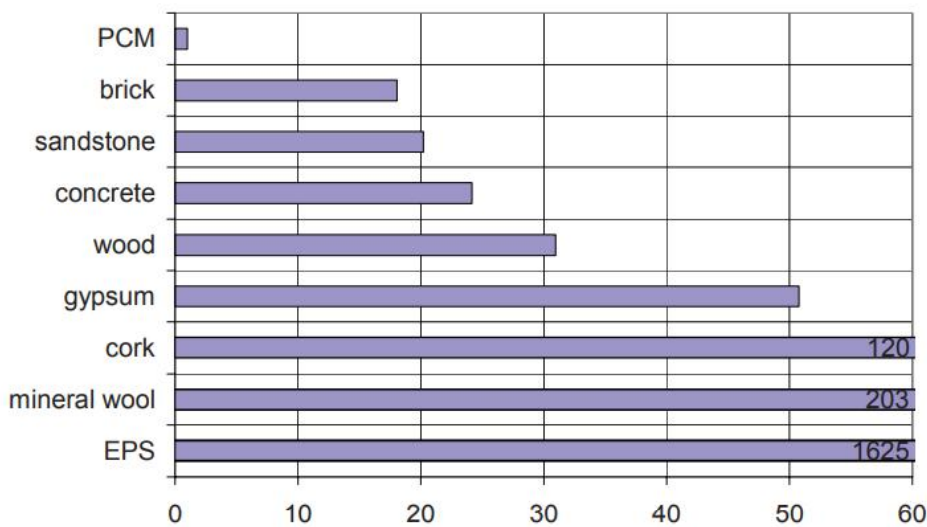


Fig. 1.2 - thickness in cm equivalent to 1cm of PCM [2]

1.3 classification and properties

There are different commercial PCMs which differs one to each other depending on their chemical nature and properties.

Here's a schematic of the classification of PCMs.

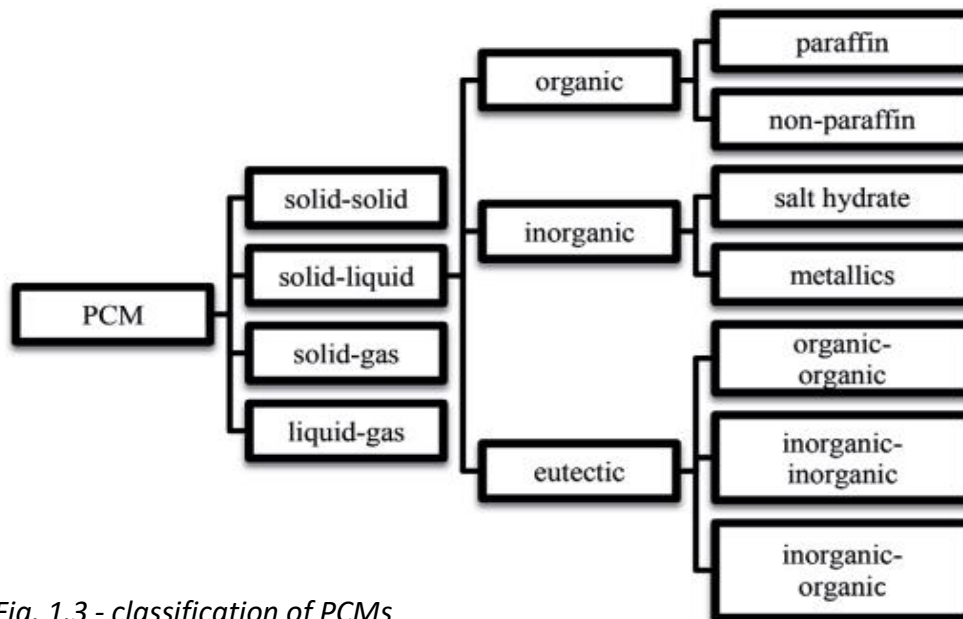


Fig. 1.3 - classification of PCMs

The two main families of PCM are the organic and the inorganic one. An example of both is respectively the paraffins and the hydrated salts. These two families regard materials with solid-liquid phase transition.

To be suitable for a generic application, each PCM should have some characteristics, like:

- Phase change temperature coherent with the application considered
- High latent heat storage capacity
- High thermal conductivity
- Non-toxic, non-flammable, non-corrosive, safe
- No properties degradation after plenty of cycles
- Cheap and abundant
- No subcooling

Since there are no materials that satisfy all these characteristics, one should choose the material more suitable depending on its applications. For example, hydrated salts are quite good regarding the thermal properties having a large energy storage density and high thermal conductivity respect to the paraffins, but they're corrosive, they present subcooling and tends to phase segregation and so they often require nucleating agents to start the solidification.

Paraffine waxes, if pure, are very expensive and so only commercial ones are used (even though nowadays also the commercial ones reach high level of purity). They are easier to manage but have lower thermal energy storage and lower thermal conductivity, and hence, they require large surface area and additives to increase the thermal conductivity.

Paraffins in general presents a lower density when liquid and so if 2 phases are present, the liquid tends to remain at the top of the container; and usually as solid they present about 10% less volume than when they're liquid.

Another advantage of paraffins is that they present less or no subcooling respect to salt hydrates.

Here is reported a table which compare and summarize differences between different energy storage materials:

Property	Rock	Water	Organic PCM	Inorganic PCM
Density, kg/m ³	2240	1000	800	1600
Specific heat, kJ/kg	1.0	4.2	2.0	2.0
Latent heat of fusion, kJ/kg	-	-	190	230
Latent heat, kJ/m ³	-	-	152	368
Storage mass for 10 ⁶ kJ (kg)	67,000	16,000	5300	4350
Storage volume for 10 ⁶ kJ (m ³)	30	16	6.6	2.7
Relative storage mass	15	4	1.25	1.0
Relative storage volume	11	4	2.5	1.0

Tab. 1.2 - Comparison of various heat storage media (stored energy = 106 kJ = 300 kWh; DT = 15 K) [5]

The more evident data is that PCM require a very small mass and volume to store the same energy compared to other materials like water and rock.

1.4 main problems

An introduction of the main problems of the salt hydrates and the paraffins is done in the section 1.3, but now they will be shown more in detail.

1.4.1 thermal conductivity

The acknowledged main problem of PCM materials (especially of paraffin) is the low thermal conductivity λ (~ 0.2 [W/(m K)] for paraffins and 0.4 [W/(m K)] for hydrated salts), which decrease the heat transfer from the heat transfer fluid to the PCM. This leads to an increase in the charging/discharging operational time and so a poor performance of the PCM in energy storage devices. To solve this problem there are mainly 3 solutions:

- 1) Increasing the λ of the PCM dispersing highly conductive nanoparticles (D between 1 nm and 100 nm) in the PCM itself, or on a macroscopic scale adding metallic pieces. The latter reduces a little bit the volume percentage of the PCM.
- 2) Lowering the thermal resistance of the PCM (which is connected to 1) because increasing the thermal conductivity, the thermal resistance decreases.
- 3) Increasing the contact area between PCM and the heat transfer fluid. The most common way is by using fins.

1.4.2 stability

This is not an important problem in the short period but in the long period it could be. With the term “stability” of the PCM we mean the number of cycles that it guarantees before presenting properties degradation. This could be a problem only after a long period of time or on a specific application. For example, PCM which undergo phase change very often or works in a high-temperature environment may experience more rapid degradation than a PCM that is used in a stable environment.

1.4.3 subcooling

Subcooling is the phenomenon that occurs when during the cooling process the crystallization (solidification) of the material start at a temperature which is lower than the melting temperature and so the liquid remains liquid also at a temperature lower than the melting temperature. Usually it affects mostly inorganic PCMs (like hydrated salts) and not the organic ones (like paraffines)

Subcooling occurs because the material has difficulty to solidify, and so a possible solution is to add some *nucleators* which helps the beginning of solidification.

However, not always subcooling occurs. For example, if the cooling/heating process is very slow, it may not happen.

CHAPTER 2.

Overall setup

2.1 description of the heat exchanger

The heat exchanger used for the experiment consists in two coaxial cylinders in PVC (plexiglass) with a thickness of 5 mm the inner one and 3 mm the outer one. The inner one has an internal diameter of 19 cm and the outer one 23 cm.

Between the two cylinders there is an air gap which works as insulant. The HE is 50 cm high and inside it is present a smooth stainless-steel coil with an external diameter of 18 mm, 9 turns of spiral and 40 mm between the centres of adjacent coils. The length of the coil is approximately 3.3 m. The inner volume is 0.0142 m³ (approximately 0.0134 m³ if we consider the volume of the coil which reduces the volume available for the PCM)

In that way, knowing the density of the material, it's easily possible to calculate the quantity of material that is possible to store in the HE:

$$\text{PCM}_{\text{MASS}} = 14.2 \text{ [L]} * 0.77 \text{ [kg/l]} = 10.934 \text{ [kg]}$$

Note that 0.77 [kg/l] is the density of the liquid paraffin.

Here is reported a picture of the HE as it was before start to work on it:



Fig. 2.1 & 2.2 - Initial state of the heat exchanger

The main initial problem was that the coil was not perfectly in the centre of the cylinder and since the intention was to operate in configuration as symmetrical as possible, it was necessary to think about how to solve this issue. This was done with a column drill by enlarging the holes in which were inserted the supply and return coil and moving them until the coil was well centred.

The reason why we want it centred is because later we would make all the supports for the thermocouple of the same dimensions, and they should perfectly fit all around the coil to obtain comparable temperature measurements in different positions.

2.2 recirculation circuit

There was the need to think about an external circuit to recirculate the liquid PCM from the bottom to the top to guarantee a good mixing inside the HE. At the end it was chose to make the circuit in PVC-U (unplasticized polyvinyl chloride) which is a PVC material that thanks to its thermal stability and resistance to chemical agents will be suitable also if in future it is decided to use a hydrated salt as PCM, which would corrode the normal PVC.

The melted PCM is collected at the bottom of the HE and sent back on the top of it. To do this a pump is used, specifically a **Grundfos Alpha1L 15-40 130** which has a cast iron body and an impeller in PES + 30% of glass fibre. A manual exhaust valve is placed at the bottom of the system, so in case of necessity is possible to expel the PCM or simply discharge the system. Then a valve is placed after the pump to introduce a localized loss.

The idea was to also put in flow meters to know exactly the amount of PCM that is recirculated.

Here is showed a preliminary setup which was under investigation:



Fig. 2.3 - First investigation of the setup for the external circuit

Then, as this configuration was deemed to present certain problems, several modifications were added, and the final configuration differs from the one above for the following things:

- The pump can be disconnected from the circuit thanks to 2 sleeves
- It is used a mechanical flow meter while the digital one was placed in the return water circuit to the bath
- A feed valve is added on the top to feed the system with the liquid PCM
- After chose the most appropriate configuration it was realised that there was another big problem: after the complete solidification of the PCM inside the HE and in the external circuit, if the melting process started after sending hot water into the coil, the PCM present in the external circuit obviously doesn't melt. So, it was inserted a heating cable that was wrapped all around the external circuit to keep it always at the melting temperature.

Then the circuit was thermally insulated. At the end, it appears like that:



Fig. 2.4 - Heating cable wrapped around the external circuit



Fig. 2.5 - Thermally insulated external circuit

The heating wire was connected to an on/off thermostat in which was set a setpoint temperature of 40 °C. The thermocouple of the thermostat was placed in contact with the body of the flow meter, which is maybe one of the most critical parts of the circuit to melt the solid PCM inside it.

2.3 acquisition system

The acquisition system is the set of devices useful for detecting temperatures and flow rates.

The main tool used is the Datalogger DT80 which is shown in the figure below:



Fig 2.6 - Datalogger DT80 acquisition system

It has 16 analogical and 4 digital channels. In the analogical ones are connected the thermocouples and in the digital one the digital flow meter.

Since the thermocouples are quite a lot, to be able to connect all of them, the *shared terminal* connection was chosen.

Each channel has four terminals named, in order from the left to the right “* + - #”.

To connect three TC in each channel, each one should have the positive wire in a different terminal (*, + or -) and all the negative wires connected together in the # terminal.

In that way in each channel is possible to connect 3 TCs and we are therefore able to connect all the 30 TCs to a single Datalogger.

The Datalogger is connected to the internet network and thanks to its PC software is possible to configure the setup, specifying the different channels and connection and fix an acquisition time interval. It's also possible monitoring in real time the temperature inside the system and build graphs which shows the temperature trends over the time.

Here there is a schematic which report the positioning and the nomenclature of the TCs inside the HE:

The following scheme must be read like a section of a half cylinder from the centre (where there is the return coil) to the outer wall. Only the first part of the coil is drawn but consider that above each TC in position "4" runs the supply coil.

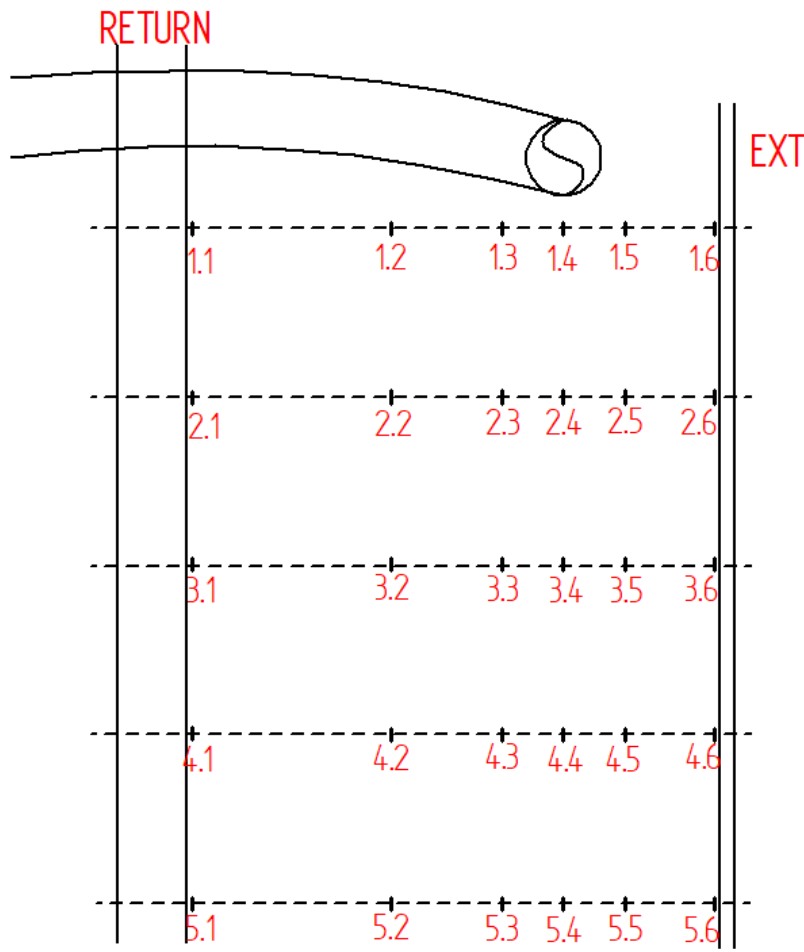


Fig. 2.7 - Schematic of thermocouple's placement inside the heat exchanger

To better understand:

- 1.1 is the TC in the centre of the HE (close to the return line) in the highest position.
- 5.6 is the TC most far from the centre of the HE (close to the external plexiglass) in the lowest position.

In the figures of the next chapters, will be called **level** the set of thermocouples at the same height. So, there will be 5 levels: from 1 to 5 respectively from the top to the bottom.

Will be called **position** the set of thermocouples that are in the same radial distance from the centre of the HE. So, there will be 6 positions: from 1 to 6 respectively from the centre towards the outer part of the cylinder.

2.4 Thermo Scientific circulator



Fig 2.8 & 2.9 - Water circulator

This is the circulator that allows to send hot and cold water into the coil to perform melting and solidification cycles, fixing the temperature and the flow rate.

The circulator is a **Thermo Scientific HAAKE PC 200 / A25** which allows to set temperatures and perform temperature cycles with ramps to see if the thermocouples follow the same temperature trend, and if not correct them. In the experiment it was used setting a set point temperature that must be maintained in all the solidification and melting process (in particular 11 °C in solidification and 45 °C in melting).

Some data about the circulator in heating operation:

Temperature range [°C]	+13 / +200
Temperature stability [°C]	± 0.01
Capacity (230 V) [W]	2000
Max flow rate [l/min]	24
Max pressure [mbar]	560
Max suction [mbar]	380
Pump speed	Variable 40% to 100%

Tab. 2.1 - Heating operation data of the circulator

In cooling conditions:

Temperature range [°C]	-24 °C / +200 °C
Capacity [W]	500
refrigerant	R134a

Tab. 2.2 - cooling operation data of the circulator

Since in the circulator is only possible to set the speed of the pump from 40% to 100%, initially is not possible to know which is the flow rate of water that flows into the coil.

For this purpose, two different flow meters are placed in the return line from the HE to the circulator. The first one is a traditional flow meter which was used to calculate manually with a chronometer the amount of water which flows in the unit of time. It results that, with the pump set at 80%, 8 litres of water each minute flows inside the coil. It means 480 litres/hour. This number was used to calibrate the digital flow meter which gives as output a flow rate which is function of a frequency.

According to the datasheet of the producer:

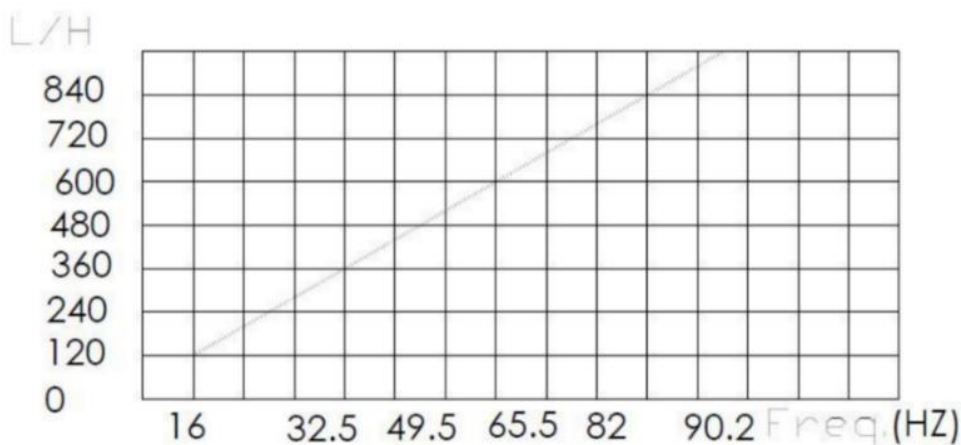


Fig. 2.10 - characteristic flow VS frequency curve of the flow meter

FLOW [L/h]	FREQUENCY [Hz]
120	16
240	32.5
360	49.3
480	65.5
600	82
720	90.2

Tab. 2.3 - flow and frequency output from the digital flow meter

Initially with the pump at 80% the digital flow meter gives as output 505 l/h. It was easy to calculate the corresponding frequency with the proportion:

$$65.5 : 480 = x : 505$$

So, the frequency was 68.9155 Hz.

With this number it was adjusted the characteristics of the digital channel of the Datalogger by imposing that a frequency of 68.9115 Hz corresponds to a flow rate of 480 l/h which means in practical terms to give a minor slope to the straight-line characteristic of the flow meter.

Chapter 3.

Choice for the experiment

In this section are explored the main choices that were done to perform the experiment and the main reasons why they were done.

3.1 Material: the PCM

It was chosen to use an RT28 by *Rubitherm Technologies GmbH* which is a paraffin and has the following characteristics:

- Latent heat storage capacity (latent + sensible) = 250 [kJ/kg] \pm 7.5%
- Specific heat capacity = 2 [kJ/(kg K)]
- Melting temperature: 27-29 °C
- Density ρ (solid) = 0.88 [kg/l]
- Density ρ (liquid) = 0.77 [kg/l]
- Volume expansion: 12.5 % (from solid to liquid)
- Thermal conductivity = 0.2 [W/(m K)]
- Maximum operational temperature: 50 °C

Let's see the partial enthalpy distribution, given by the manufacturer:

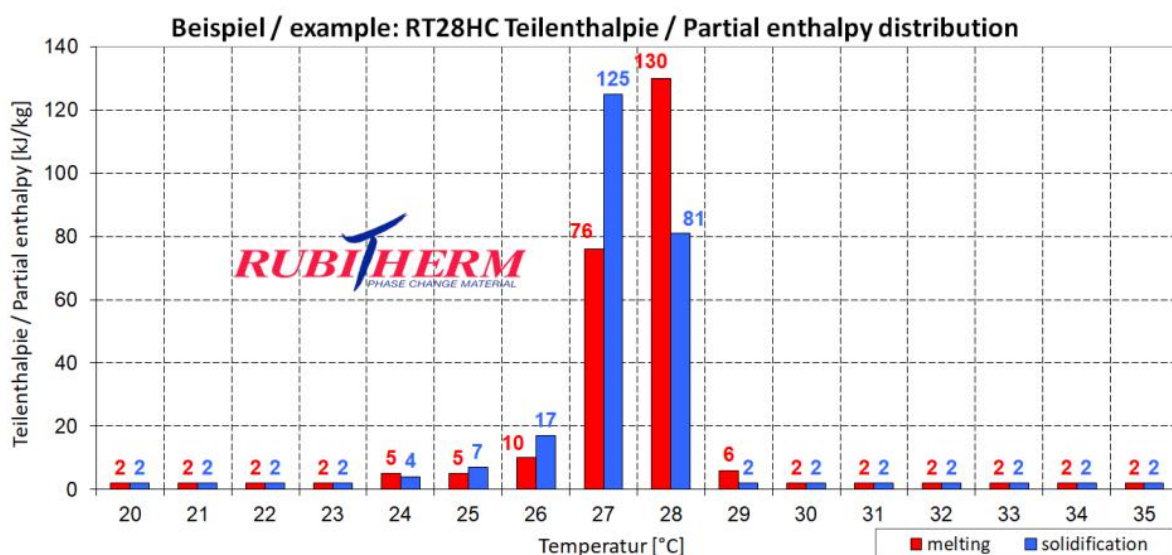


Fig. 3.1 - partial enthalpy distribution of RT28 paraffin

3.2 Temperature sensors

Type-T thermocouples (TCs) were chosen, and their characteristics are the following:

- Insulated with Teflon (PFA)
- Range of temperature [-75 +260 °C]
- Class of tolerance: 1 (± 0.5 °C or $\pm 0.4\%$)
- Thickness of the 2 conductors: 0.315 mm
- IEC standard satisfied

The TC are “built” by us from a 50 m TC coil. They were cut of different lengths depending on the positioning inside the HE. So, an extremity was stripped and prepared to be connected to the Datalogger; the other was stripped, and the 2 wire were twisted and then welded together with tin to form the junction:

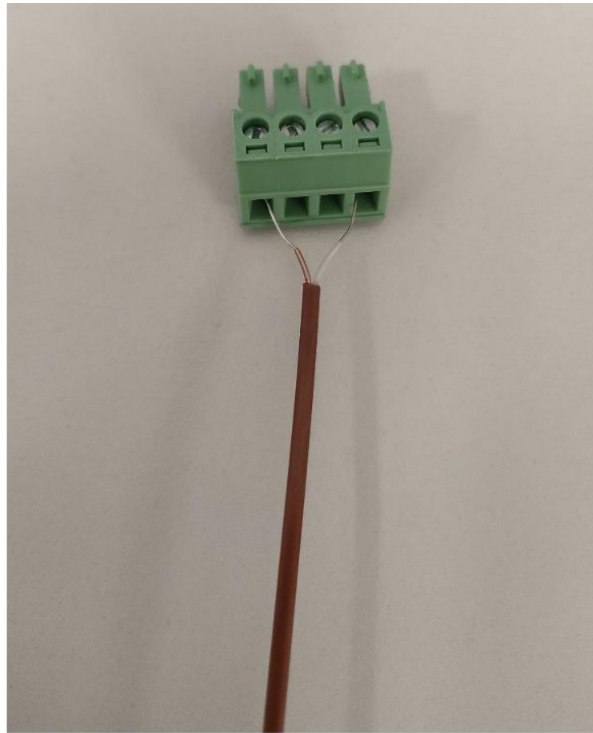
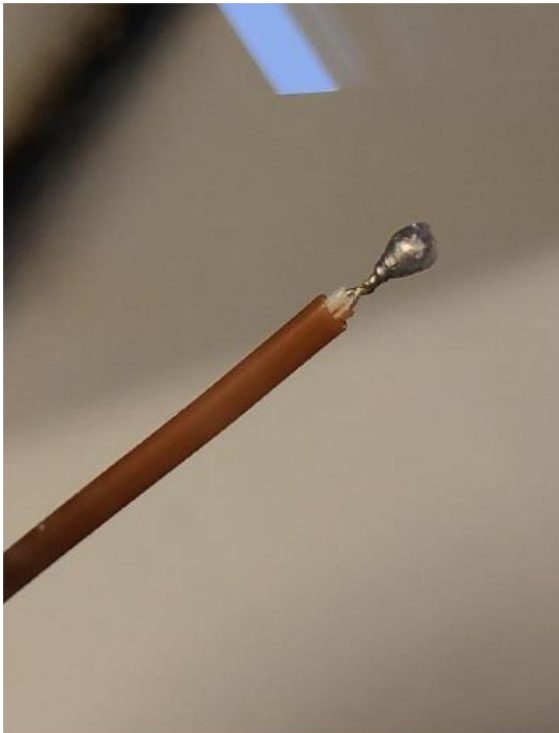


Fig. 3.2 & 3.3 - The two extremities of the thermocouple

3.3 Design of the supports

Since there was a need to measure the temperature inside the HE it was necessary to think of a system that would allow the measurement to be carried out quite easily. The system must be rigid, so not to have problem of stability during phase change and possibly to be as small as possible so not to “disturb” the measurement and the behaviour of the system.

Supports for the thermocouples were designed in 3D with the software *Solid Edge* and then printed with a 3D printer in PLA material.

Different projects were done, but at the end it was chosen a support where two hooks are fitted into adjacent coils of the spiral, while holes are needed for put the thermocouples inside to be stable and not move within the operations.

These supports are placed at different height inside the HE and their function is to let the thermocouples measure the temperature at different radial distances in the HE. The holes are placed at increasing distances from the coil (which correspond the position 4) both towards the internal and the external part of the cylinder to have the two outer holes as outer as possible as we can see from this 3d view:

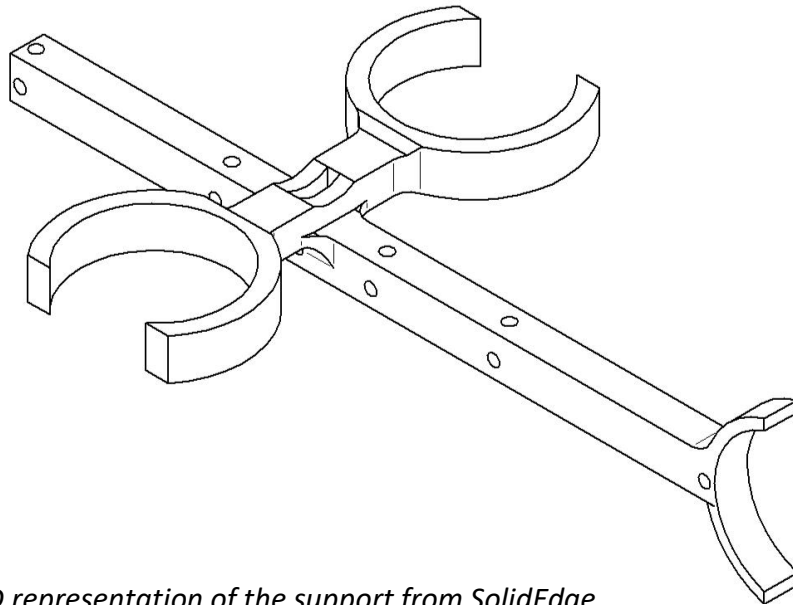


Fig. 3.4 - 3D representation of the support from SolidEdge

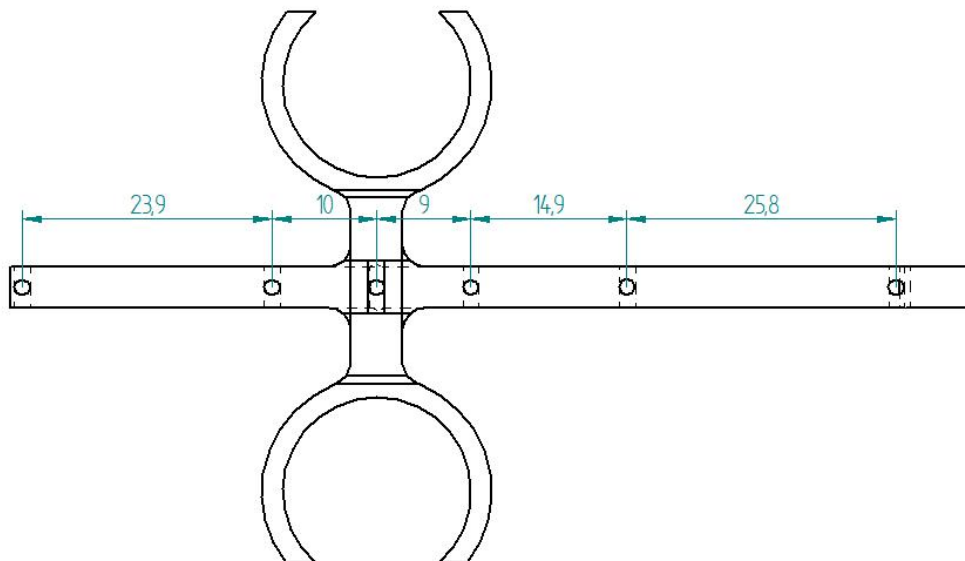


Fig 3.5 - top view with dimensions of the support – quotas in [mm]

At the end it was decided to put 5 supports in 5 different heights inside the HE and in each support put 6 thermocouples in different radial distance from the coil.

This is how it appears when support is positioned in the coil:



Fig. 3.6 & 3.7 - inside and outside view of supports in helix pipe

Chapter 4.

Characterisation of the HE and temperature calibration

4.1 calibration of the thermocouple

The calibration of the TC was done in this way:

After TCs were all installed in the supports and all the system is in the working setup, the system was filled with water. So, a temperature was set in the circulator bath (for example 30 °C which is near to the melting point of the PCM) and water was sent at that temperature inside the coil. Meanwhile the recirculation pump was set to maximum speed to guarantee an optimal mixing of the water inside the HE.

So, it was wait until the system reaches an equilibrium and all the thermocouples should measure the same temperature. Based on this, it was given an offset to those TC which measure temperatures that were not precise.

We end up to a calibration which is enough precise for our purposes. In fact, TCs were calibrated in a range of error of about ± 0.20 °C. As an example, are now reported the temperatures measured when the system reaches the equilibrium at 20.4 °C:

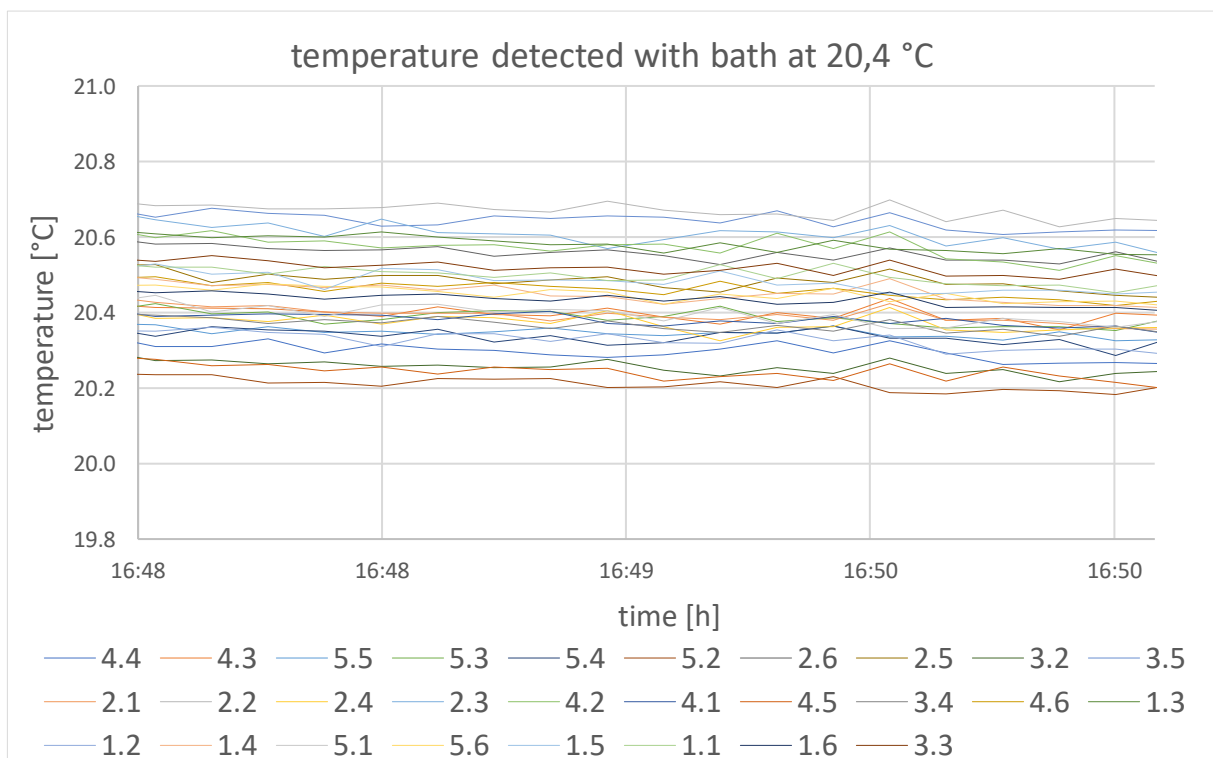


Fig 4.1 - temperature trend at 20.4 °C

4.2 characterisation with water

To start to characterize our system we perform different trials with water before substituting it with PCM. It will be interesting to compare the performance with water and those with PCM.

In particular, the initial tests were carried out performing cycles from 20 °C to 40 °C and then from 40 °C to 20 °C.

This procedure was done with different boundary conditions:

- With and without the external cylinder: to see how much it isolate especially during the phases when there was no water circulation in the coil.
- With and without the recirculation pump: to see how much stratification occur when the pump does not work.

Let's see first the typical trend of the temperatures for some random TCs (it's the same for each TC):

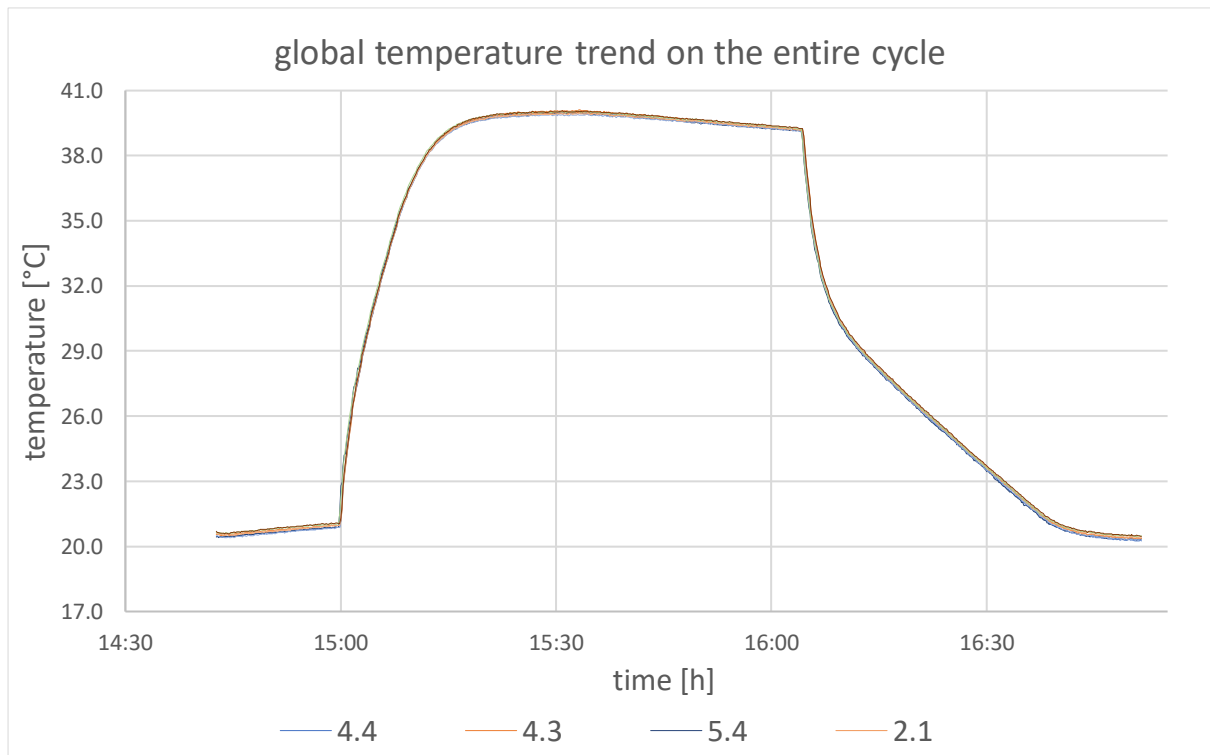


Fig 4.2 - complete cycle temperature trend

It is clearly possible to see several stages:

- I. The initial plateau at 20 °C
- II. The heating phase from 20 °C to 40 °C
- III. The plateau at 40 °C
- IV. A transient phase in which there is no circulation of water into the coil while the bath is brought from 40 °C to 20 °C. in that period (about 30 minutes) there is a small decrease in the temperature due to the losses toward the external environment. (Note that the one presented above is the case without the external cylinder and with the circulation pump turned on)
- V. The cooling phase from 40 °C to 20 °C
- VI. The final plateau at 20 °C

In all the cases the trend is obviously the same. The only big difference is the stratification that is present when the circulation pump is not working. As an example, is now shown the different trend of the mean temperatures at the top level (TC from 1.1 to 1.6) and at the bottom level (TC from 5.1 to 5.6) during the heating phase, with the presence of the external cylinder when the pump is working or not:

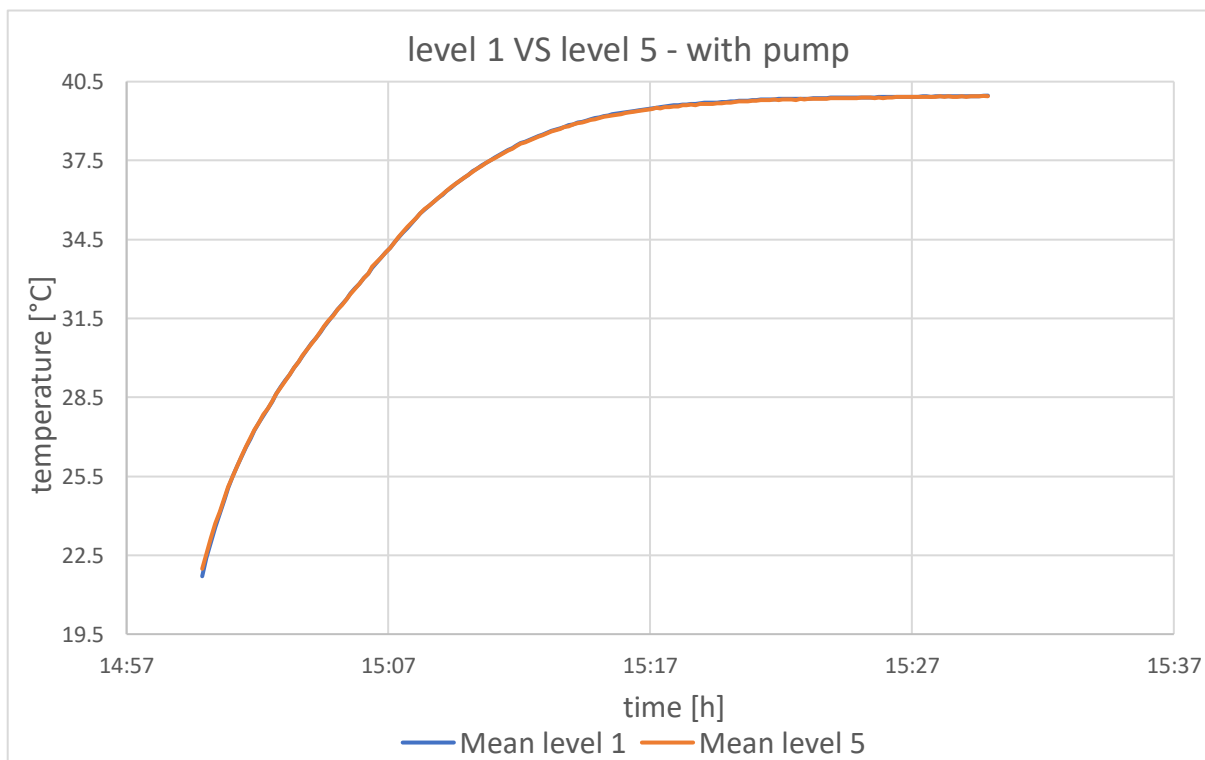


Fig 4.3 - stratification with pump (basically no stratification at all)

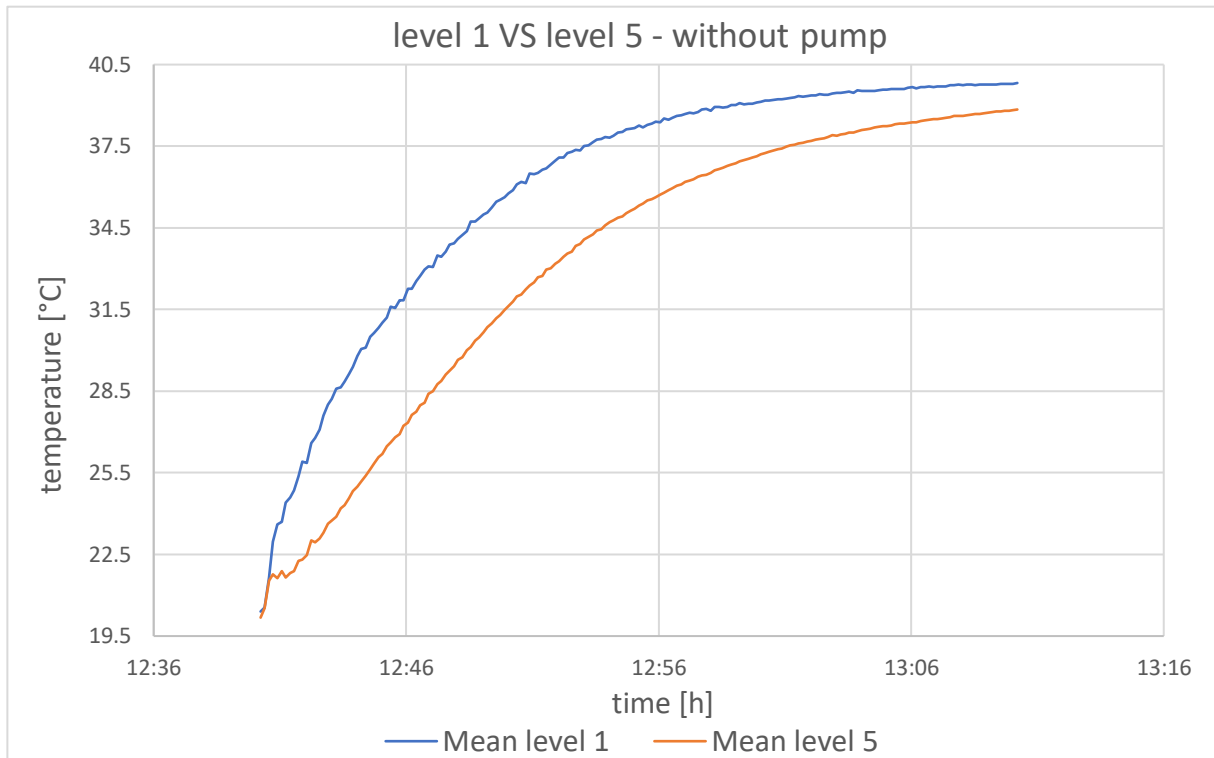


Fig 4.4 - stratification without pump

Is evident that the pump can perfectly mix the water inside the HE, in fact there is no stratification at all in the case with the pump in operation. While without the pump the stratification is present and is quite big. In fact, there is a maximum of 5 °C between the top and the bottom of the HE; and since the TC aren't placed at the absolute extremity of the cylinder but there is some water below and above the last TC, something more than 5°C of stratification is expected to be present. It means about 1 °C each 10 cm.

Another unusual behaviour that was noticed is during the period when there is no circulation of water into the coil because the bath is brought from 40 °C to 20 °C. Especially when the circulation pump is not working and is not present the external PCV cylinder.

In that case there is a lot of stratification in the lowest level and the trend of the decreasing temperature is not linear as in the other cases and in all the other levels:

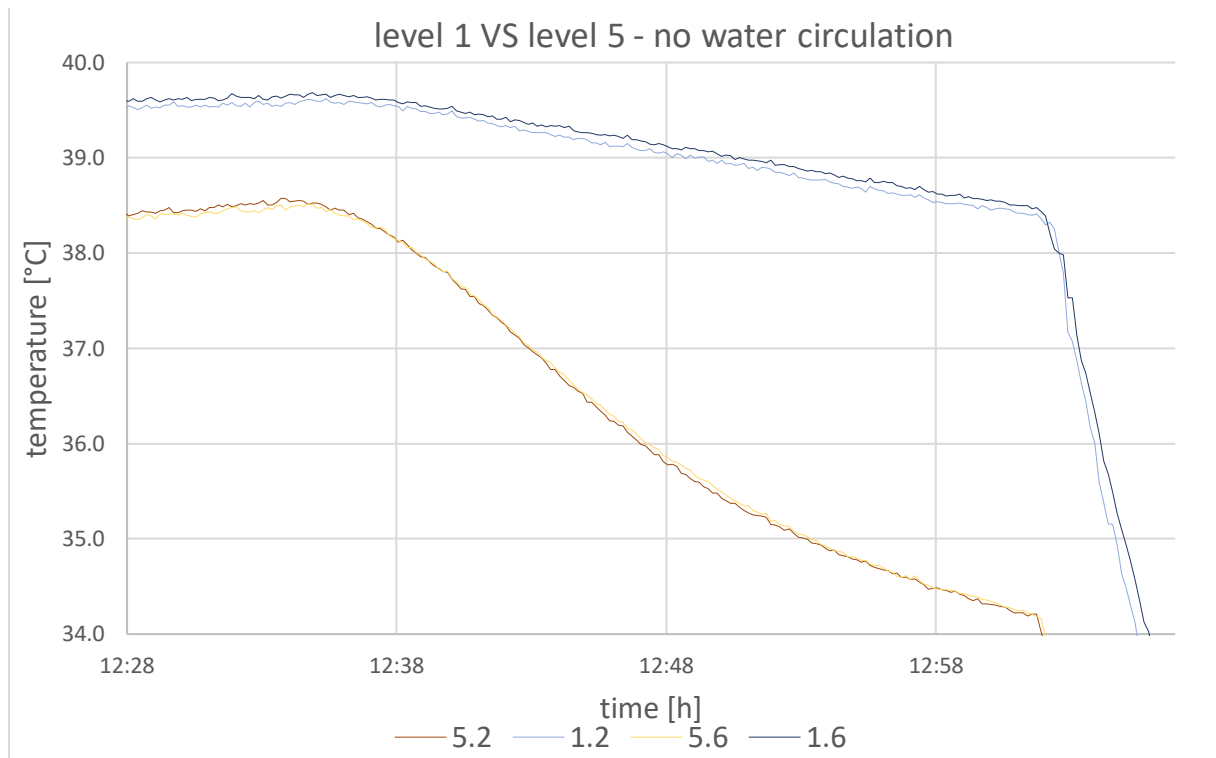


Fig 4.5 - stratification in the lowest level

So, only the lowest level presents such a stratification and a decrease of temperatures that doesn't follow a linear decrease. All the other levels behave like the 1.2 and 1.6 TC.

The tests just described were done only to understand how much the cylinder isolated from the surroundings and how much does the pump mix well the material inside the HE.

To compare the behaviour with the water and the one with PCM tests in the same conditions must be carried out.

So, we perform the cooling from 45 °C to 11 °C and heating from 11 °C to 45 °C.

The flow rate was kept constant at 105 l/h.

The flow rate was kept at that value because at higher flow rates the water would remain in the coil for very little time, so it would not have time to exchange heat and the ΔT_{in-out} would be too small. With this flow rate, considering a length of the coil of almost 3.3 m, the water remains in the coil for about 23 seconds.

4.3 Powers and energies

Let's calculate some powers and energy regarding these trials with water.

The boundary conditions of these tests were:

- Flow rate 105 l/h
- $\Delta T = 34\text{ }^{\circ}\text{C}$
- $T_{\text{amb}} = 22\text{ }^{\circ}\text{C}$
- 10.5 kg of water
- No water circulation in the external circuit (also valve closed)

Cooling:

In the first hour, the average power is 266 W and after this hour the mean temperature inside the HE is already $14.5\text{ }^{\circ}\text{C}$.

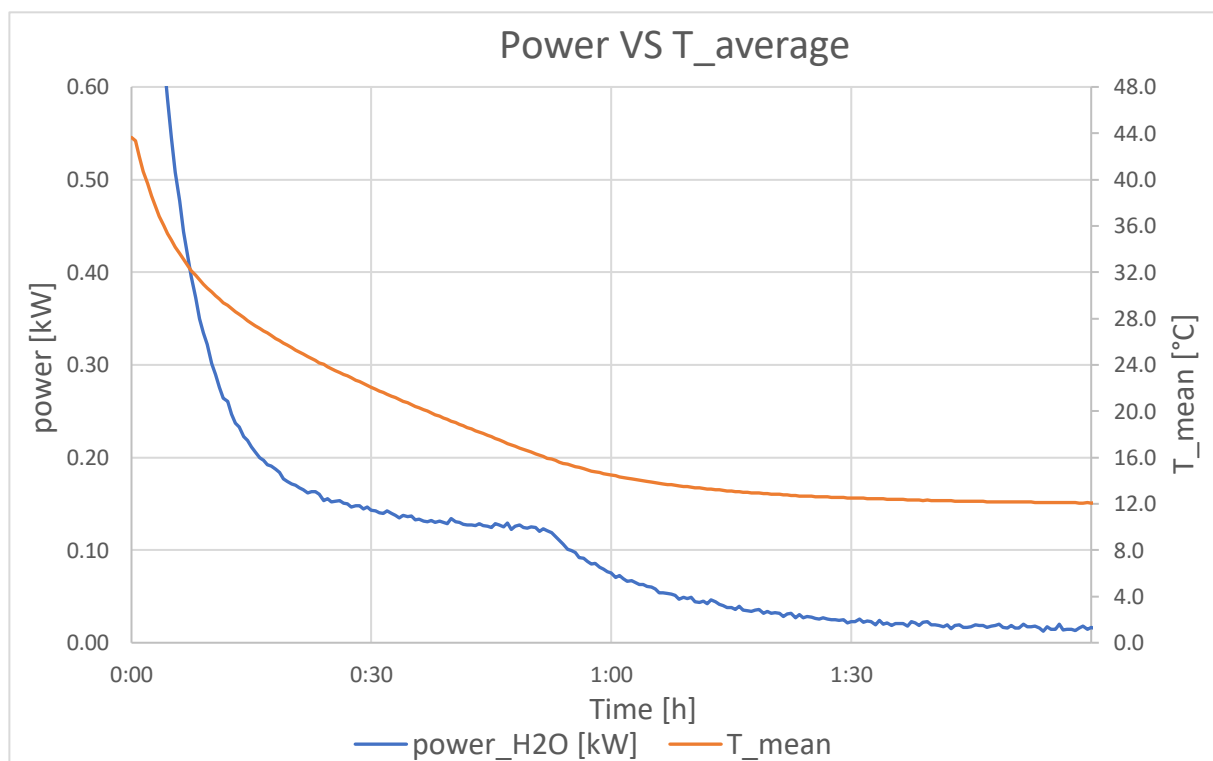


Fig. 4.3.1 - trend of power and average temperature of the water

At the beginning the power of the system is higher than the power of the circulator, in fact the latter is not able to maintain the fixed temperature of $11\text{ }^{\circ}\text{C}$.

The moment when there is a change in the slope of the power curve (a little before one hour) is the moment when the power of the bath starts to be higher than those of the system and it's able to maintain a supply temperature of $11\text{ }^{\circ}\text{C}$.

In the figure below is shown the temperature of the water in the bath (and so the supply temperature). It's possible to see that initially the temperature inside the bath increases a lot.

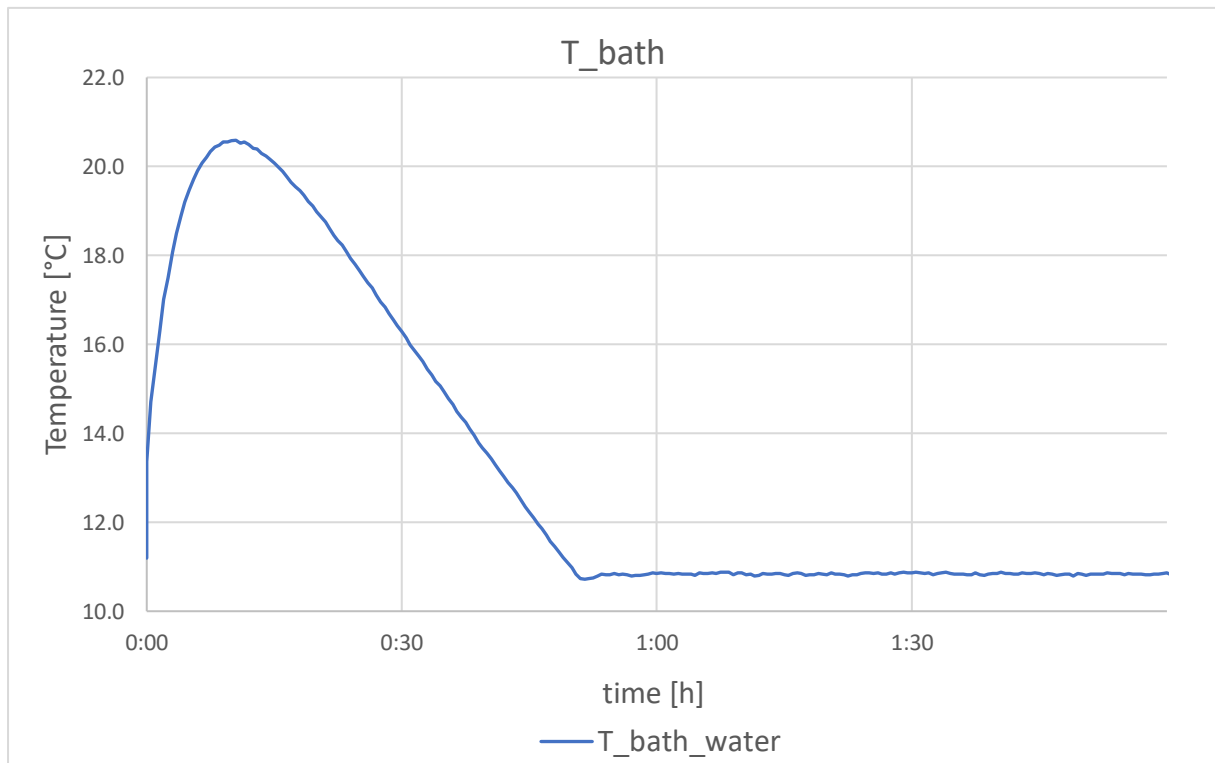


Fig. 4.3.2 – bath temperature trend in cooling operation

So, up to 52 minutes the bath cannot stabilise its temperature because the power exchanged is greater than the power of the chiller itself.

We can see this behaviour also in the temperature difference between supply and return water.

also in this case, the knee of the slope change is very visible at the instant when the bath reaches the fixed temperature, and its power becomes greater than that of the exchanger.

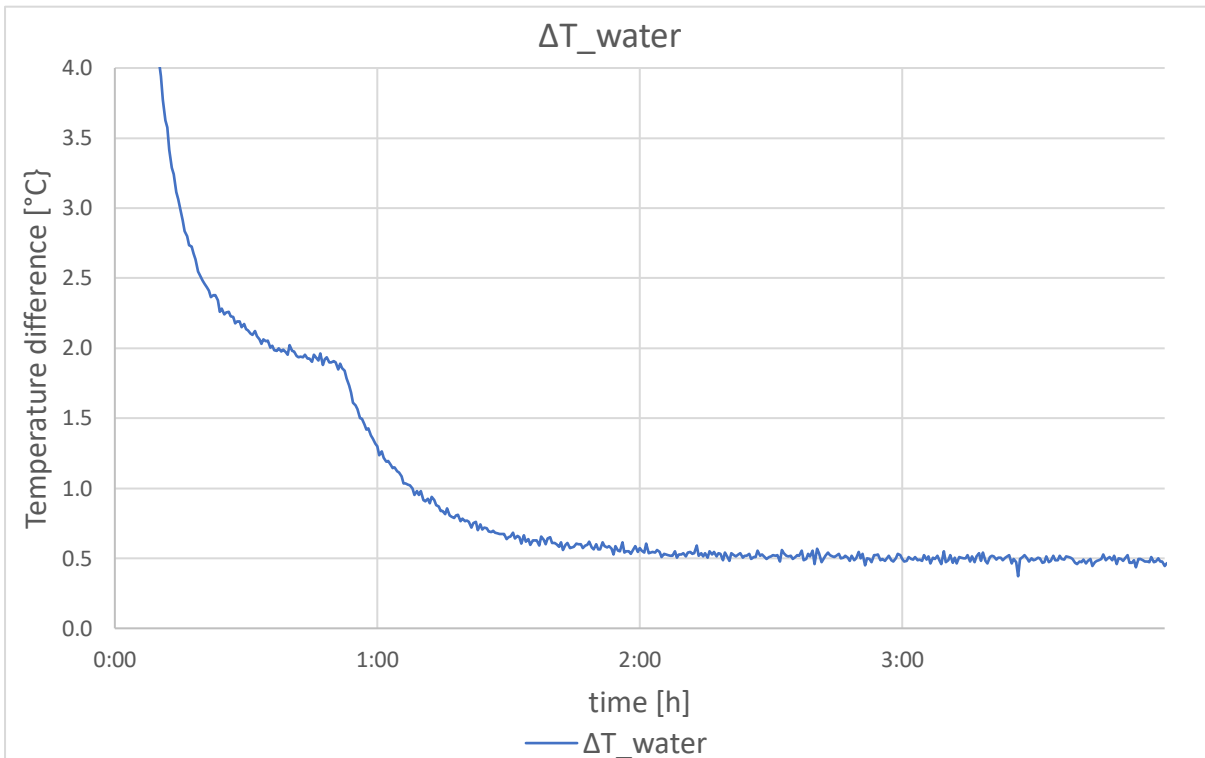


Fig 4.3.3 – temperature difference supply-return

To calculate the energy of the entire process, the system was allowed to reach an equilibrium performing the cooling for 17 hours.

The initial mean temperature of the water was 43.64 °C and the final one 11.91 °C.

So, the expected theoretical energy is:

$$E_{\text{theoretical}} = 10.5 \text{ [kg]} * 4.2 \text{ [kJ/(kg °C)]} * 31.73 \text{ [°C]} = 1399.3 \text{ [kJ]} = 0.3887 \text{ [kWh]}$$

The variation of the internal energy calculated with the data collected is:

$$\Delta U = 1403.3 \text{ [kJ]} = 0.3898 \text{ [kWh]}$$

The energy calculated by the data collected (power in the unit of time) results:

$$E_{\text{experimental}} = 1407 \text{ [kJ]} = 0.3808 \text{ [kWh]}$$

So, it is possible to confirm that to a first approximation the acquisitions system is sufficiently accurate.

Heating:

Also in heating the energy should be approximately the same.

In this case the system pass from a mean temperature of 44.3 °C to 12.4 °C; so the theoretical energy is:

$$E_{\text{theoretical}} = 10.5 \text{ [kg]} * 4.2 \text{ [kJ/(kg °C)]} * 31.9 \text{ [°C]} = 1406.8 \text{ [kJ]} = 0.3908 \text{ [kWh]}$$

The variation of the internal energy calculated with the data collected is:

$$\Delta U = 1408.5 \text{ [kJ]} = 0.3912 \text{ [kWh]}$$

The energy calculated (power in the time) results:

$$E_{\text{experimental}} = 1405.6 \text{ [kJ]} = 0.3904 \text{ [kW]}$$

Note that these energies just calculated are not directly comparable with the PCM ones that will be calculated later since in this case there is almost 3 kg kilograms more material in the cylinder.

So, when the energies between water and PCM cases will be compared, the calculation will be normalized by mass to consider the behaviour of the system with the same amount of material.

Also in heating is interesting to see the temperature of the bath because the power in heating conditions, as seen before in the specifics of the bath, is four times bigger than the one in cooling:

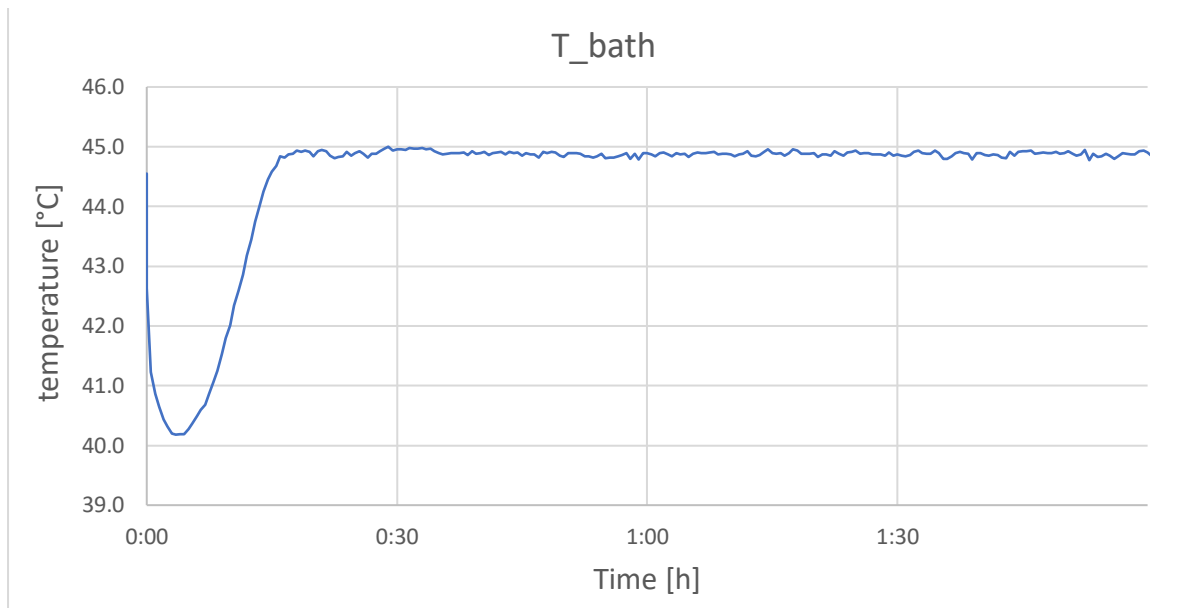


Fig. 4.3.3 – bath temperature trend in heating operations

As expected, the time required by the bath to reach the fixed heating temperature is almost 4 time less than one required for reach the cooling temperature in cooling operations as it was seen before.

Chapter 5.

Characterisation with PCM

Once the water trials are over, the entire system was discharged. So, the remained water has been dried and the PCM was filled into the cylinder.

The exact quantity of paraffin charged in the cylinder was 8.714 kg (11.32 litres).

Here there is a picture of the dismantled HE with the liquid paraffin inside that is perfectly transparent.



Fig. 5.0 - PCM pouring into the cylinder



Fig. 5.1 - micrometric flow valve

Before performing the reference tests both in melting and solidification, the boundary conditions, which remains the same for all the successive tests, were set:

- Ambient temperature: 22 ± 1 °C kept constant with the heating system of the room and controlled also with a TC
- Water pump of the circulator set at 40%
- Flow rate: 105 l/h (fixed with a micrometric valve in the return line of the circulator as shown in the figure above)
- Acquisition time: 30 seconds
- All the pipes (supply, return and external circuit) thermally insulated

5.1 Reference test in solidification

The liquid PCM, before starting the solidification, is brought at almost 45°C sending hot water at that temperature into the coil. When the whole system has reached the same temperature, cold water at 11 °C was sent to start and see the solidification process. A video of the solidification was taken and all the temperatures inside the HE were monitored for the entire process.

It was seen that the solidification process starts around the coil and expand radially from it, both from the supply and the return coil. Becoming solid, the paraffin loses its transparent properties and so it's quite difficult to see if the entire amount of paraffin is solid or not, but we can understand that watching at the temperatures. In fact, the solidification starts from the coil and expand; since the coil is near to the external surface, the solid front reaches first the external wall making it opaque and not allowing you to see inside.

Here there is a picture that shows how it appears after 20 minutes of cold water at 20 °C and when it is completely solidify. In the latter is possible to see the decrease in volume in of the solid-state respect to the liquid



Fig.5.1.2 & 5.1.3 - solidification beginning and completed solidification with clear volume reduction



Start



5 min



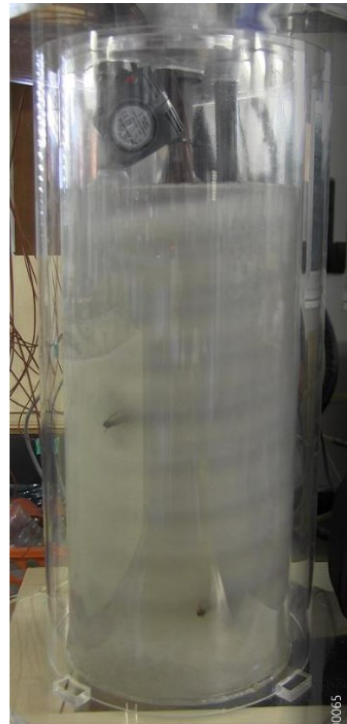
10 min



15 min



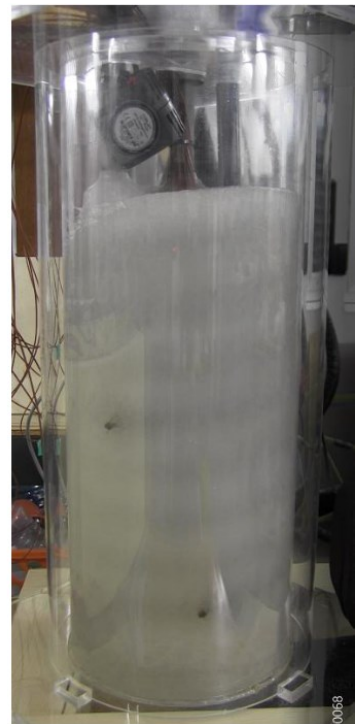
30 min



60 min



120 min



170 min

Fig. 5.1.4 - solidification process in different time interval

To have an idea of the solidification time, based on measurements, the required time to have the last TC (the 2.6) that reaches 25 °C is 5 hours 54 minutes.

This data about the time seems to be very big, in fact looking at the HE already after 2 hours it seems that all the material is solidified, but looking at the temperature it is not like that.

At that time by the way, the mean temperature of the PCM inside the HE is 14.4 °C.

But all the most external TCs take a huge amount of time to reach low temperature, because they're far from the coil and near to the external environment which is at 22 °C.

Let's calculate some energy:

The exact quantity of PCM that was filled into the HE is 8.714 kg.

During the operations, little losses of paraffin occurred in the junctions of the external circuit. They were fixed but a small amount of paraffin was lost. Moreover, there was a small quantity of paraffin that remains in the external circuit and does not participate to the heat exchange process. It was estimated the amount of "lost" material in almost 200 gr, and so the amount of paraffin that was considered *operative* was **8.5 kg** (because this will be the quantity we will extract later when we prepare the 1.5% graphene solution).

According to the producer, the heat storage capacity is **250 ± 7.5%** [kJ/kg] (which include both the sensible and the latent heat in the range [21 °C ÷ 36 °C]).

Since experimental results were very far in terms of energy from the theoretical expected energy based on the latent heat provided by the manufacturer, a sample of paraffin for a DSC analysis was sent to the CNR laboratory in Padova and the result confirmed the doubt: the **latent heat** in the temperature range [24 ÷ 31 °C] turns out to be almost **106 [kJ/kg]**, thus far from the approximately 220 [kJ/kg] declared by the manufacturer's datasheet.

So, considering our mass of PCM, the energy due to the latent heat for the entire process is:

$$E_{\text{latent}} = 106 \text{ [kJ/kg]} * 8.5 \text{ [kg]} = 901 \text{ [kJ]}$$

According to the producer, in addition, the specific heat capacity is 2 [kJ/(kg K)], so the theoretical sensible cooling in the range of 30 °C (T mean from 42.2 °C to 12.2 °C) is:

$$E_{\text{sensible}} = 2 \text{ [kJ/(kg K)]} * 30 \text{ [K]} * 8.5 \text{ [kg]} = 510 \text{ [kJ]} \text{ (it means 60 [kJ/kg])}$$

This number exactly matches the total internal energy variation calculated based on the measured temperatures (it was obtained 510.11 [kJ]). So, we can say again that the temperature acquisition system is well representative of the reality.

So, the theoretical energy of the solidification cycle is:

$$E_{\text{solidif_teo}} = E_{\text{sensible}} + E_{\text{latent}} = 901 \text{ [kJ]} + 510 \text{ [kJ]} = 1411 \text{ [kJ]} = 0.392 \text{ [kWh]}$$

Then, we calculate in each time interval the power exchanged in the water side easily with the formula:

$$P = \frac{\dot{m} \text{ [l/h]} * c_p \text{ [kJ/(kg K)]} * \Delta T \text{ [K]}}{3600} = \text{[kW]}$$

and so, the experimental energy of our solidification process was calculated and results:

$$E_{\text{solidif_exp}} = 1412.2 \text{ [kJ]} = 0.392 \text{ [kWh]}$$

So, the theoretical and the experimental energy matches perfectly.

To have an idea of the trend of the energy during the time is now reported a graph:

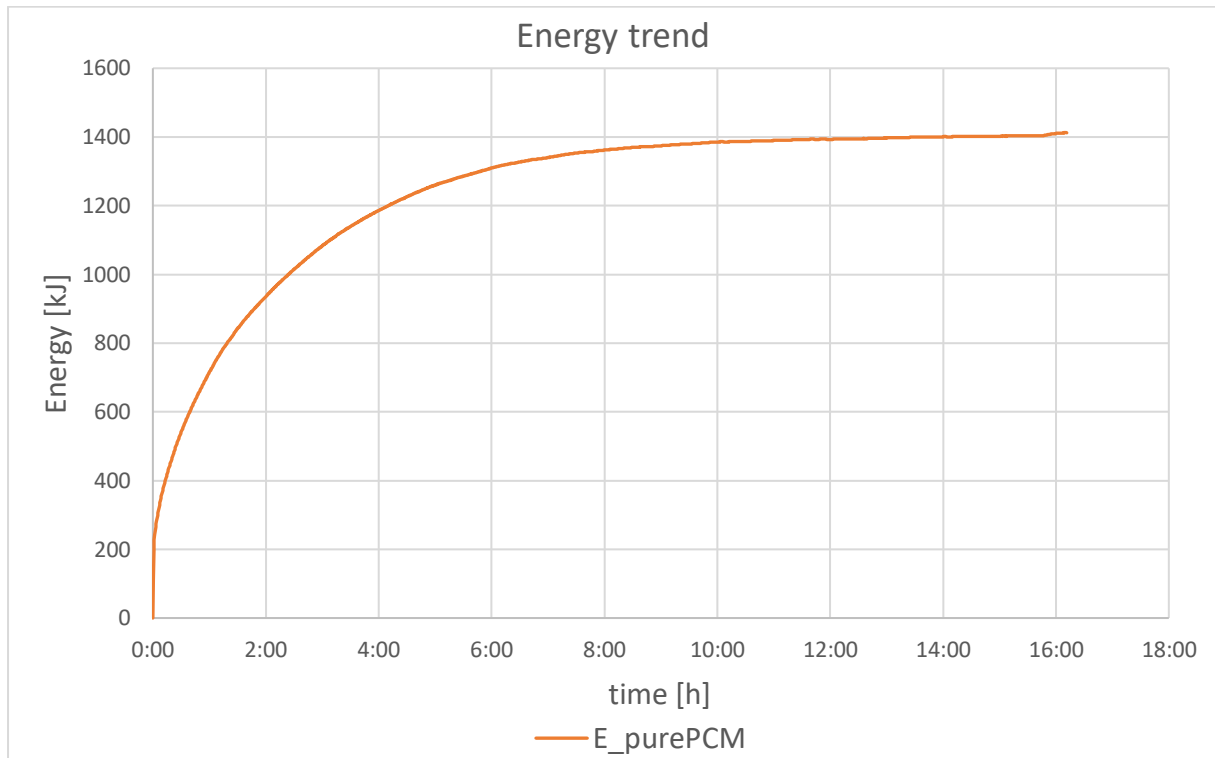


Fig. 5.1.5 – energy trend for pure PCM

In some tests, it was noticed that after 16 hours of operation, when the temperatures (supply, return and average of the PCM) are constant and the system should have reached an equilibrium, there was still present a residual power that can vary from zero to 30 W and which was considered as the tare weight of the system for these reasons:

- there are some losses through the envelope which is not adiabatic (we'll calculate them in a few).
- there are some losses through the water circuit from the bath to the coil. Even though we isolate it, some losses are still present especially in brass junctions (for example in the flow meter) which are not isolated. It was not possible to consider that kind of losses.
- The accuracy of the acquisition system is not perfect. Let's think for example at the TC of the supply and return water. Although it has been tried to calibrate them as accurately as possible, if there is a difference in measurement of only 0.1 degrees this would result in a power output of 25 W that would not exist.

➤ **The heat that is entering/exiting the HE through the plexiglass**

Some data and hypothesis:

- λ of the PVC = 0.2 [W/(m K)]
- convective coefficient for the still air gap $h_1 = 7$ [W/(m K)]
- convective coefficient for the ambient air $h_2 = 13$ [W/(m K)]
- surface of the external cylinder $A_2 = 0.373$ [m²]
- surface of the internal cylinder $A_1 = 0.306$ [m²]

So there was 5 resistances to be considered: the two by conduction through the PVC (R_{cond}^1 and R_{cond}^2), the two convective inside the air gap (R_{conv}^1 and R_{conv}^2) and the one convective on the external wall of the HE ($R_{conv ext}$).

Let's calculate them:

$$R_{cond}^1 = \frac{s}{\lambda * A_1} = \frac{0.005 [m]}{0.2 \left[\frac{W}{mK}\right] * 0.306 [m^2]} = 0.082 \left[\frac{K}{W}\right]$$

$$R_{cond}^2 = \frac{s}{\lambda * A_2} = \frac{0.003 [m]}{0.2 \left[\frac{W}{mK}\right] * 0.372 [m^2]} = 0.040 \left[\frac{K}{W}\right]$$

$$R_{conv}^1 = \frac{1}{h_1 * A_1} = \frac{1}{7 \left[\frac{W}{m^2K}\right] * 0.306 [m^2]} = 0.467 \left[\frac{K}{W}\right]$$

$$R_{conv}^2 = \frac{1}{h_1 * A_2} = \frac{1}{7 \left[\frac{W}{m^2K}\right] * 0.372 [m^2]} = 0.384 \left[\frac{K}{W}\right]$$

$$R_{conv ext} = \frac{1}{h_2 * A_2} = \frac{1}{13 \left[\frac{W}{m^2K}\right] * 0.372 [m^2]} = 0.207 \left[\frac{K}{W}\right]$$

So:

$$R_{tot} = \sum R_i = 1.18 \left[\frac{K}{W}\right]$$

And thus, the power lost or gained through the envelope is:

$$q = \frac{\Delta T}{R_{tot}} = \frac{(22 - 15.7)}{1.18} = 5.34 [W]$$

Note that 15.7 °C is the mean temperature of the PCM in all the solidification process.

The energy losses through the envelope are quite small but still a part of the residual power.

Note that we don't consider the heat exchanged in the top and bottom surfaces.

Let's see some temperature trend inside the cylinder during the solidification process:

For example, for the highest level (the level 1):

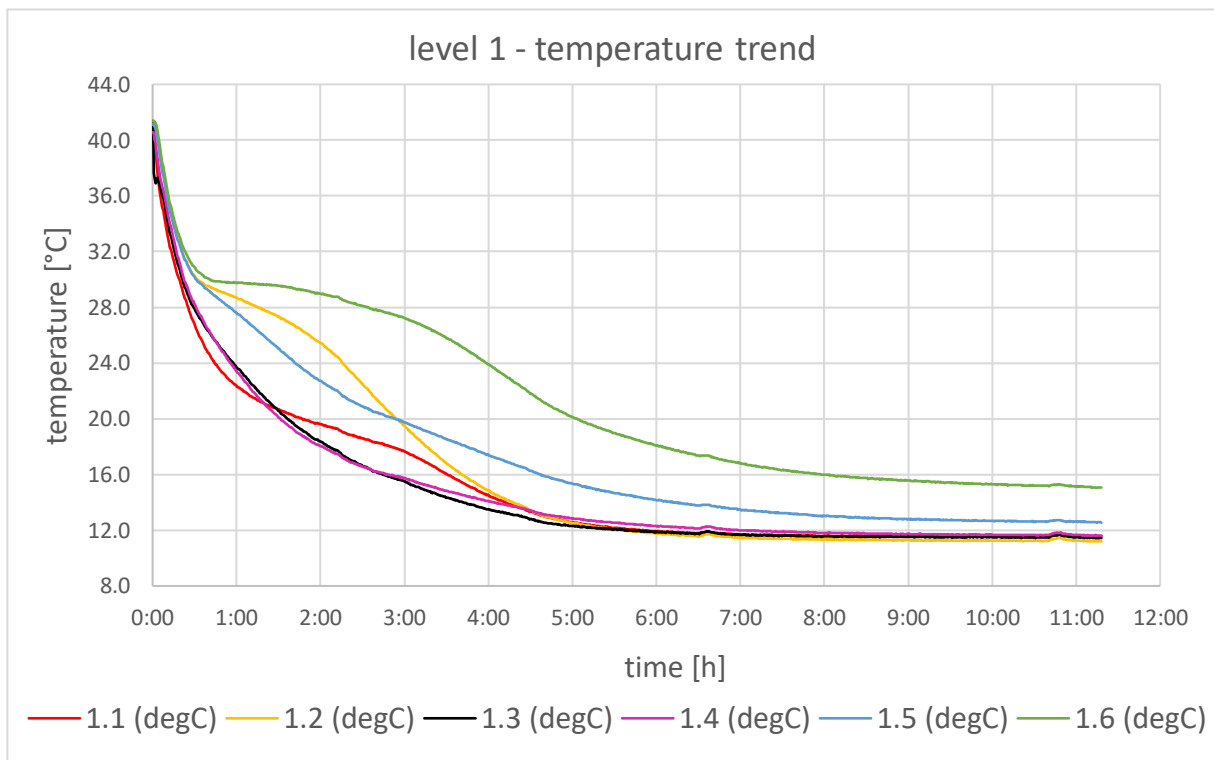


Fig. 5.1.6 – temperature trend in the highest level

It is possible to see first that the solidification process is very slow. In fact, the TC near to the external wall (the 1.6) takes 2 hours and a half only to reach the melting temperature and then reaches 18 °C after 6 hours.

In general, it can be seen that the farther the thermocouple is from the coil, the slower it cools; In fact, the solidification start from the coil and propagate basically only by conduction through the PCM itself.

TC 1.4, 1.1 and 1.3 solidify essentially in the same way since they're all near to the coil.

1.2 and 1.5 are quite slower because 1.2 is in the middle of the 2 coils (supply and return) but far from both, while 1.5 is quite near to the supply but also near to the external environment which is at 22 °C.

The trend represented in the figure 5.1.5 is the same for each level.

Another interesting trend that we can compare is the same radial position but in different height level.

For example, we can see what happens in the TC nearest to the supply coil (the TCs in position 4):

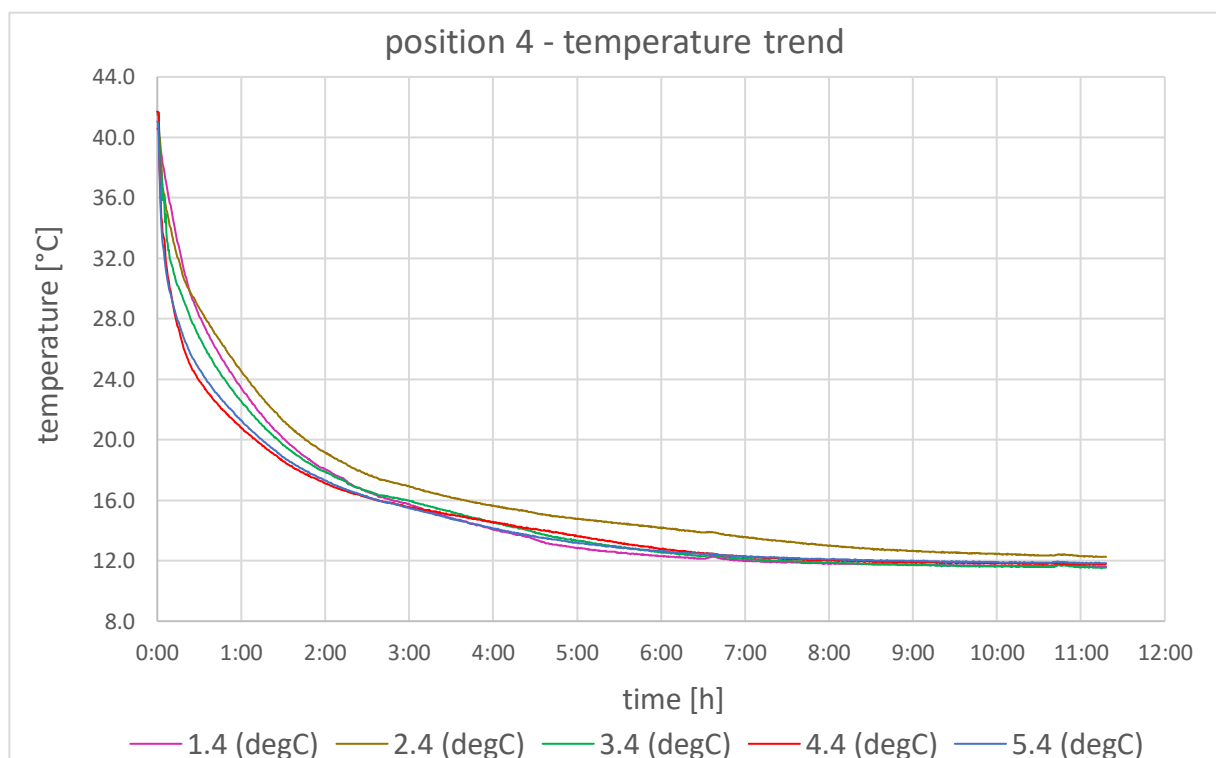


Fig. 5.1.7 – temperature trend in position 4

In this case it can be seen that the temperature trend is the same in all the levels. It makes sense because the solidification start at the same time in all the PCM in contact with the coil (even though flowing through the pipe, the cold fluid heats up a little bit, but its influence is limited and not appreciable).

We can also notice that there is still a difference of about 15 minutes between the first and the last TC that reaches the melting temperature. This is also because during the period in which the bath is brought to 11 °C, the circulation pump is stopped and so some stratification occurs. So, when the cold water flow into the coil start, at the bottom of the HE the temperature is quite lower than on the top (0.5 – 1 °C difference) and so the solidification occur first. In addition, the cooled paraffin lowering its temperature, increase its density and tends to move downwards into the HE while the hotter one tends to rise, and so in the high levels the solidification occur later.

This can be seen also in the position 5:

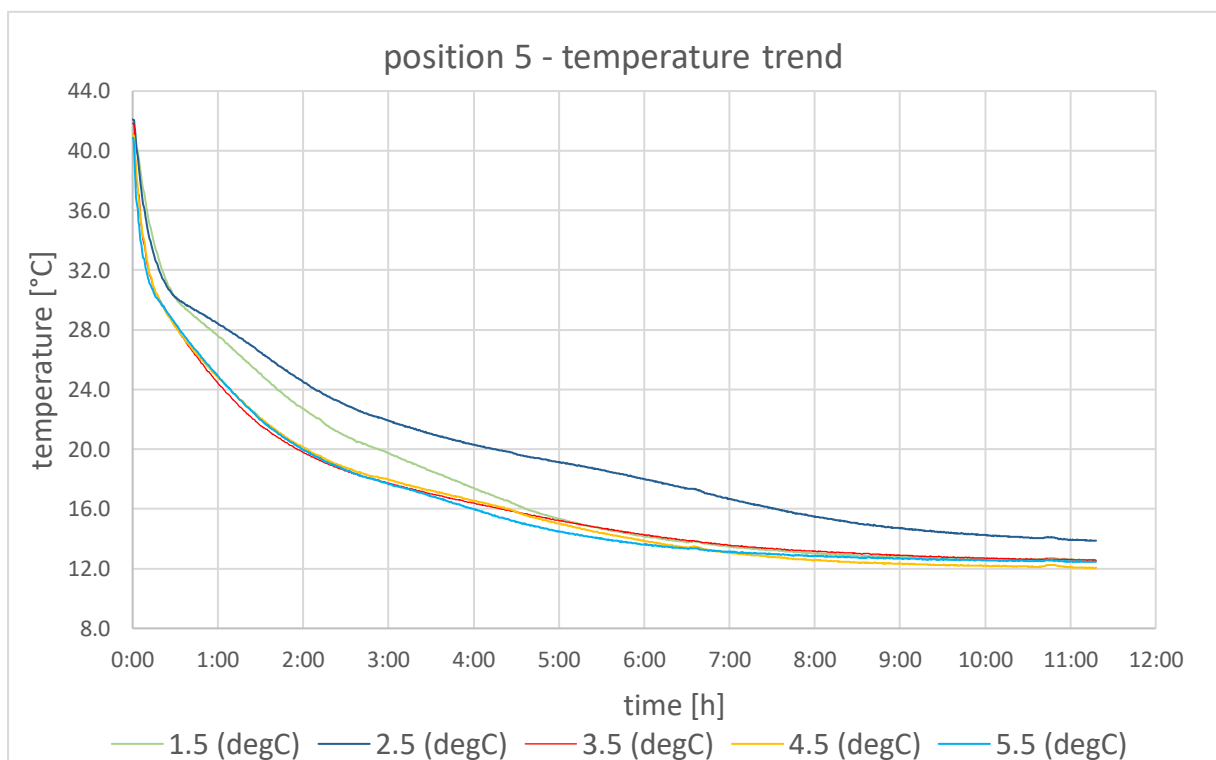


Fig. 5.1.8 – temperature trend in position 5

The same behaviour of the previous case happens: the three TCs in the lower levels (3.5 – 4.5 - 5.5) solidify basically at the same time while the 2 higher levels are slower.

Regarding the powers, to have an idea of the trend, here are reported the mean powers in different time intervals:

Time interval [min]	Mean power [kW]
0-10	0.659
10-20	0.160
20-30	0.131

Tab. 5.1 mean solidification power in time

The following is the path of the instant powers excluding the first 5 values to have a clearer graph:

In the x axis is reported the time in hour from the beginning of the solidification process, and in the y axis the power in kW.

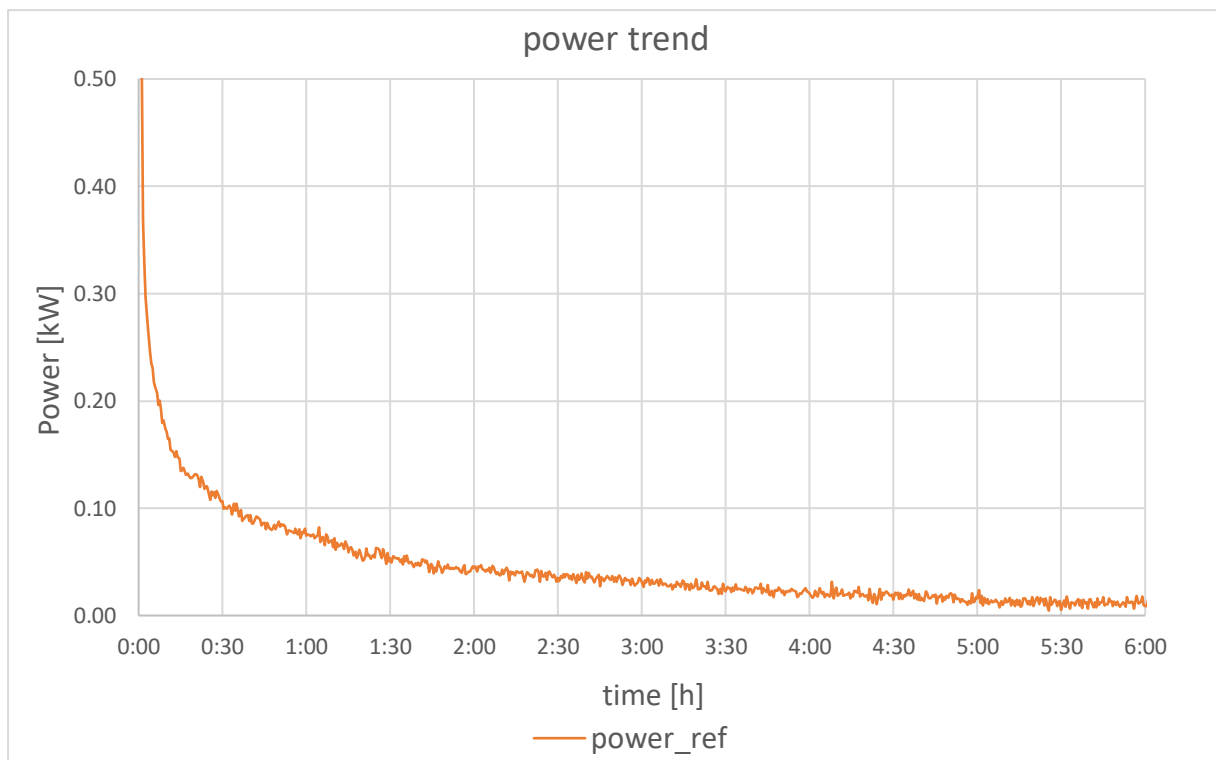


Fig. 5.1.9 - global trend of the power in solidification

One can see that initially the power is very high, in fact in the first two minutes, the mean power is 1.79 kW. It means that the power of the exchanger is more than three times that of the chiller, to the extent that the latter was not able to maintain the 11 °C in the supply coil.

But let's zoom into the first hour, and see how the power behave:

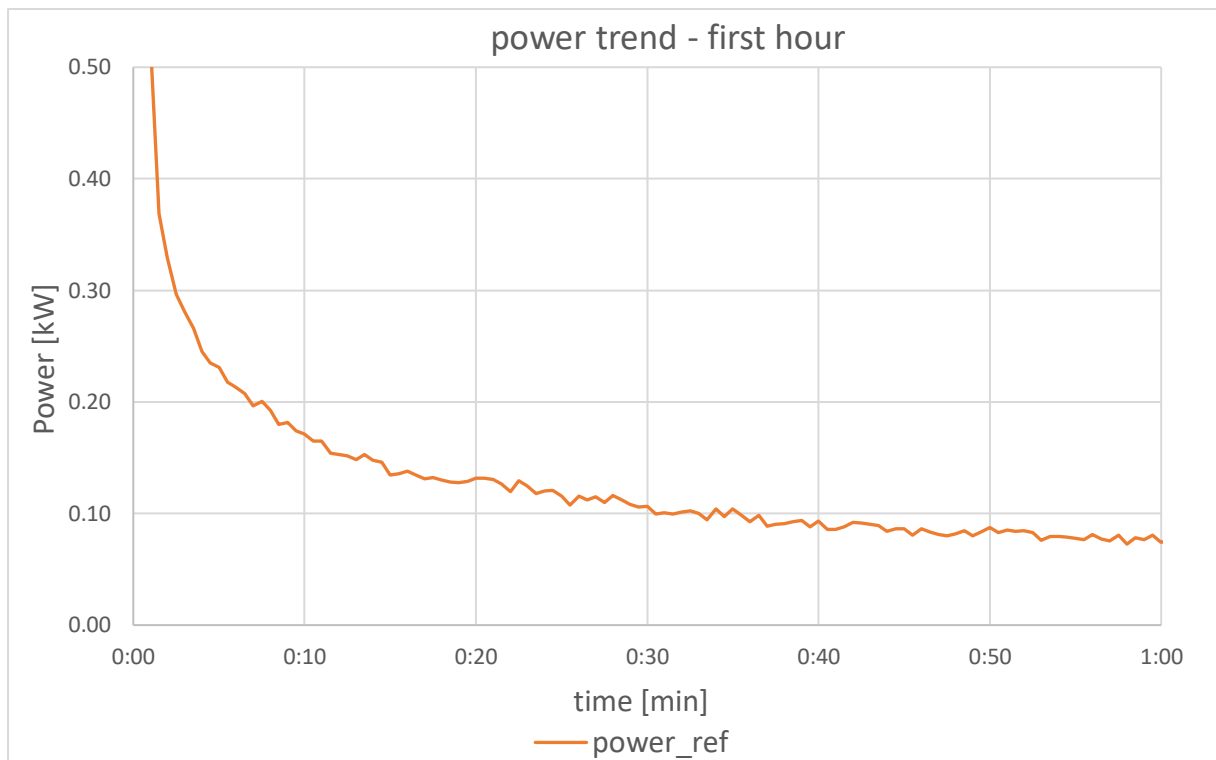


Fig.5.1.10 - trend of power in the first solidification hour

Is evident that in first 10 minutes the power is quite high because the cold water is extracting a lot of heat from the hot PCM and so the ΔT between supply and return water is big. After these 10 minutes the slope of the curve decrease and after one hour is already less than 100 W.

After first two hours the power decrease under 50 W mostly because the latent heat to be transferred is almost exhausted and only sensible heat is being exchanged, until the system reaches an equilibrium.

Let's compare graphically the water case and the pure PCM case, regarding the thermal power:

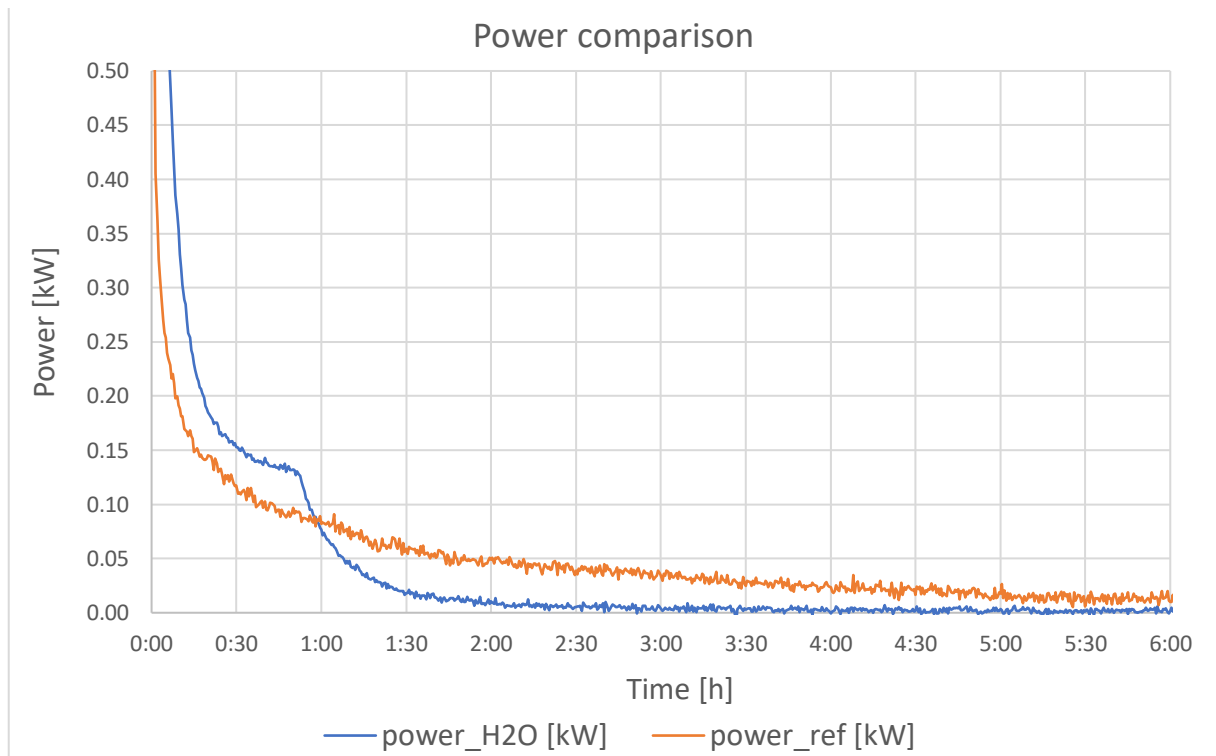


Fig 5.1.11 – power comparison, water and reference case with PCM paraffin

One can see that in terms of power, the system with water is better in the first hour due to the higher thermal conductivity of the water respect to the PCM (0.6 [W/(m K)] for the water and 0.16 [W/(m K)] for the PCM), and then it became worst because the latent heat of the PCM is involved.

It is possible to see that there is a big difference also in the temperature of the bath between the two tests (water and PCM):

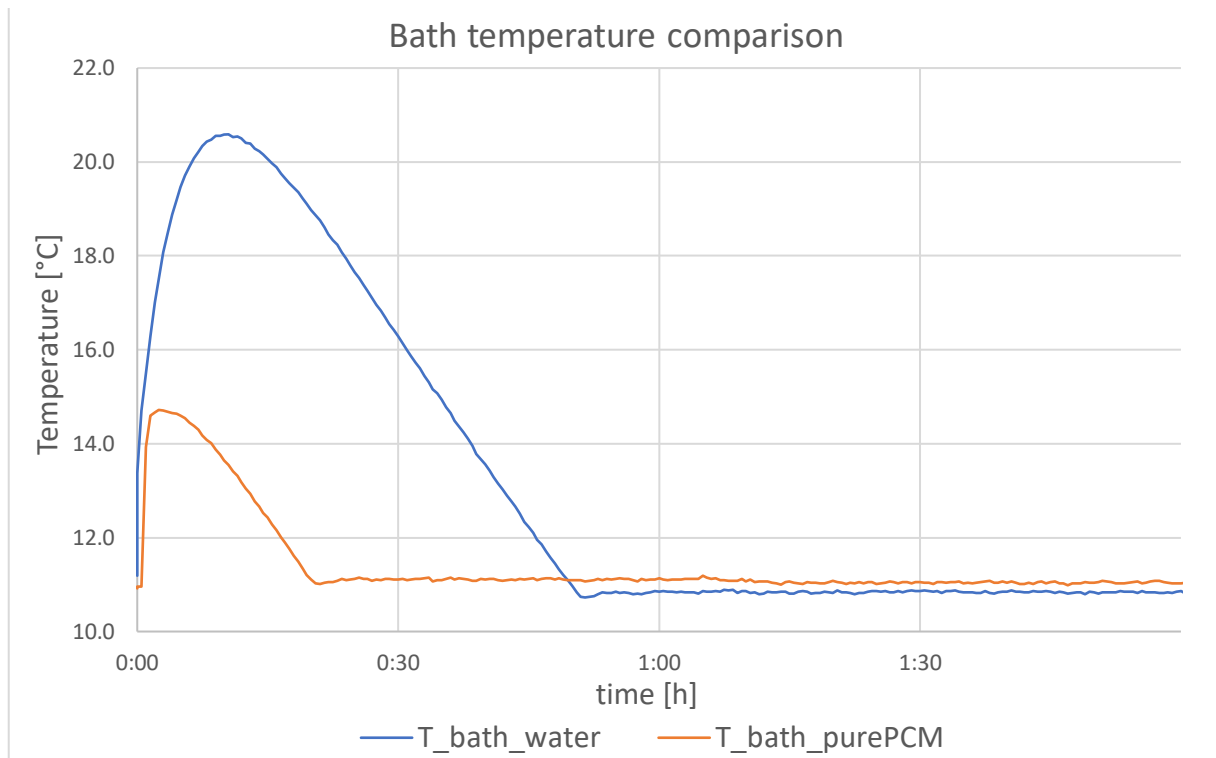


Fig 5.1.12 – bath temperature comparison between water and pure PCM

The figure above shows a significant difference between the two cases. In fact, in the case with water the temperature of the bath reaches a temperature that is almost 6 degrees higher than the case with PCM.

This graph is coherent with the one shown in the figure 5.1.11. The temperature of the bath is higher, so the ΔT between supply and return is bigger and so the power.

For completeness is now reported the comparison between the ΔT of supply and return in the two cases:

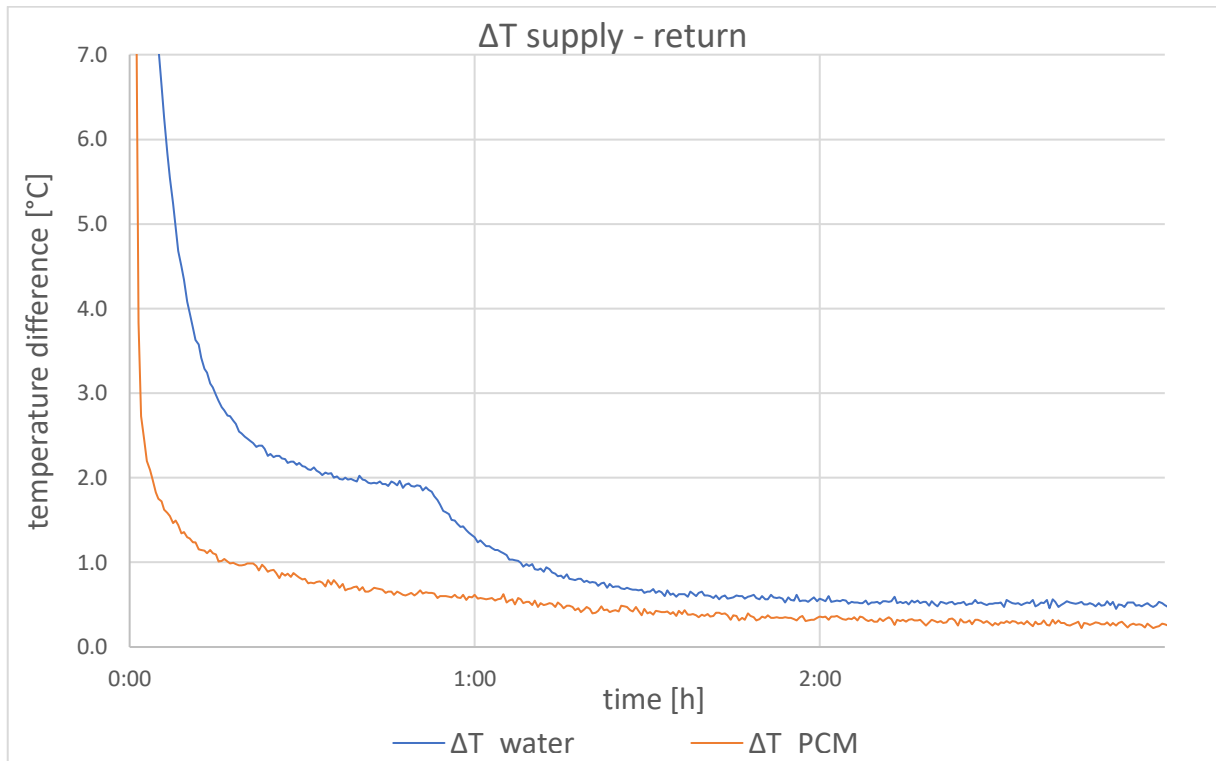


Fig 5.1.13 - ΔT supply-return comparison

The trend confirms that with water since the ΔT is bigger, also the power is bigger as shown in figure 5.1.11. The ΔT drop at almost 52 minutes in the exact moment in which the power of the bath become higher than the power of the heat exchanger as is shown in figure 5.1.12.

5.2 Reference test in melting

The melting process was performed sending water at 45 °C when the solid was at a mean temperature of 12.3 °C.

Here there are some pictures taken in different moments during the melting process:

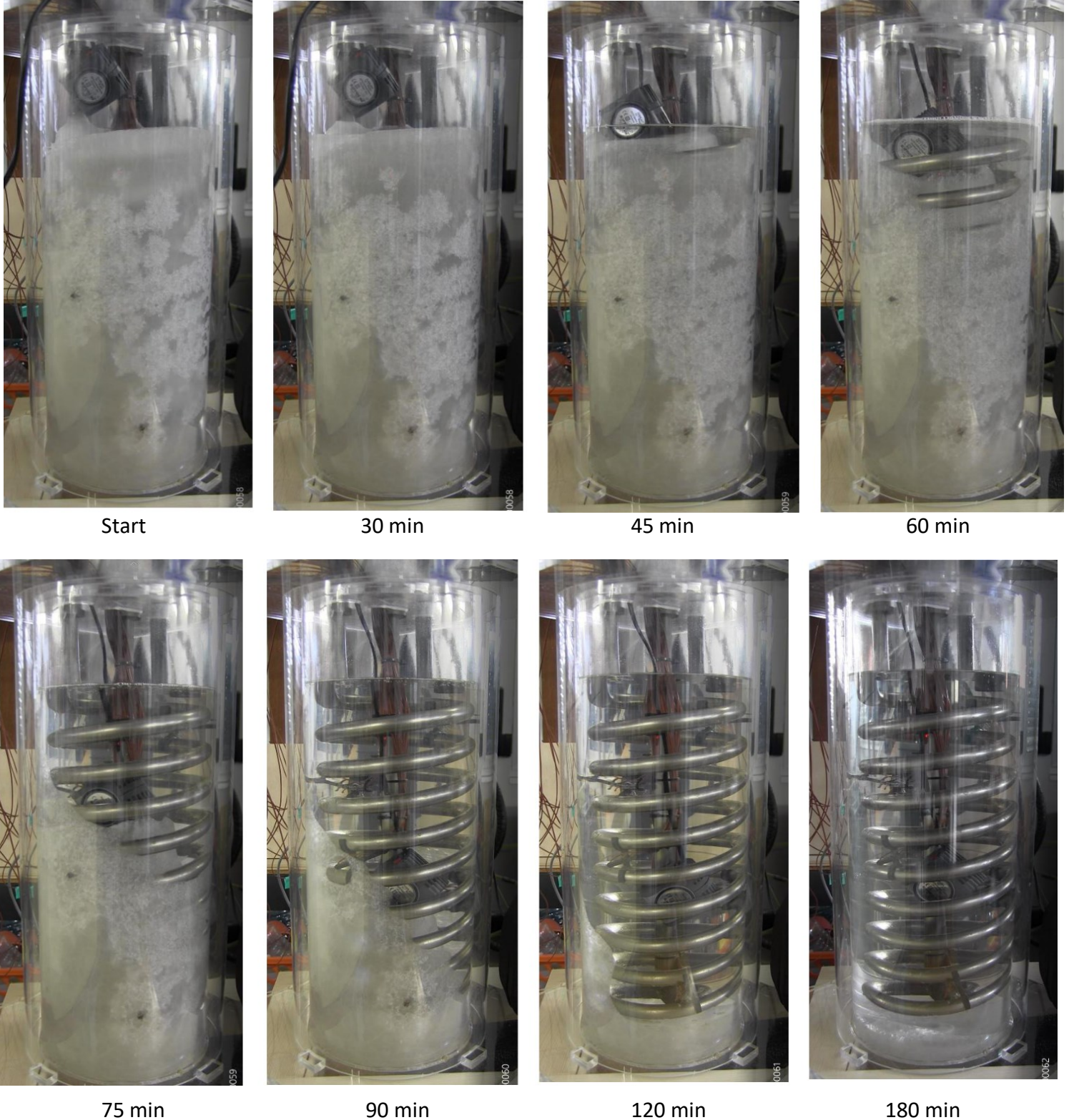


Fig. 5.2.1 - melting process in different time intervals

In this case clearly the last TC to reach 30 °C was the one at the bottom towards the external environment (the 5.6) and it reaches 30 °C after 1 hour 32 minutes; but when those TC reached 30 °C there was still present an amount of PCM at the bottom of the HE (in fact the 5.6 TC is about 7-8 cm from the bottom) estimated in 4-6 cm. It means that there was still a portion of latent heat that has to be exchanged.

During melting, since liquid paraffin is lighter than the solid one and tends to rise inside the cylinder, in the suction of the external recirculation pump remains the solid portion until the end of melting. In that way the melting process is quite slow (even though some natural convection occurs) and is not possible to enhance the convection turning on the external recirculation pump.

To overcome this problem, a small aquarium pump was inserted in the top of the HE (at the level of the liquid paraffin), so when the first portion of PCM melts, is possible to turn on the pump which increase a lot the convection inside the HE and reduce significantly the time required for completely melt the PCM.

Let's calculate some energies also for the melting process.

Theoretically for the same ΔT (between the mean temperature at the beginning and the end of the melting process) we must obtain the same energy, i.e 1411 [kJ]

Based on measurements, the variation of the internal energy of our system is:

$$\Delta U = 1411 \text{ [kJ]} = 0.392 \text{ [kWh]}$$

The resulting energy in the water side instead:

$$E = 1412.2 \text{ [kJ]} = 0.393 \text{ [kWh]}$$

And now we consider the same aspect as for the solidification regarding the power exchanged through the envelope:

➤ **The heat that is entering/exiting the HE through the plexiglass**

$$q = \frac{\Delta T}{R_{tot}} = \frac{37.8 - 22}{1.18} = 14.2 \text{ [W]}$$

In the melting case it is necessary to consider also the power of the aquarium pump that is inserted:

➤ **The power that is put into the PCM with the aquarium pump**

The aquarium pump has a power of 7 W, so a part of the residual power that is present in melting is due also to this.

Let's see also for the melting process, some temperature trends:

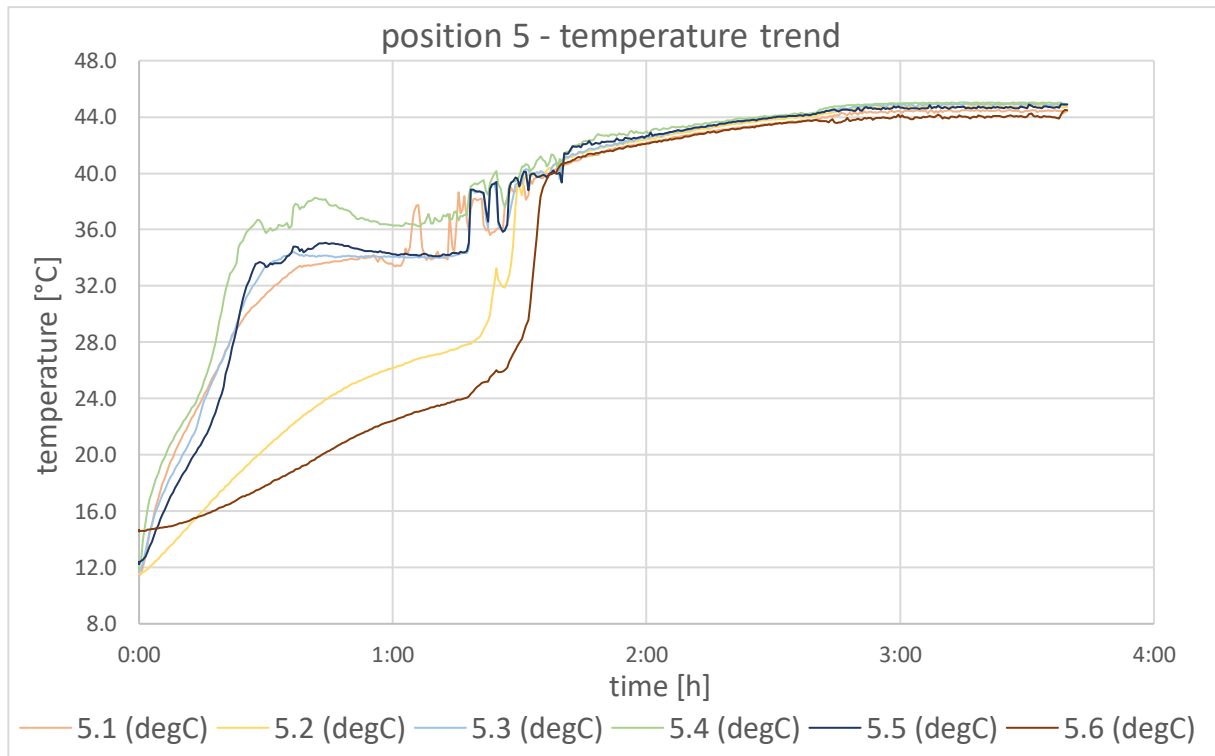


Fig. 5.2.2 – temperature trend in level 5

In melting one can see several things: For example, that the trend is less linear and more jagged. This is probably because the melting the process is not only driven by conduction but also by convection since the melted liquid moves up towards the top of the cylinder due to buoyancy and also the convection is enhanced by the aquarium pump that was inserted in the HE (in the case of level 5, the effect of the pump is very limited because the pump doesn't reach such a depth inside the HE and so it doesn't move the paraffin around the level 5 sensors, making the convection limited in that zone).

Anyway, also in this case we can see that the temperatures in the TCs near the coil are the first to melt. In fact, 5.1, 5.3, 5.4, 5.5 reaches the melting temperature at the same time (3 minutes difference between the first and the last).

Instead, 1.2 and 1.6 are much slower. They reach the melting temperature more than one hour later.

Almost for each TC is also possible to see that at certain point there is an instantaneous increase of the temperature, and this is due to the effect of the aquarium pump that push the hot paraffin close the sensors and so the temperature increase is not gradual as it would be in “normal” conditions.

The effect of the pump can be seen more clearly in the higher levels.

Note that the small pump was turned on after 50 minutes from the beginning of the melting process.

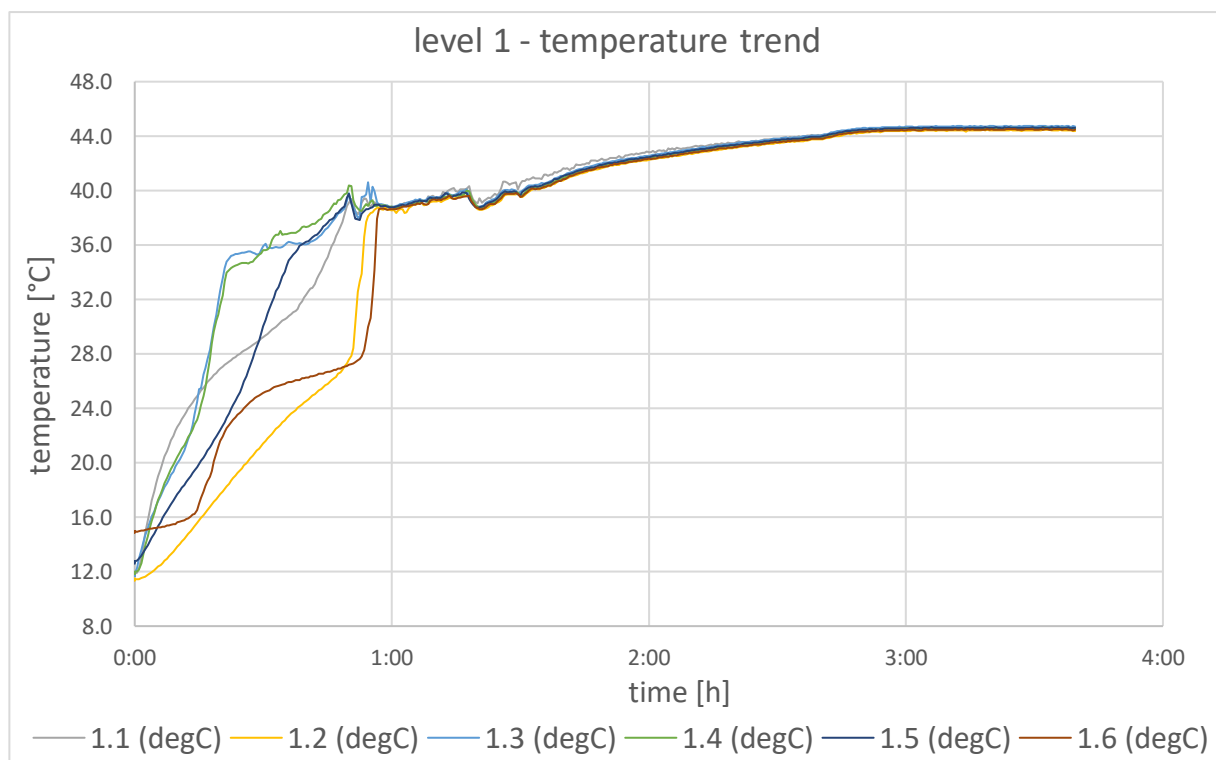


Fig. 5.2.3 – temperature trend in level 1

In this case, after 50 minutes is possible to see the effect of the aquarium pump. In fact, at that moment all the other TCs present an increase in temperature. In particular 1.1, 1.3, 1.4, 1.5 presents a slightly increase around 40 °C while the 2 most far from the coils, i.e 1.2 and 1.6 has a bigger increase from 27 °C to almost 38 °C.

Is also possible to see after 1 hour 17 minutes that there is a small temperature drop in all the TCs. That is the moment when the pump was moved downwards into the cylinder due to the increased level of the liquid present. This cause a mixing of the stagnant and stratified liquid paraffin pushing the colder one into the upper levels where is present the hotter PCM.

Let's see also what happens in different radial positions.

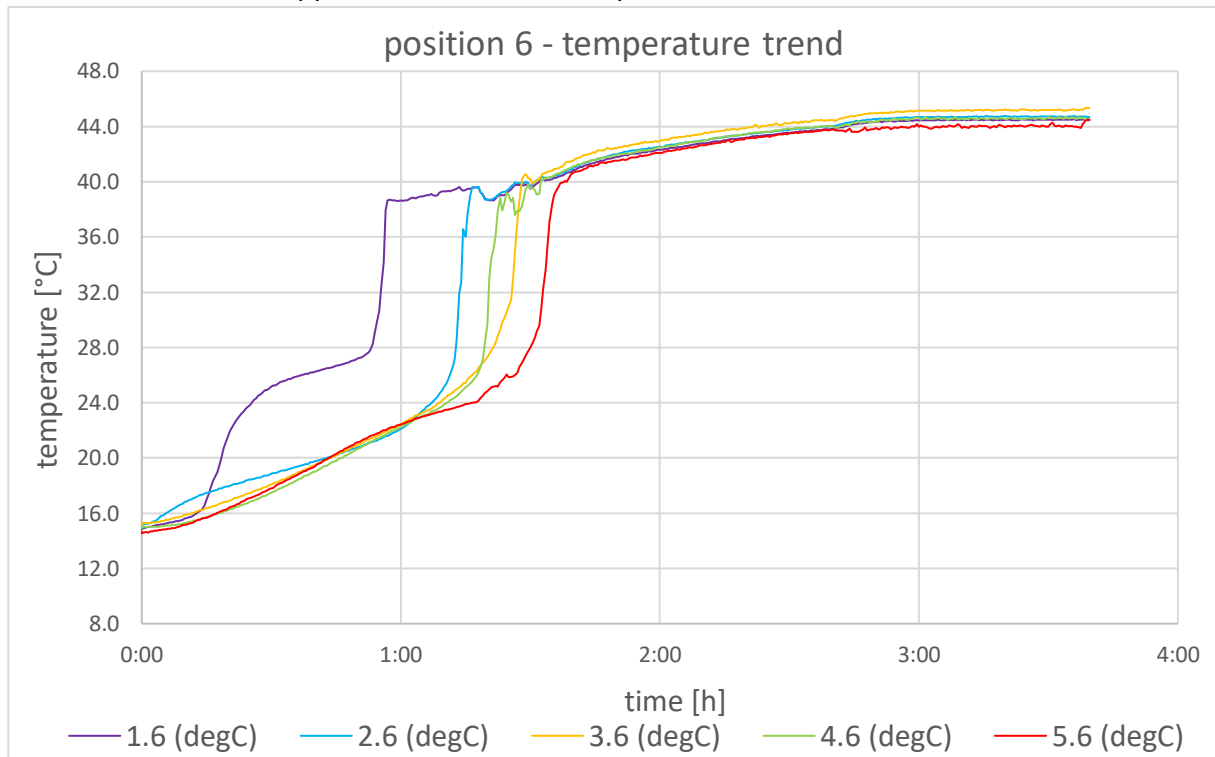


Fig. 5.2.4 – temperature trend in position 6

The TCs in position 6 are the last ones to reach the melting temperature. As we expected, since the liquid front moves towards the bottom during the melting process, the first TC to reach the melting point is the highest one (the 1.6) and the last is the lowest one (5.6). The only two TC that, according to reaching of the melting temperature are reversed, are the 3.6 and 4.6 but the difference is quite negligible (2 minutes).

Looking at the other positions, the behaviour changes a little bit. In fact, usually the first two TC to melt are the higher ones (level 1 and 2), then there is the level 5 and finally the levels 3 and 4.

As an example of what has just been said, here is reported the behaviour in the position 3:

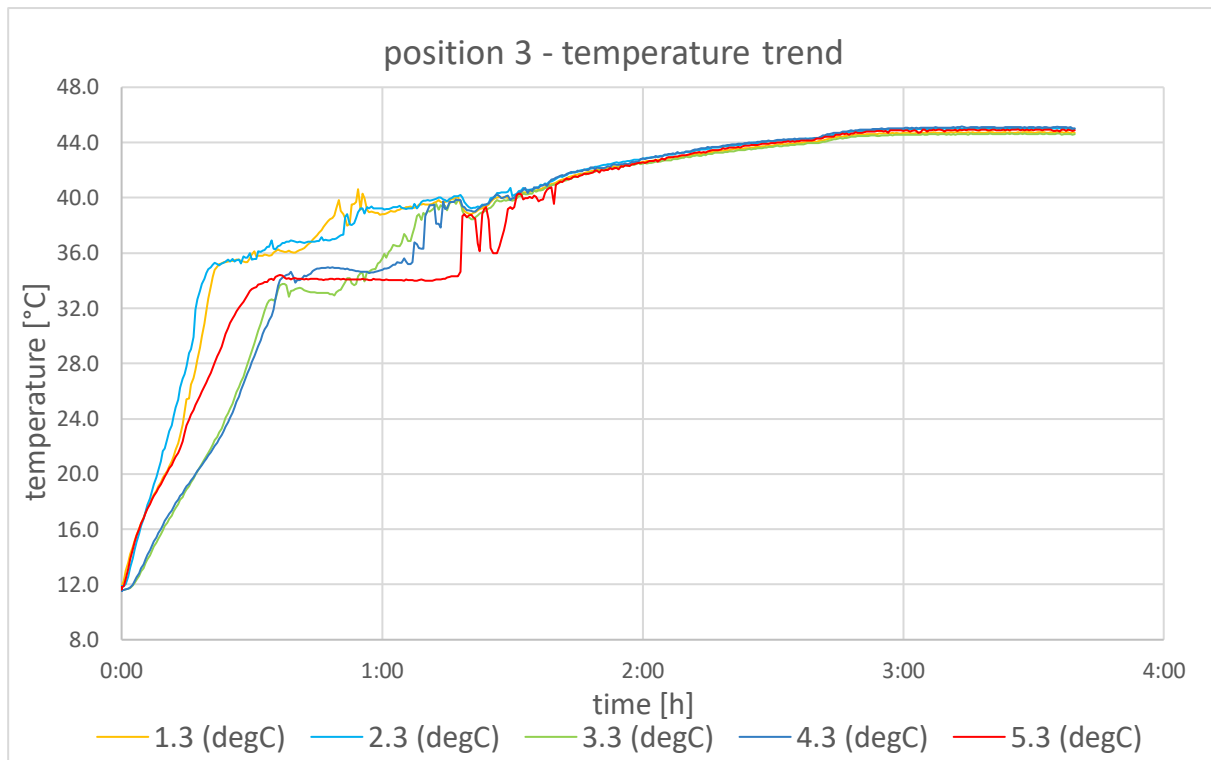


Fig 5.2.5 – temperature trend in position 3

Regarding the powers, to have an idea of the trend, also for the melting, are here reported the mean powers in different time intervals:

Time interval [min]	Mean power [kW]
0-10	0.650
10-20	0.163
20-30	0.168

Tab. 5.2 mean melting power in time

Instead of looking at the power trend during the time as we done for the solidification, to have a more interesting view, are now directly compared the power in melting and solidification in a unique graph.

5.3 powers comparison: solidification VS melting

Let's see the comparison of the powers in melting and solidification in the first three hours of operation:

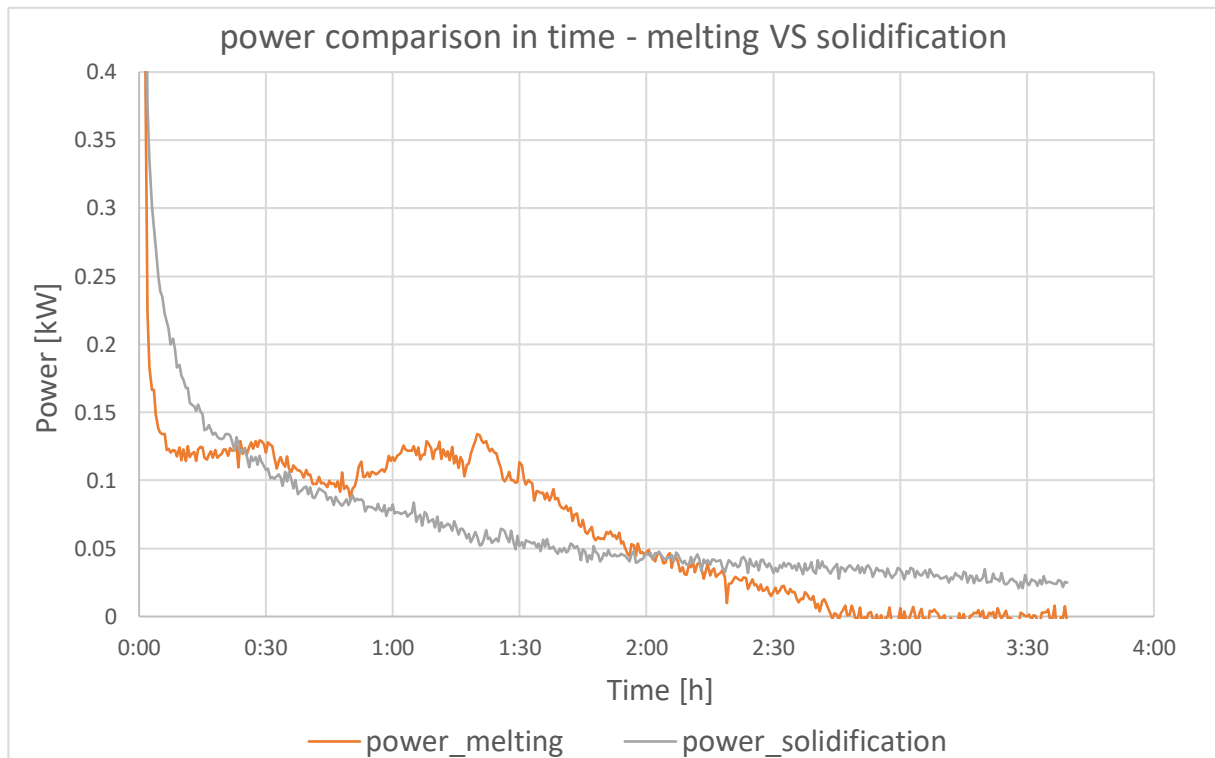


Fig 5.3.1 - solidification & melting power comparison in the first hour

One can see that the melting process is faster than the solidification one, but since the energy exchanged in the entire process is the same, it is normal that the average values of the powers during melting is a little bit higher in the first hours. Remember that the main reason of the much faster process is the presence of the aquarium pump that increases so much the convection of the liquid PCM inside the HE (from the minute 50 in fact we can see that the power in melting increases and remains high for about one hour and then starts to descend again).

While the power in solidification remains quite constant because it's a more slow and stable process, the power in melting decreases especially after 1 hour 20 minutes and intersects the power of the solidification after 2 hours. This decrease in melting power is related to the fact that the fraction of solid PCM remaining is little compared to the initial one, and as we can see in fig. 5.2.1 after 2 hours there are only few cm of solid PCM at the bottom, but

the aquarium pump can't go so down and so convection phenomena is very limited in that region of the HE.

The melting power decrease and decrease until there is no solid PCM at all and the system reaches the equilibrium after the sensible heating. While the solidification, as before, continues to exchange a little quantity of sensible + latent heat and even if it's difficult to see if there is a liquid part remaining, it is easy to check it through the TCs placed inside the HE.

Since the powers in the time represents the energy, the areas under the two curves must be the same as was calculated in the chapters before.

Chapter 6.

ϵ -NTU characterisation

We want also to characterize our HE in terms of efficiency. To do this, it is simply calculated dividing the actual real power by the maximum theoretical one:

$$\epsilon = \frac{\sum m * cp * (T_{in} - T_{out})_{water}}{\sum m * cp * (T_{in_{water}} - T_{mean_{PCM}})}$$

It results an average efficiency of 14%.

Another way to calculate the efficiency of a tube-tank PCM heat exchanger is by using the equation provided by [10]:

$$\epsilon = 0.830477 - 17.2411 * \frac{\dot{m}}{A} + 1848.522 * \left(\frac{\dot{m}}{A}\right)^2 - 1038.48 * \left(\frac{\dot{m}}{A}\right)^3 + 3022.2 * \left(\frac{\dot{m}}{A}\right)^4 - 4065.01 * \left(\frac{\dot{m}}{A}\right)^5 + 1717.23 * \left(\frac{\dot{m}}{A}\right)^6$$

Where \dot{m} is the mass flow rate of water which is “fixed” with the micrometric valve at 105 l/h and A is the surface area of the coil in contact with the PCM which is calculated and equal to 0.187 m².

Using this empirical equation, it results an efficiency of 15.45%

Chapter 7.

Small scale tests with graphene

7.1 Type of graphene

The used graphene is named CANAM (**C**arbon **n**anostructured **a**dvanced **m**aterial) and is produced by *Futura Srl*.

CANAM is a nano-structured material of ultra-pure carbon (no less than 99.76% of carbon) and there is no trace presence of solvent or heavy metals.

It is also totally stable (until about 600 °C), chemically inert, hydrophobic (wettability angle greater than 90°), electrically conductive, constant in corrosive environments and has no impact in the environment itself.

Its density ranges from 0.01 to 0.001 g/cm³ and its specific surface area can reach up to about 2000 m²/g



Fig. 7.0 - CANAM in the undisturbed state

The CANAM cost us 150 €/kg. When putting the 3% of graphene in the PCM it means that the price of graphene is 4.5 €/kg of PCM.

Considering an average price of the paraffine of 8 €/kg it means that the paraffin enhanced with 3% of graphene have a cost of 12.5 €/kg.

Since there is initially 8.5 kg of pure PCM, the cost of the whole material we use including the graphene is about 106 €.

7.2 Test explanation and conductivity enhancement results

Before adding the graphene directly into the HE, some tests were carried out in lab tubes to see first if the conductivity of the pure PCM is equal to the one given by the producer and then what happens to the conductivity if different percentages of graphene are added into the PCM.

The lab tubes used are the one in the following photo:



Fig. 7.1 - lab tubes

Four tests were done (named from 0 to 3). 35 ml of PCM was put into each tube and then different percentage by weight of graphene were inserted into each tube. Specifically:

N° test	Tare with cap [g]	Tare without cap [g]	Gross without cap [g]	NET PCM [g]	Weight of graphene [g]	% of graphene
1	13.90	11.20	36.80	25.60	0	0
2	14.35	11.50	35.60	24.10	0.1	0.41
3	14.10	11.35	35.10	23.75	0.25	1.05
4	14.10	11.35	35.35	24.00	0.35	1.46

Tab. 7.0 data of different tests

This is how they look like after PCM was melt, well mixed with the graphene and then solidified:

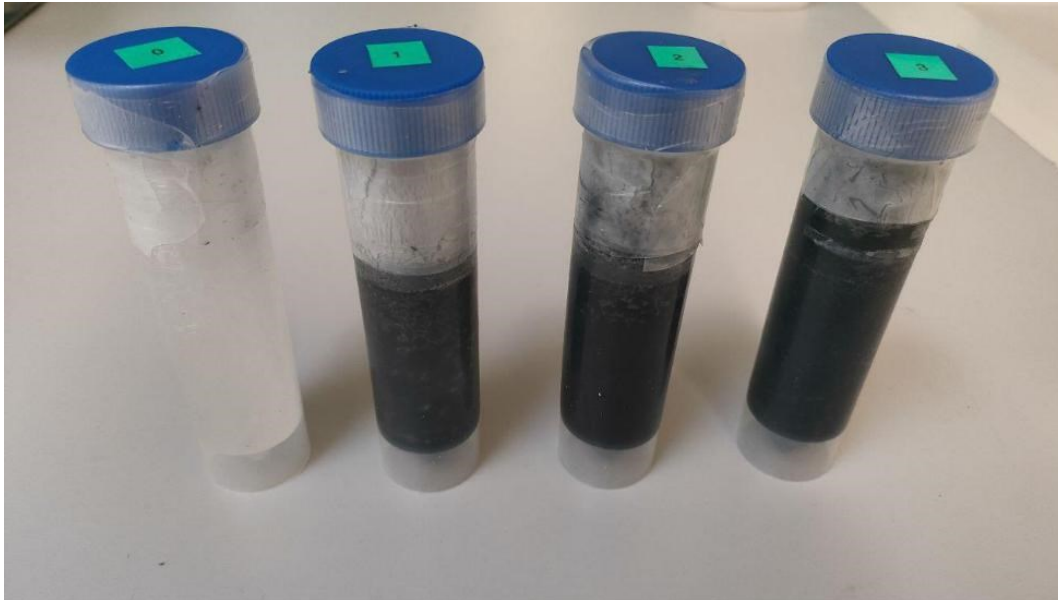


Fig. 7.2 - lab tubes with different % of graphene

To measure the thermal conductivity was used a **Thermtest portable MP-2** with the sensor **THW-L3** appropriate for liquids, pastes and powders.

The specifics of that sensor are the following:

materials	Liquids, Pastes, and Powders
Measurement capabilities	Bulk Properties
Thermal conductivity	0.01 to 1 W/(m K)
Measurement time	1 second
Reproducibility	± 2%
Accuracy	± 5%
Temperature range	10 to 40 °C
Minimum sample size	15 ml
Standards	ASTM D7896-19

Tab. 7.1 - specifics of THW-L3 sensor



Fig. 7.3 & 7.4 - instrument for thermal conductivity measurement

Since increasing the percentage of graphene the sensor gives some problems, we use also another one: the **TLS 150 mm**, which characteristics are:

materials	Soils, Pastes, Powders, and Solids
Measurement capabilities	Bulk Properties
Thermal conductivity	0.01 to 3 W/(m K)
Measurement time	3 minutes
Reproducibility	± 2%
Accuracy	± 5%
Temperature range	-40 to 100 °C
Minimum sample size	150 mm in length, 50 mm in diameter
Standards	ASTM D5334, IEEE 442-2017

Tab. 7.2 – specifics of TLS 150mm sensor



Fig 7.5 – Thermtest MP-2 with TLS 150 mm sensor

In fact, the tests were done immersing the sensor after bringing the solution to a temperature lower than 40°C (otherwise the instrument would give an error).

The entire measurements takes less than a minute if we use the THW-L3 sensor and some minutes using the MP-w.

At the end of the measurements the value of thermal conductivity appears on the display.

According to these tests, the increase in thermal conductivity doesn't follow a linear proportionality with the % of graphene, but higher is the % of graphene higher is the increase in thermal conductivity.

We carried out the first 6 percentage of graphene with experimental tests findings the results that are shown in the table below. The remaining values, from 4% to 10% were interpolated in excel following an exponential function and a polynomial one respectively and is noticeable that the differences become quite big:

%grafene	λ [W/(m K)]	λ [W/(m K)]
0	0.146	0.146
0.41	0.168	0.168
1.05	0.225	0.225
1.46	0.273	0.273
2	0.38	0.38
3	0.55	0.55
4	0.889	0.800
5	1.405	1.099
6	2.221	1.453
7	3.510	1.860
8	5.546	2.322
9	8.764	2.837
10	13.850	3.407

Tab 7.3 - thermal conductivity for different % of graphene

But it was noticed experimentally that already at 3% of graphene, the solution become a paste very dense to such an extent that the external recirculation pump probably will not be able to move it.

So, even though we chose to not overcome 3% of paraffin, it means that we more than triplicate the conductivity of the pure paraffin and so we expect that also the power and energy increase quite significantly.

To have a more accurate results for the conductivity, we carried out some tests also with the **HotDisk TPS 1000** and for the paraffin enhanced with 3% of graphene we obtain a conductivity of **0.68 [W/(m K)]**.

The main specifications of that instrument are the following:

Thermal conductivity	1 to 500 W/(m K)
Measurement time	2.5 to 2560 seconds
Reproducibility	Typically better than 1%
Accuracy	Better than 5%
Temperature range	-100 °C to 750 °C

Tab. 7.4 - specifics of HotDisk TPS 1000 instrument



fig. 7.6 - HotDisk TPS 1000

Since the graphene that we have available is quite coarse, we “minimize” it using a **Fisher Scientific sonic dismembrator FB-505** and a **Julabo shaking bath**.



Fig. 7.7 & 7.8- Julabo vibrating plate and sonicator FB-505

The Julabo is quite old, so we don't have a technical datasheet about it. Instead, here are reported some data about the sonic dismembrator FB-505:

Wattage [W]	500
Voltage [V]	220/230
Hertz [kHz]	20 (ultrasonic frequency)
Volumetric range [ml]	0.2 to 1000
Pulse mode	1 to 59 seconds

Tab. 7.5 sonic dismembrator FB-505 specifics

In the figure below is possible to see some differences. In fact, at 1% the mix appears more liquid while in 3% it's more like a paste and seems that is possible to add few or no more graphene at all.



Fig. 7.9 - different consistency with 1% and 3% of graphene

Chapter 8.

Enhancement of performance with 1.5% of graphene

It was decided to start with a 1.5% by weight and then move to 3%.

The graphene addition process was not carried out in a single operation but was done by taking about 0.4 kg of paraffine out of the HE, then gradually adding the graphene while sonicating it, until the 1.5% by weight is reached.

The 1.5% graphene solution was put in another container and the same procedure was done for all the rest of the paraffine.

Then, from the valve placed on the top of the HE the solution was filled in.



Fig. 8.1 - The discharged system



Fig. 8.2 - Filling with 1.5% graphene solution

During the discharge/charge processes some paraffin was lost and so the effective mass filled in at 1.5% was 8.3 kg.

Before filling the system with the solution, several conductivity tests were done. The mean calculated thermal conductivity results in 0.375 [W/(m K)]. So, since the thermal conductivity of the pure paraffine was also measured and equal to 0.16 [W/(m K)], already with 1.5% of graphene the thermal conductivity was more than doubled.

8.1 Solidification with 1.5% graphene

The test was carried out in the same boundary conditions as the case with the pure paraffin.

To have a first rough estimation, in this case the last TC reach 25 °C after 2 hours and 58 minutes, so the process becomes faster (in the pure paraffin case this happens after 4 h 33 min).

Since the solution is totally black and opaque, differently from the reference case now is not possible to see the solidification process that start from the coil and expand.

8.2 Comparison with reference case

Let's see the power trend comparison between the case with pure paraffin and the one enhanced with 1.5% of graphene in the first 6 hours:

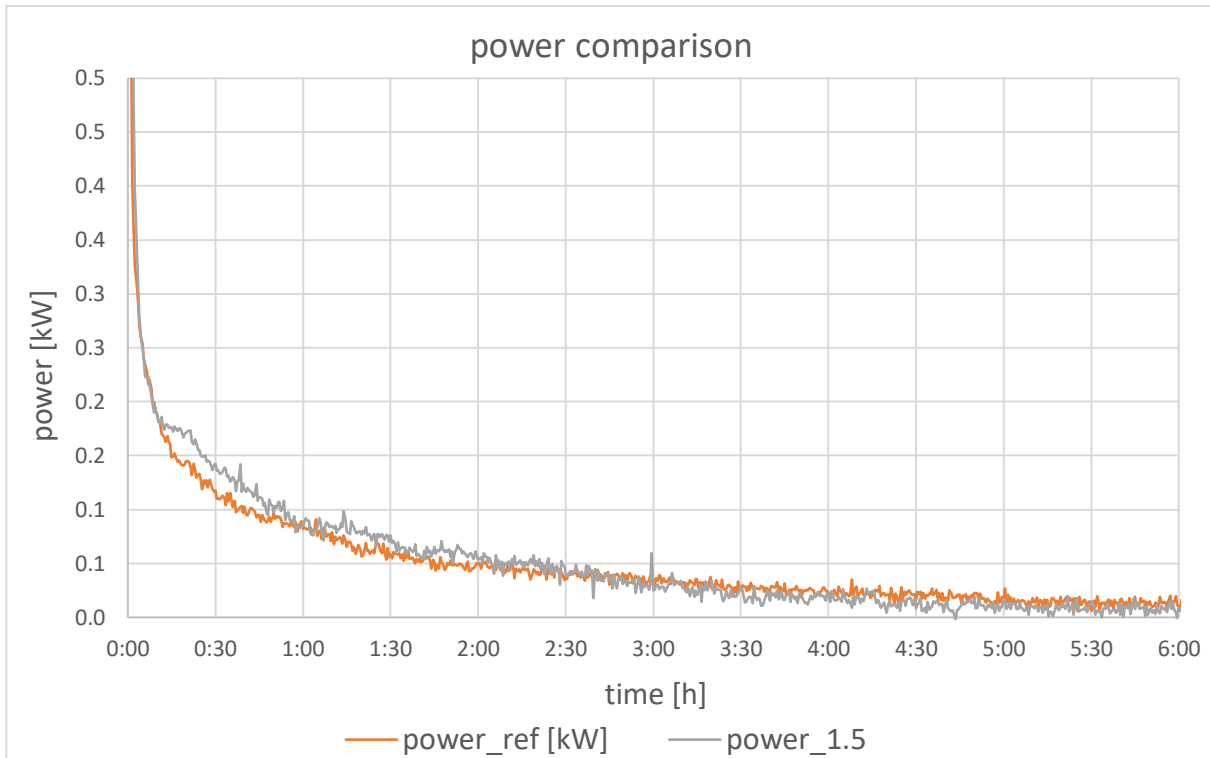


Fig. 8.2.1 – power comparison – pure PCM VS 1.5% graphene

In the first hour of solidification the mean power increases by 9%. In general, one can notice an improving especially in the first two hours, then the latent heat is exploited in both cases and the differences are quite negligible.

We can also see the improvement in solidification in terms of energy.

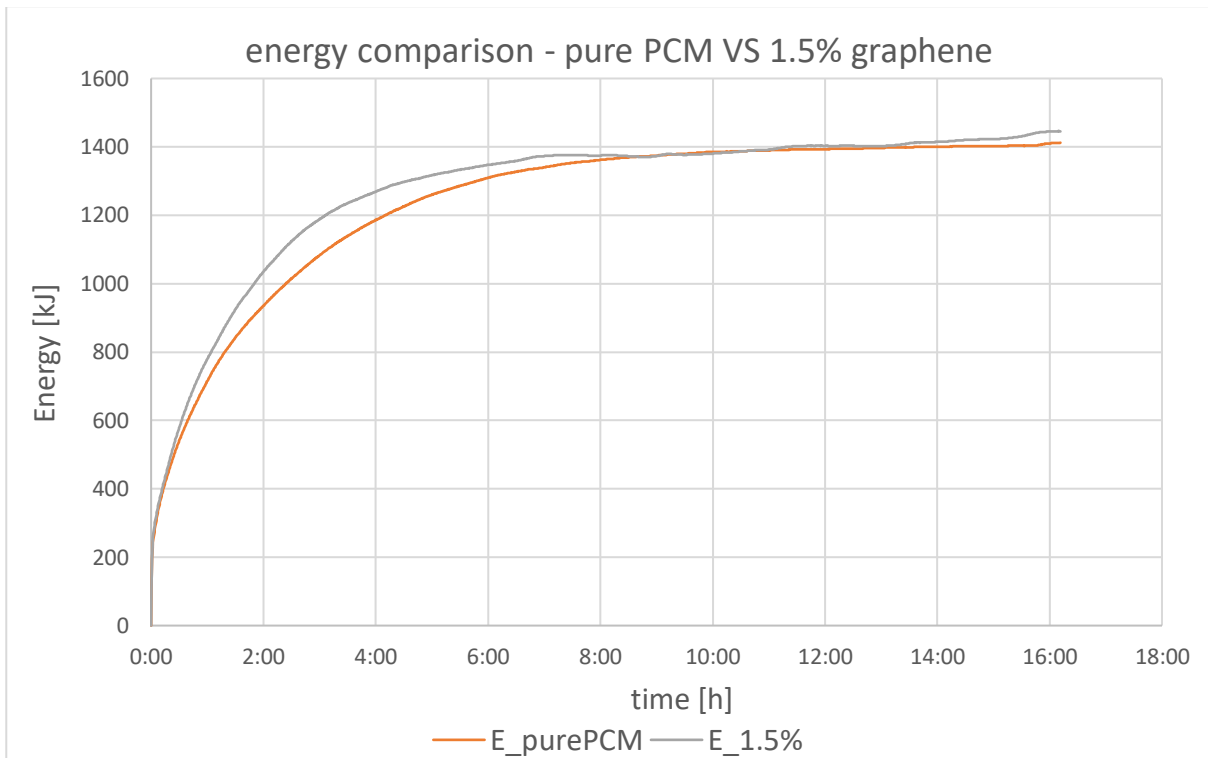


Fig 8.2.2 – energy comparison pure PCM VS 1.5% graphene

In the first hour we have an increasing of 8.7% in terms of energy.

Instead, after 3 hours the energy is increased of 9.8%.

But the most important achievement is in the velocity of the system:

For example to reach 1200 kJ (0.33 kWh) the system require 1 hour 4 minutes less than the case with pure paraffin, it means 34.4% less time. Which is not a bad result.

One can also see that the process becomes faster looking at the same TC temperature variation during the process in the same moment.

In fact, usually each TC (in the graphene enhanced case) reaches a specific temperature some time before the same TC in the reference case with the pure paraffin.

Moreover, also the initial slope of the curve is greater in the case with graphene. Is possible to see all this thing in some figure reported below:

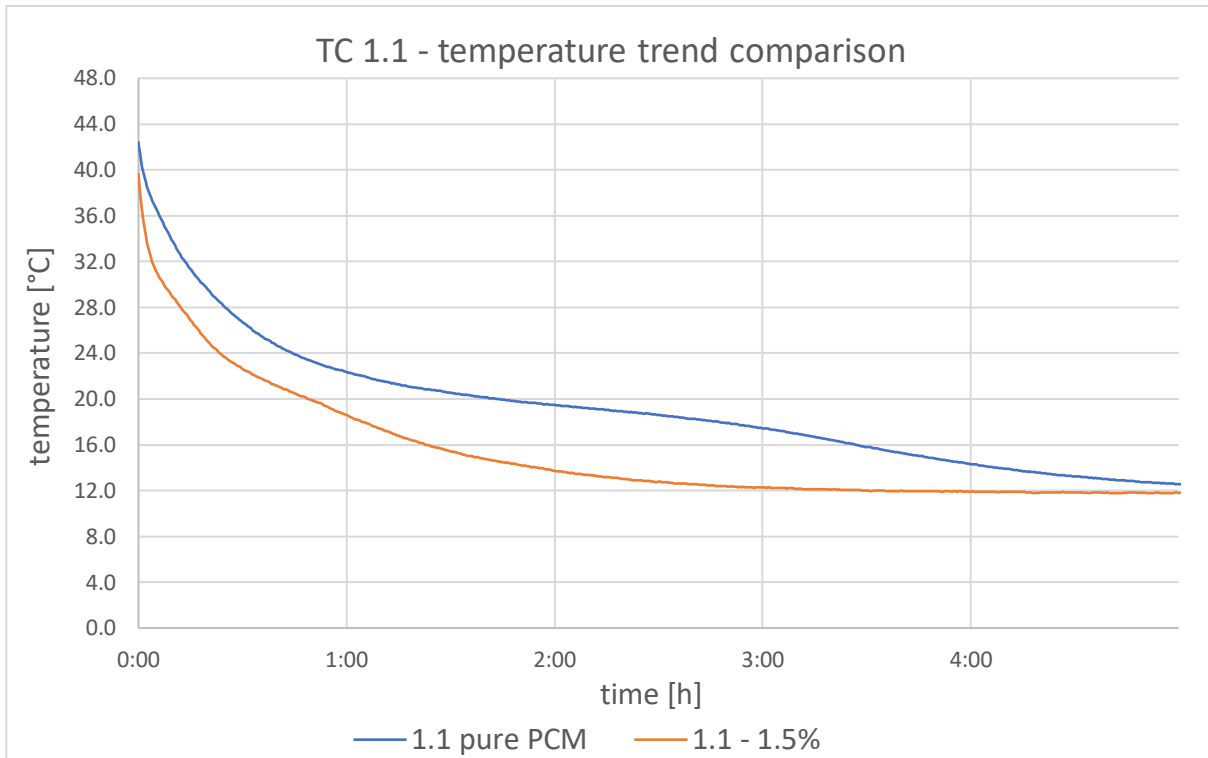


Fig. 8.2.3 - TC 1.1 temperature comparison

It is possible to see clearly that initially the temperature drop is greater thanks to the higher thermal conductivity. In this case for example, the 1.1 TC in the graphene enhanced PCM reach the melting temperature about 13 minutes before the reference case. This is a quite little improvement, but we must consider that those TC is basically attached to the coil and therefore the conduction phenomenon improvement is not yet appreciable.

The “thermal shock” is quite big and so the PCM solidify quickly making difficult to see the phase change in the temperature-time graph.

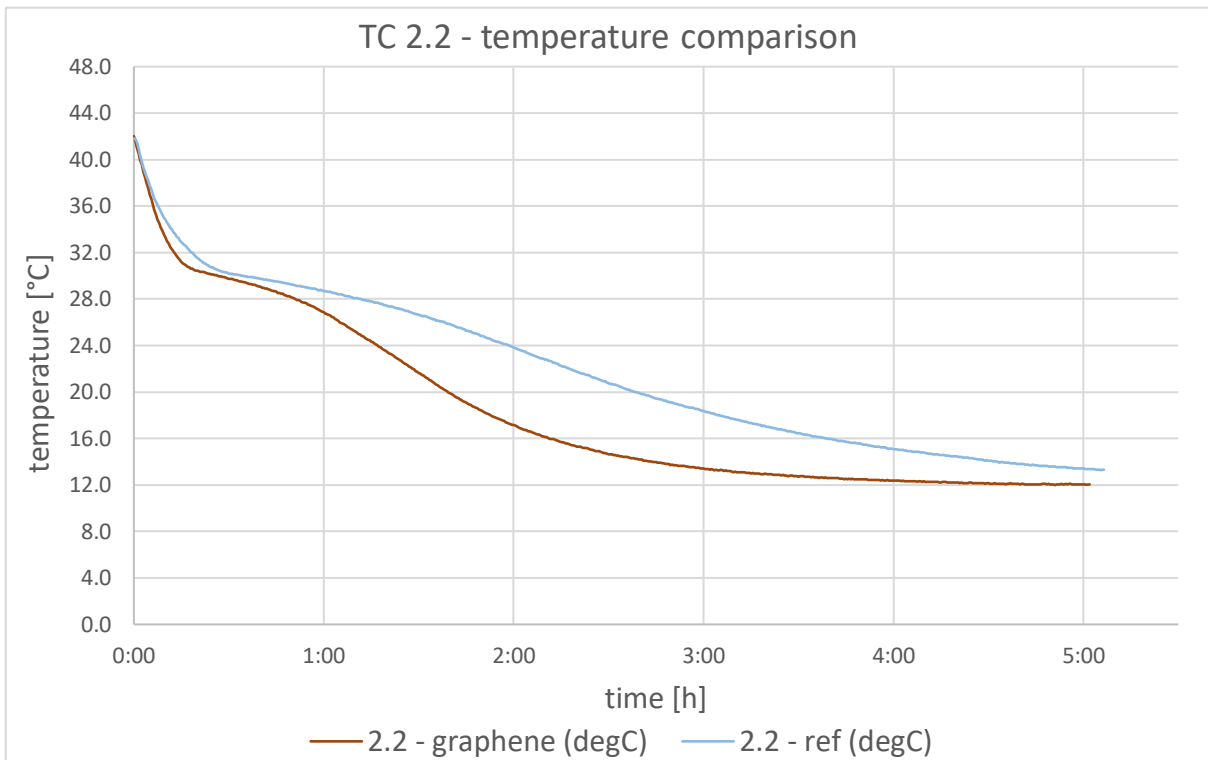


Fig. 8.2.4 - TC 2.2 temperature comparison

As already said the trend is the same and the case with graphene reach the melting temperature always before the reference case.

Differently from the case above, since the TC 2.2 is further away from a cold coil respect to the previous TC (the 1.1 which was close to it), it reaches the melting temperature after about one hour from the beginning of the cooling (the TC 1.1 reaches it about 30min after the beginning). Comparing those TCs in the 2 cases, with the graphene it reaches the melting temperature in 36% less time than the case with pure paraffin.

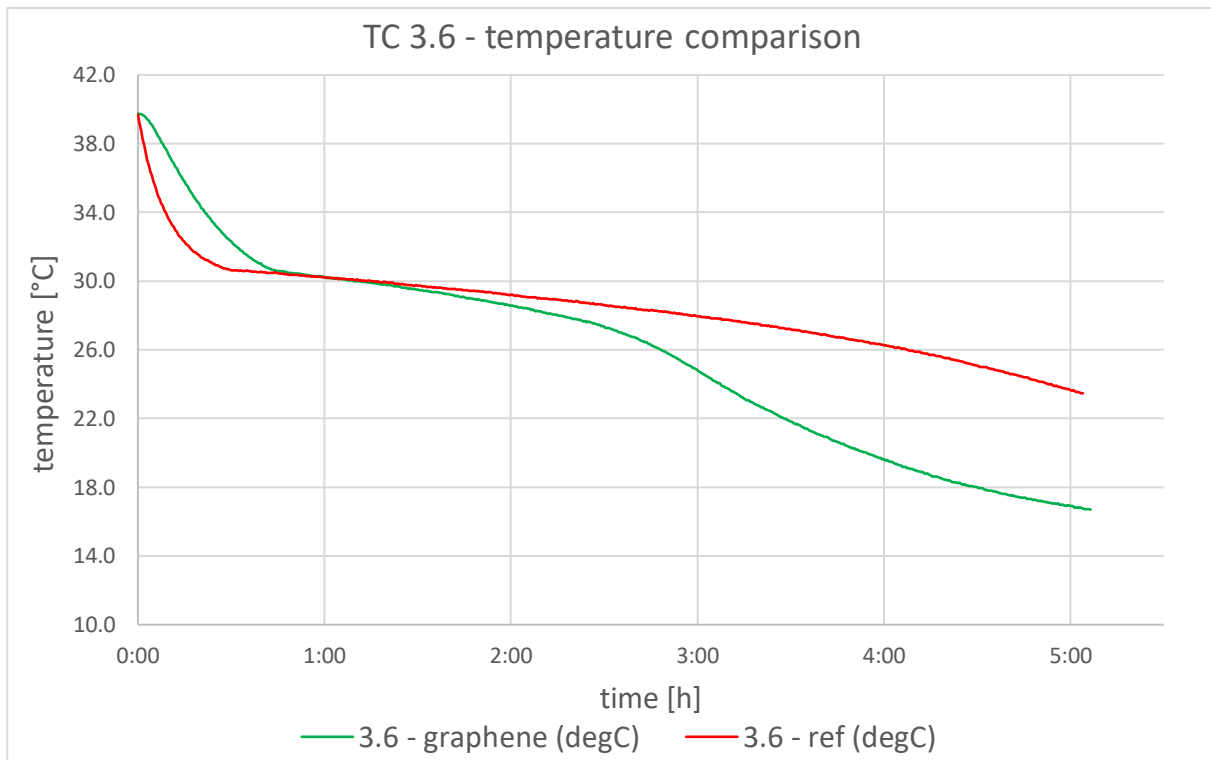


Fig. 8.2.5 - TC 3.6 temperature comparison

The TC 3.6 is the last TC that reaches the 25 °C in both cases, and as already said, the difference between the two cases is almost one hour and a half.

In addition, it is interesting to see that around 28 °C, which is the melting temperature, we can see what probably represent the phase change. In fact, around that temperature the slope change and the curve become flatter for the time necessary for the phase change, and then the slope increase again when the sensible cooling start.

For completeness we can also see the trend of the temperatures in the same height level which is useful to see that the solidification starts first at the pipe (so at TCs in position 1 and 4) than at the other closer to the supply pipe (positions 3 and 5) and finally in the more distant ones (positions 2 and 6).

Let's see for example the level 3 (note that all the levels present the same trend):

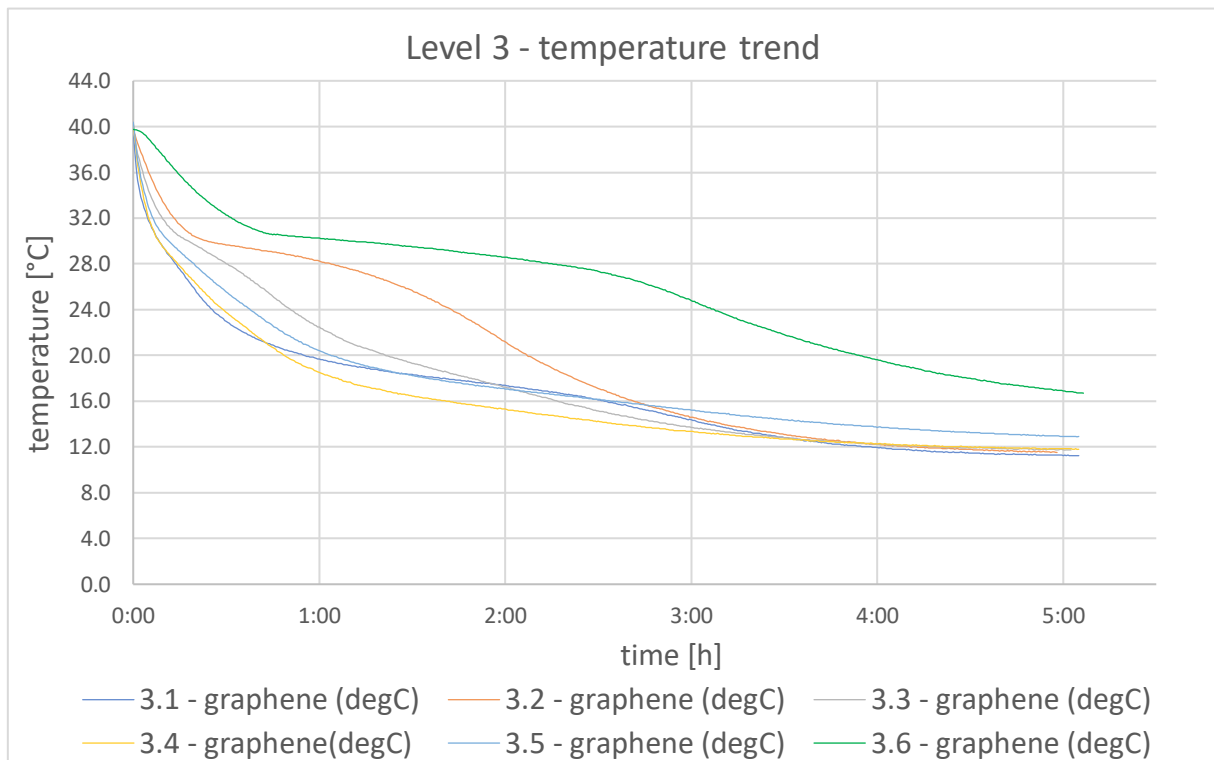


Fig. 8.2.6 – level 3 temperature trend

8.3 melting

Differently from the case with the pure paraffin, in which the melting process was considered completed when there was no PCM remaining at the bottom of the HE, now since the solution with graphene is completely black this is clearly not possible, so we rely mainly on the temperatures detected.

Although it is expected an improvement of the performance also in melting, looking at the temperatures, sometimes the opposite occurred.

To prove this, let's have a look on the last TC that reaches 30 °C, i.e the 5.6:

- In the reference case the TC 5.5 reaches 30 °C after 1 hour 32 minutes
- In the case with graphene this happens after 2 hours 42 minutes

More than one hour later!

But this is not the worst result; other TCs like the 3.6 reaches 30 °C 1 hour 30 minutes later in the case with graphene respect to the reference case with pure paraffin.

Fortunately, this happens mainly at those TCs near to the external wall, which are more influenced by the external environment. By the way, the performance doesn't improve as one could expect and at the beginning this was a very weird result.

It was discovered that the reason for these results is that voids are created during the solidification process. One cause could be that the PCM in solidification reduces its volume while the graphene remains stable. This graphene thanks to its 3 dimensional structure can decrease the phase change mobility of the PCM and this interaction causes the formation of this vacuums. These vacuums act as an insulant. In fact, if the hot coil is not directly in contact with the PCM, the latter will not begin to melt.

On the other hand, if the hot coil is in contact with vacuum, this vacuum must be heated first and the PCM begins to melt late.

The doubt about the presence of voids within the solid came from noticing cracks on the surface of the solid as we can see in the following pictures:



Fig. 8.3.1 & 8.3.2 - appearance of the solid paraffin surface

As proof of this, it was tried to cut a small block of paraffin whose solidification took place more smoothly in a freezer (i.e. in a cold environment). This is what was found inside this block of paraffin:



Fig. 8.3.3 & 8.3.4 - presence of voids inside the solid paraffin

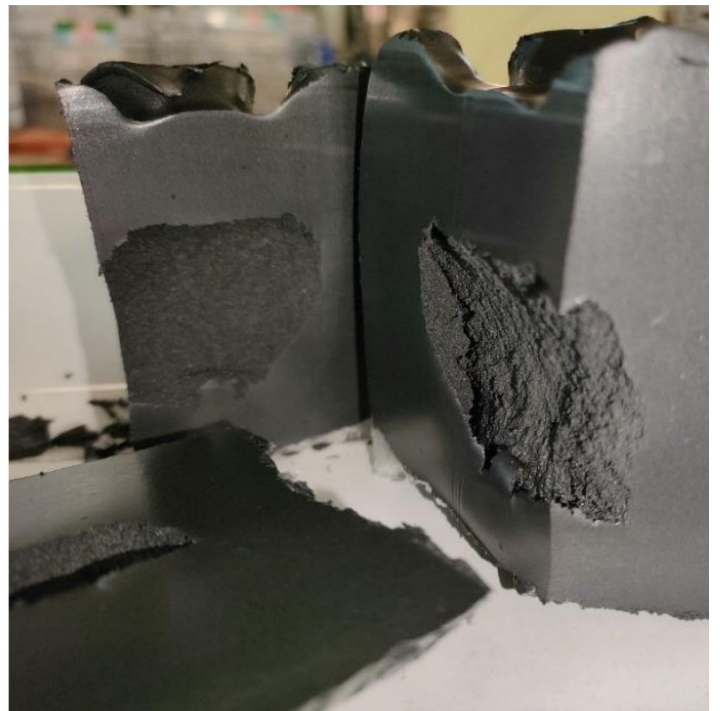


Fig. 8.3.5 & 8.3.6 - presence of voids inside the solid paraffin

The solidification inside the heat exchanger will be quite different respect to this one occurred in the freezer. In fact, we have a cold coil directly in contact with the hot PCM ($\Delta T = 34\text{ }^{\circ}\text{C}$), so the heat transfer phenomena will be different and probably also the solidification. But unfortunately, is impossible to see anything inside the HE and it's not possible to check whether any differences are present.

8.4 Comparison with reference case

Let's see the instantaneous percentage increase in the power during melting respect to the reference case in different moment of the process:

in the first 3 hours, the average power in the case with 1.5% of graphene is 3% higher than in the reference case with paraffin alone.

Melting temperature tends to be reached earlier in high levels in the case with graphene respect to the reference case. Moreover, the melting temperature tends to be reached earlier in the centre of the cylinder and later in the outer part.

Let's see some graphs that show this:

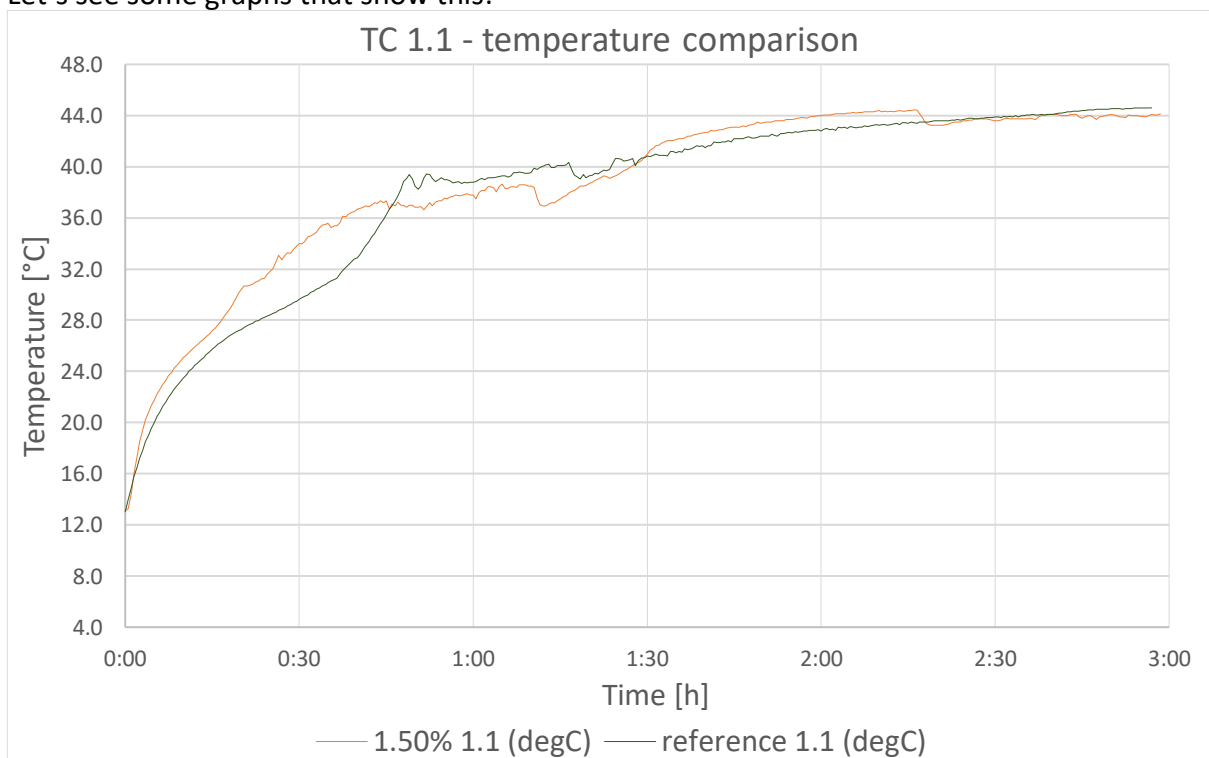


Fig. 8.4.1 – TC 1.1 temperature comparison

One can see that the melting process for this TC becomes faster; in fact, the melting temperature is reached 8 minutes earlier respect to the case with pure paraffin, i.e 32.7% less time

Another example that shows the faster melting rate in the high levels and near the centre of the cylinder could be the example of the TC 2.2:

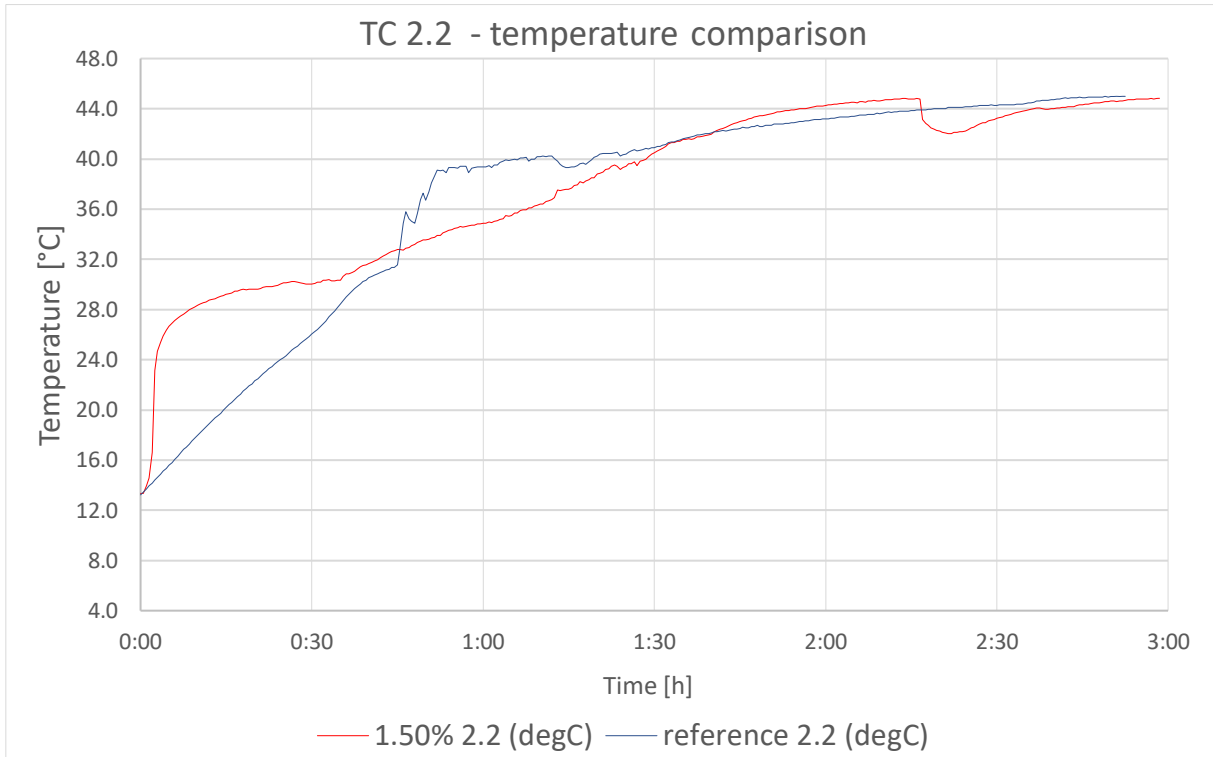


Fig 8.4.2 - TC 2.2 temperature comparison

In this case the difference is very impressive, in fact the case with graphene is much faster. Those TC reaches the melting temperature 32 minutes before respect to the same TC in the reference case with pure paraffin.

The trend tends to revers moving downwards and towards the outer walls. Let's see for example the TC 3.3:

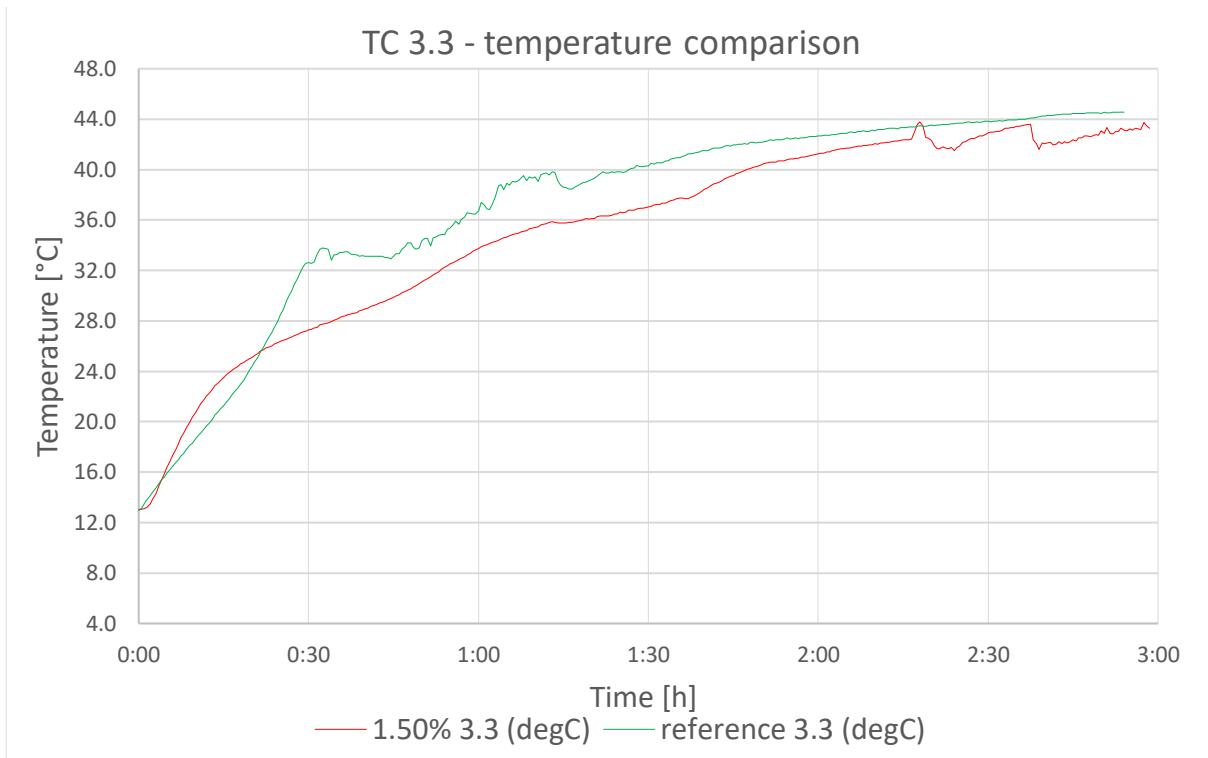


Fig 8.4.3 - TC 3.3 temperature comparison

In the figure above one can see that the initial slope of the graphene enhanced test is higher like in the previous cases, but then the slope change and it reaches the melting temperature after the reference case (about only 4 minutes later in this case).

In the position 5, instead, except for the highest level, the melting temperature is reached almost at the same time (less than 2 minutes difference) both for the reference and the graphene enhanced case. As an example, here is reported the case of the 5.5 thermocouple:

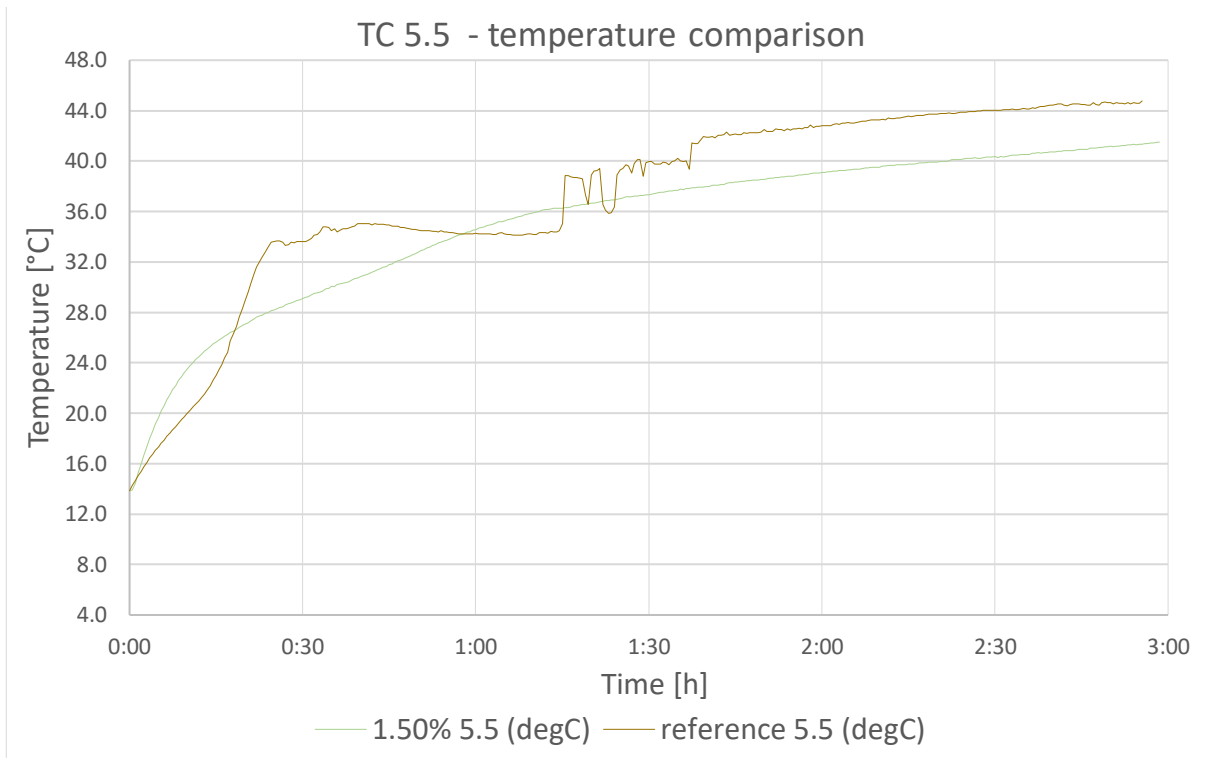


Fig 8.4.4 - TC 5.5 temperature comparison

The trends are basically the same as the previous figure (8.4.3). A thing that one can notice in almost all the graphs is that in the tests with graphene, the lines are more linear and smoother. This could be because the solution with graphene has a higher viscosity respect to the pure paraffin and so the convective action of the small aquarium pump is less present.

A completely different trend can be seen in all the TC in the outer position (position 6).

In the level 1 and 2 the trends are similar but the reference one is faster:

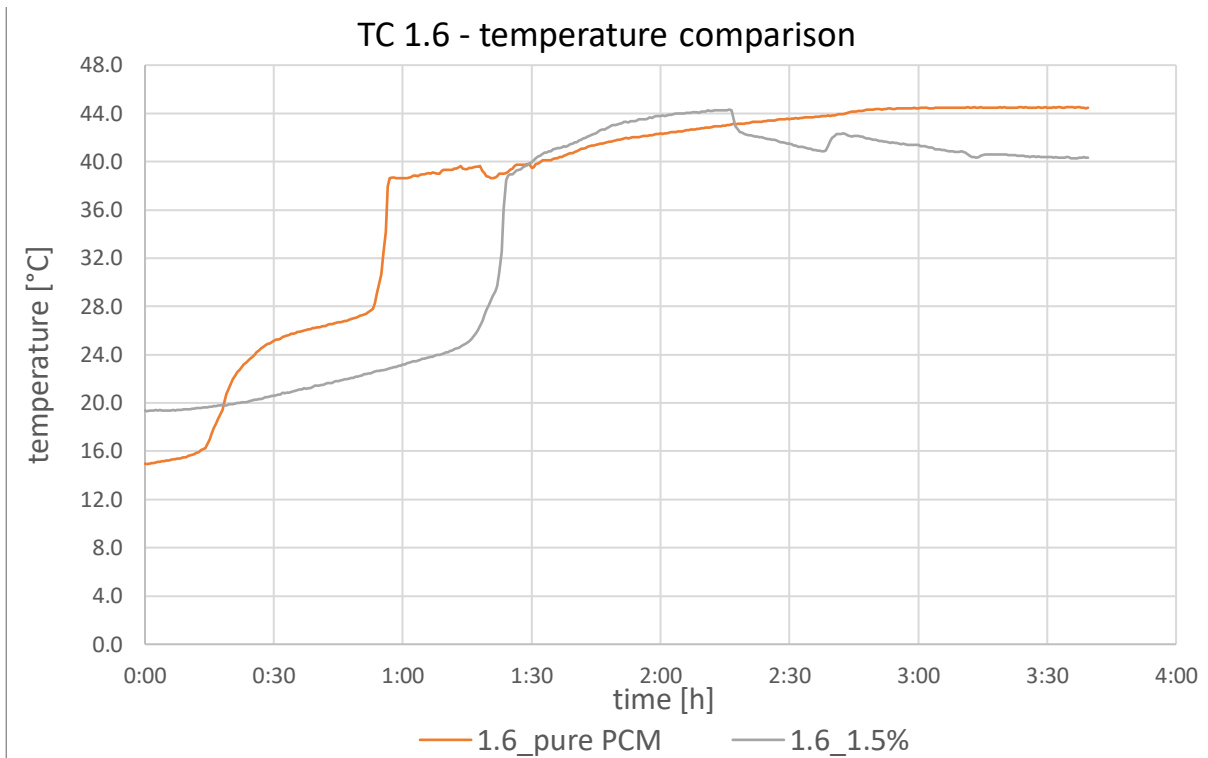


Fig. 8.4.5 – TC 1.6 temperature trends

The test with paraffin + graphene reaches the melting temperature about 27 minutes later than the one with only paraffin.

Even more extreme is the case of thermocouples in position 6 in levels 3 to 5. In those cases, the phase change is perfectly visible and takes more than 3 hours to take place as we can see in the following figure:

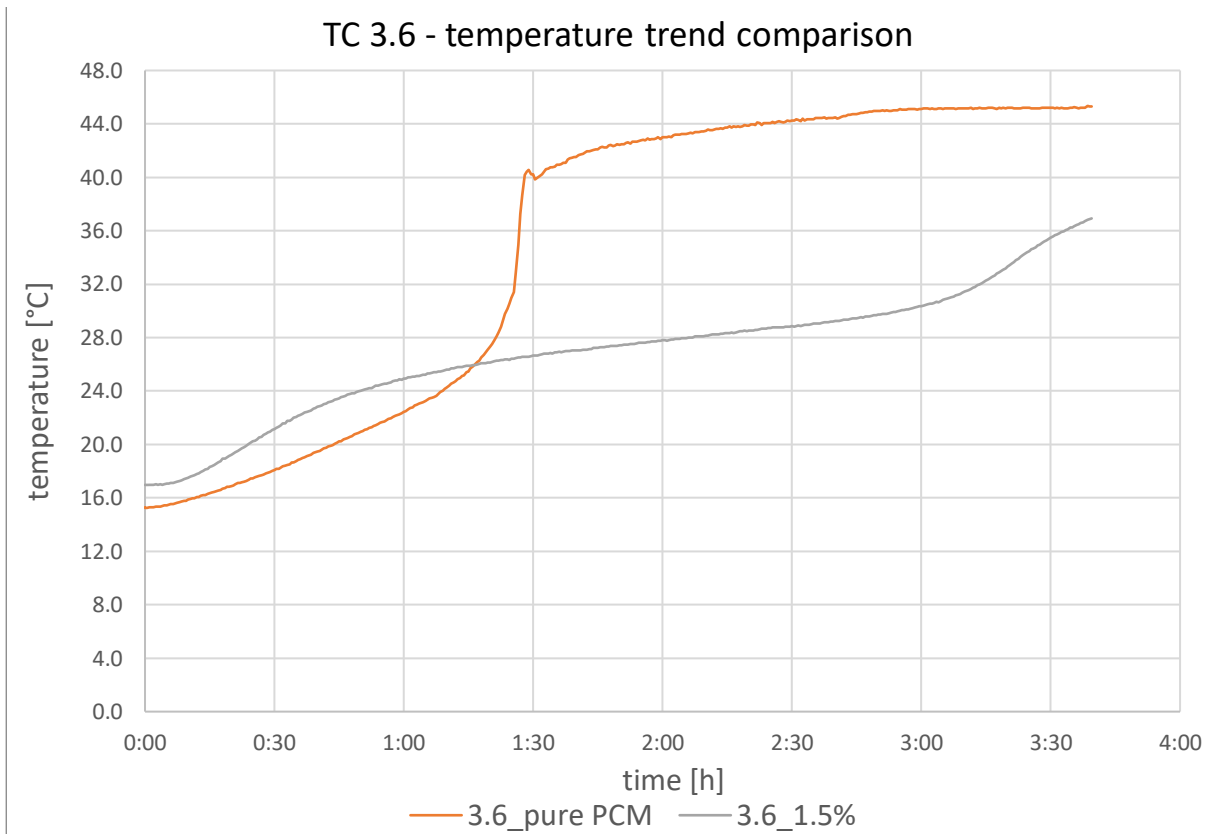


Fig. 8.4.6 – TC 3.6 temperature trend

Note that the only small difference in the two cases is the ambient temperature since for the case with graphene is 0.7 °C less as average in the entire process, but this doesn't justify such a different behaviour.

Note also that the graphs during melting process are not smooth like the one in solidification and moreover can change a little bit each time due to the possible differences in solidification and so in the void formation.

Let's see the energy comparison between the pure paraffin and the enhanced one.

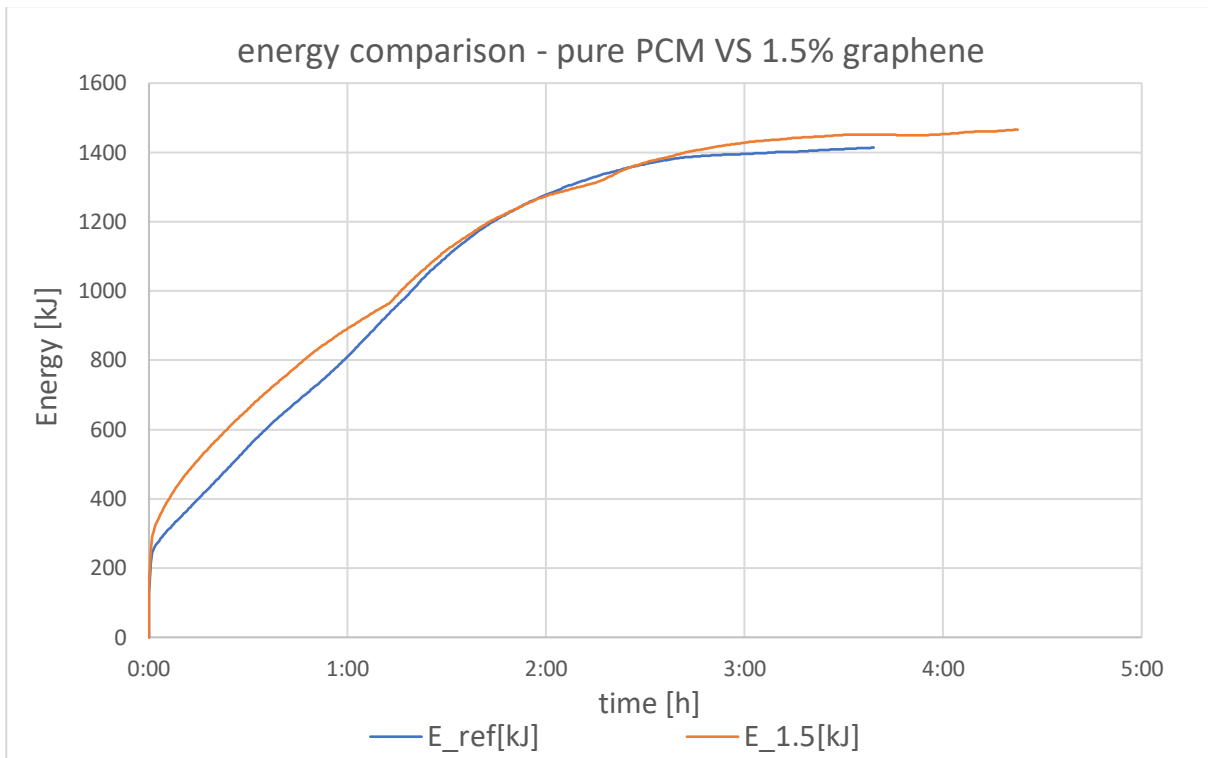


Fig. 8.4.7 – energy comparison in melting with 1.5% of graphene

It is possible to observe that the differences are quite limited, but anyway in the first hour in general the melting process becomes faster.

In fact, to reach an energy of 600 kJ it takes 12 minutes less passing from 36 to 24 minutes, i.e. 33% less time than the reference case.

Moreover, after one hour the system with 1.5% of graphene exploited 10.3% more energy than the reference case with pure paraffin.

Chapter 9.

Enhancement of performance with 3% of graphene

As before, during the addition of graphene, some paraffin was lost and so 7.5 kg at 3% were added at the end.

Before putting the 3% solution into the HE, some conductivity tests were carried out.

As we already said, the thermal conductivity of the paraffin with 3% of graphene measured with the *HotDisk* is almost $0.68 \text{ W}/(\text{m K})$ which is more than four times bigger than the one measured for the pure paraffin (which was $0.16 \text{ W}/(\text{m K})$)

We tried also to do measurements on the solid paraffin with 3% of graphene with the *Thermtest Portable* instrument with the *MP-2* sensor, and the conductivity results was $0.15 \text{ W}/(\text{m K})$. This probably indicated that there were voids in the solid (otherwise there was no other explanation), which would be a further explanation for the worsening of the melting process.

To verify that, again the solid paraffin was cut in a half in which the conductivity sensor was inserted, and this is what was found:



Fig. 9.1 - void created in solidification

9.1 Solidification

The behaviour in solidification improves further. Indeed, the temperatures are reached earlier respect both the reference case and the case with 1.5% of graphene.

First, let's see graphically the trend comparison of the power respect to the reference case and the 1.5% case:

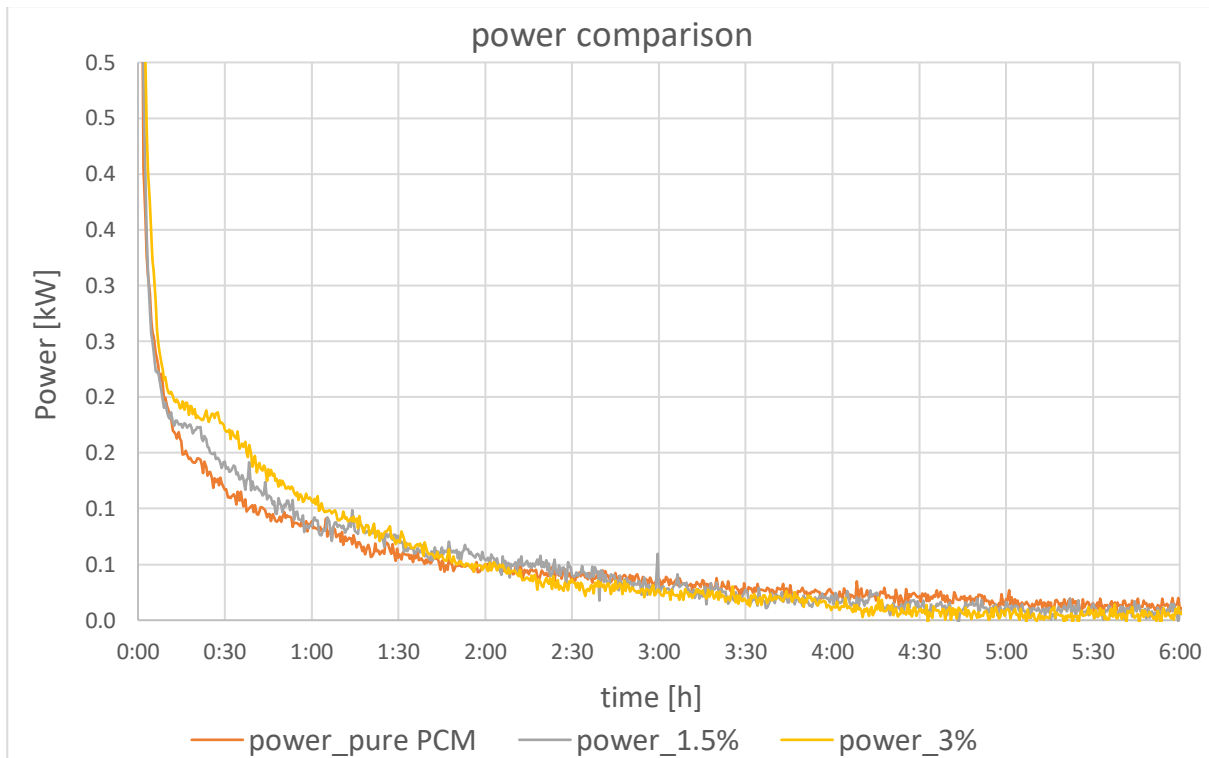


Fig 9.1.1 – power comparison

One can see that the thermal power increase, in fact especially at the beginning (in particular in the first one hour 30 minutes) the power in the case with 3% of graphene is higher due to the greater heat exchange because of the increased thermal conductivity of the paraffin.

It is possible to see for example that in the first 30 minutes the mean power of the system passes from 0.322 kW to 0.377 kW increasing by the 17%

The improving of the system can be seen also in terms of energy:

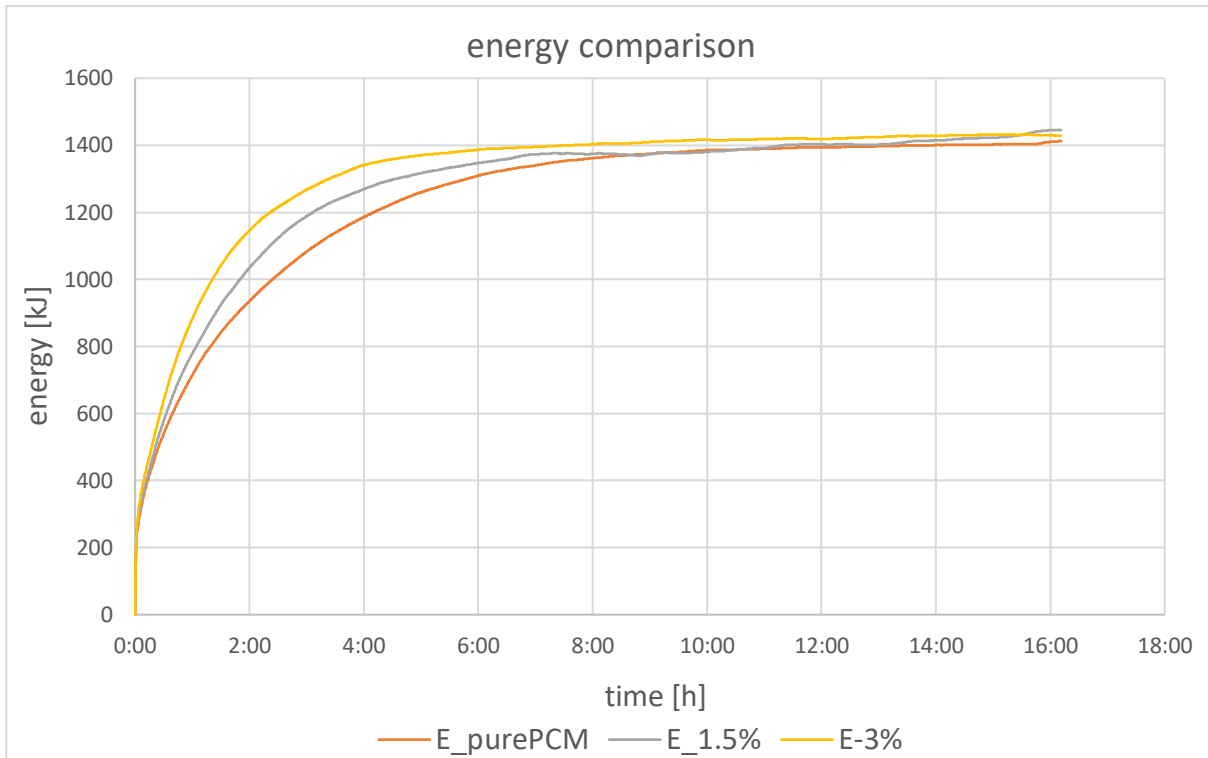


Fig. 9.1.2 – energy comparison in solidification, 3%, 1.5%, reference

It is evident that with 3% of graphene the system becomes even better.

In fact, for example, to reach 1200 kJ (0.28 kWh) in the case with pure paraffin it takes 4 hours and 10 minutes, while with 3% of graphene it takes 2 hours and 22 minutes. So, the system velocity improves by 76% which is a good result.

In addition, in the first hour, the system exchange 23.5% more energy passing from 715 kJ to 883 kJ.

Let's see some temperature trend comparison:

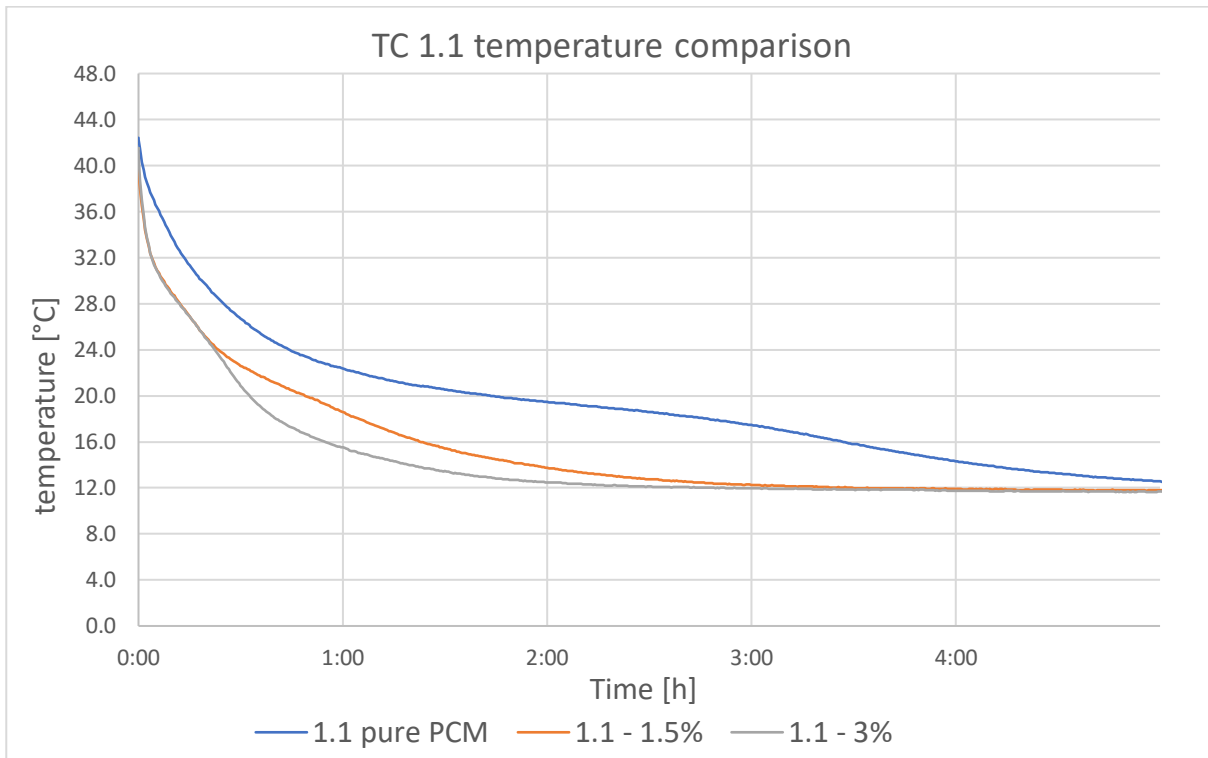


Fig. 9.1.3 – TC 1.1 temperature trend comparison

In this case, since this thermocouple is very close to the return coil, the difference between 1.5% and 3% is negligible until 24 °C, then the 3% paraffin cool down quite faster.

While the difference between the pure paraffin and the 3% enhanced is very evident: in fact, until 24°C the cooling rate is almost doubled, then for example to reach 20 °C the enhanced paraffin takes 3 times less than the pure paraffin case.

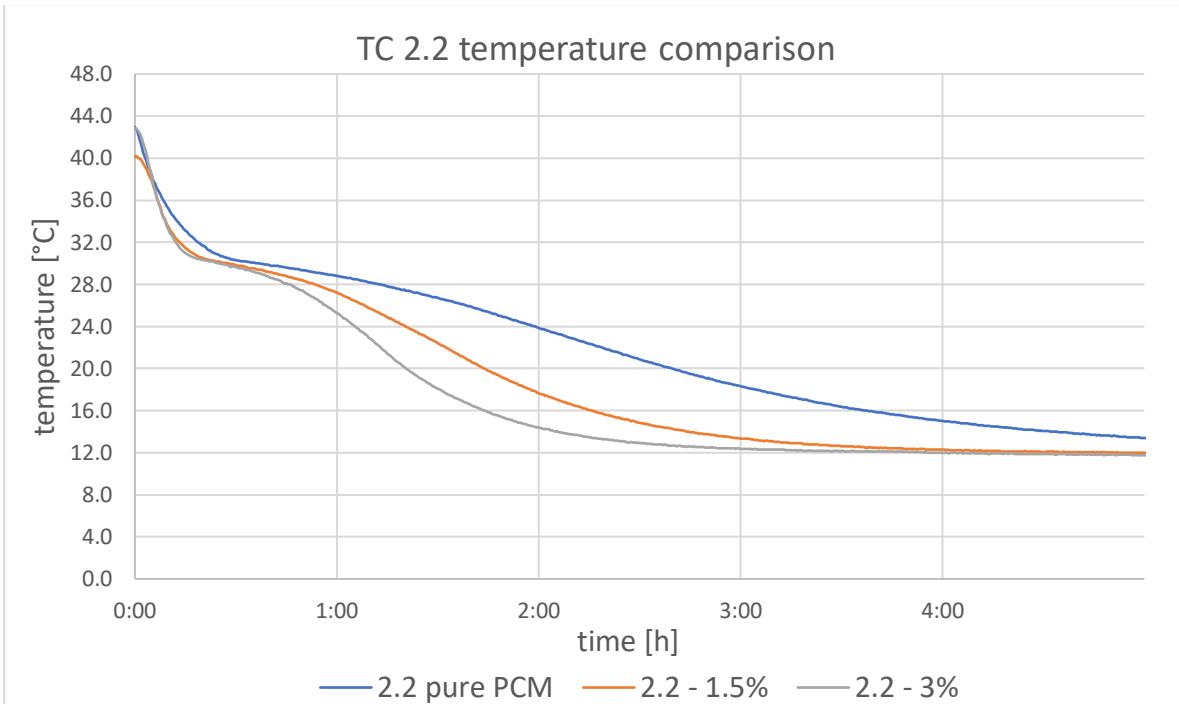


Fig 9.1.4 – TC 2.2 temperature trend comparison

The trend is similar also for this thermocouple and almost all the others.

In conclusion, after reach the melting point the differences between the pure paraffin case and the enhanced ones becomes much more evident.

As another example is now reported the trend for the thermocouple 3.3

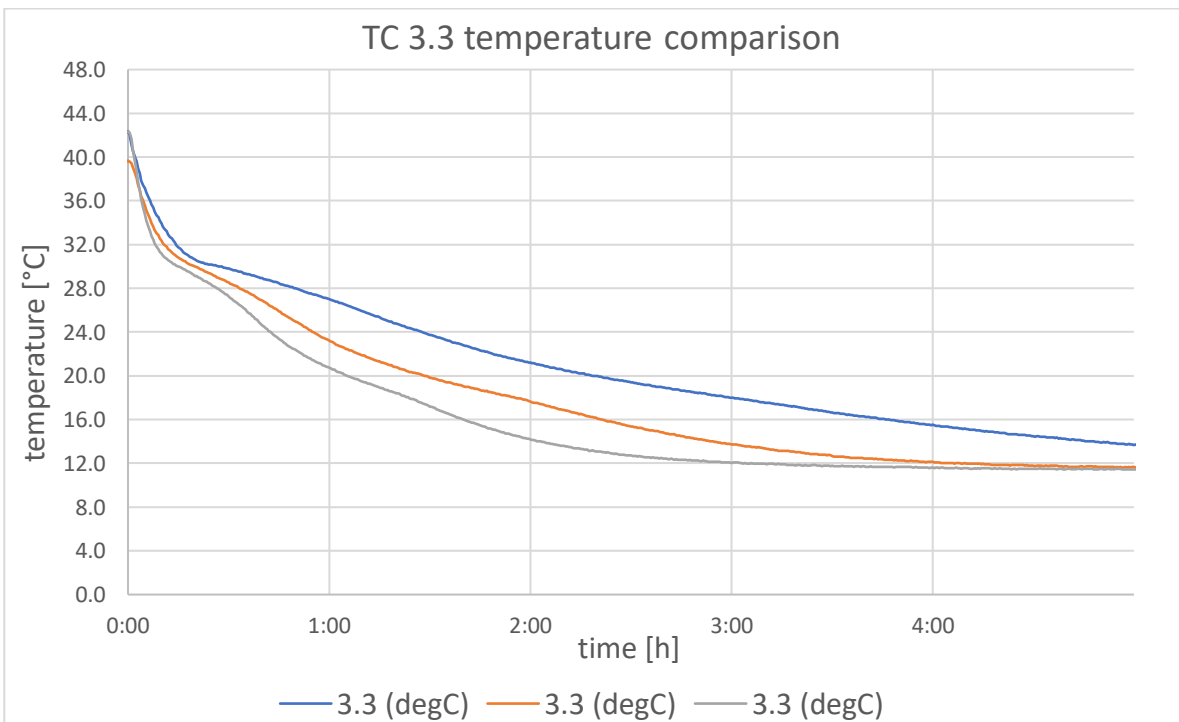


Fig 9.1.5 – TC 3.3 temperature trend comparison

9.2 Melting

Let's see the improving of the system in terms of energy.

As it happened in solidification, also in melting the system becomes faster thanks to the increased thermal conductivity:

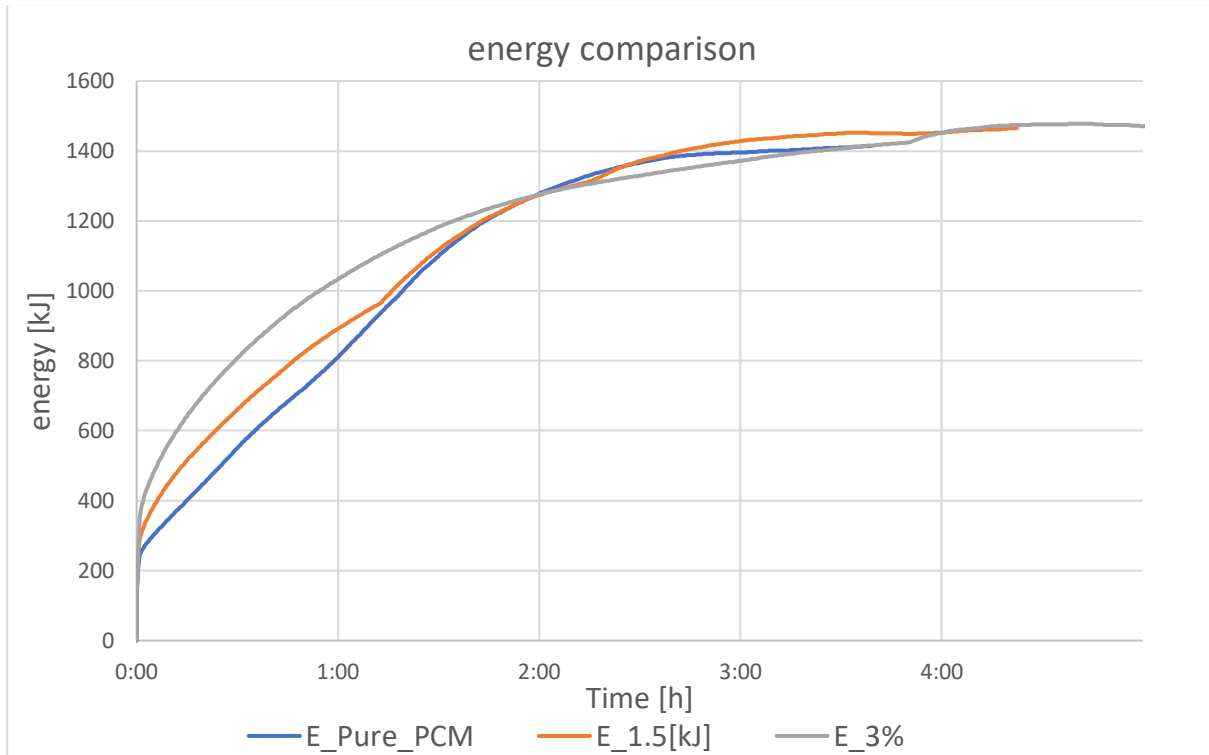


Fig. 9.2.1 – energy comparison between pure PCM, 1.5% and 3% of graphene

The improving is quite visible:

For example, to reach 800 kJ of energy the system with 3% of graphene takes exactly half time respect to the one with pure paraffin.

Moreover, after one hour, the system at 3% has exchanged 28% more energy than the reference case.

We can now look at some temperature trend comparison between the case with pure paraffin and the one with 3%.

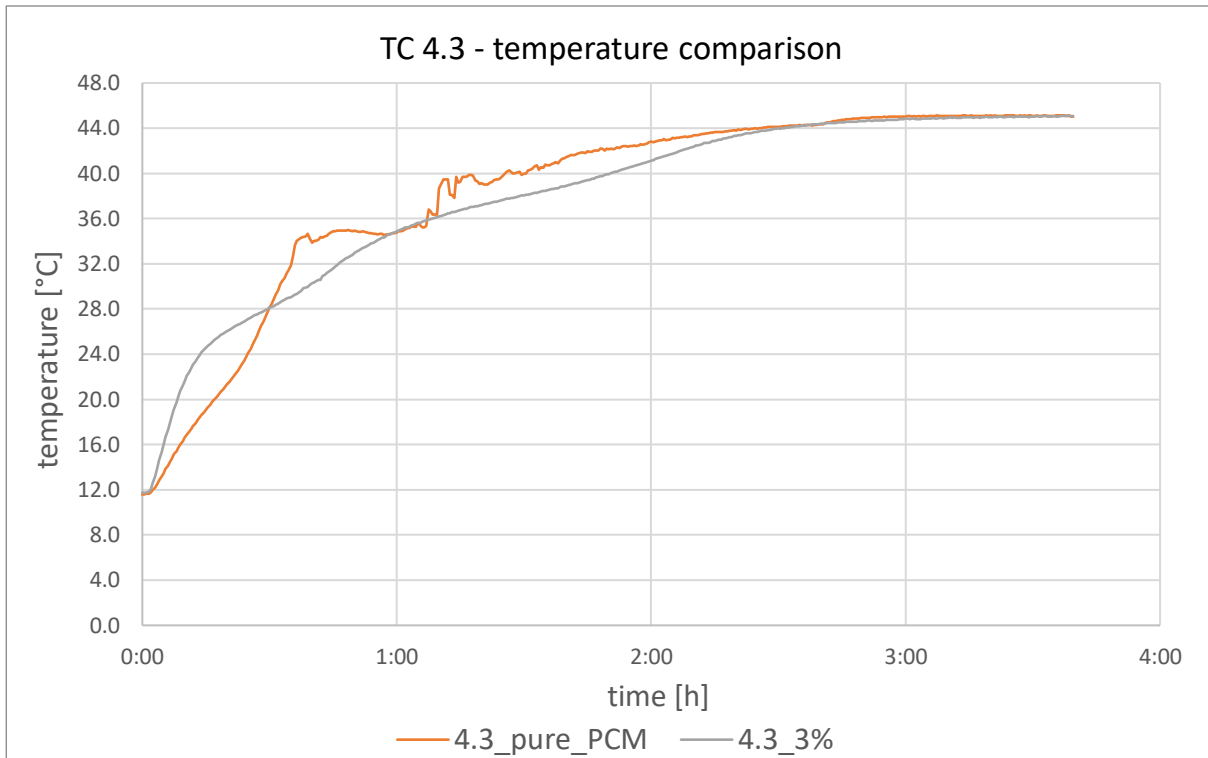


Fig. 9.2.2 – TC 4.3 temperature comparison

During melting as it has been seen, in the initial moment the heating is faster in the case of graphene respect to the reference one. But then the slope decreases, and it reach the melting temperature in the same instant than the case with pure paraffin.

According to what has been seen inside the solid paraffin, this could be due to the voids that are present inside the solid and which slow down the process.

Note that all the thermocouples behave like the one above and there is also the small difference consisting in the more convection given by the aquarium pump after one hour in the case with pure paraffin.

Chapter 10.

Graphene 3% enhanced VS Water

Since the 3% graphene case improves quite a lot the performance respect to the pure paraffin case, let's see in terms of power and energy which are the difference between the case with water and the case with 3% of graphene.

The theoretical energy of the system is a little bit higher for the PCM. In fact, as we already calculate, it results:

WATER: 1323 [kJ]

PCM: 1411 [kJ]

By the way, to make the 2 cases comparable, we also consider the water case operating with 8.5 kg of material and also, we consider also the same temperature range (i.e a ΔT of 30°C).

With this normalization, the theoretical energy of the system in operation with water becomes:

$$E_{\text{water_teo}} = 8.5 \text{ [kg]} * 4.2 \text{ [kJ/(kg K)]} * 30 \text{ [K]} = 1071 \text{ [kJ]}$$

10.1 Solidification:

Here is reported the power trend comparison:

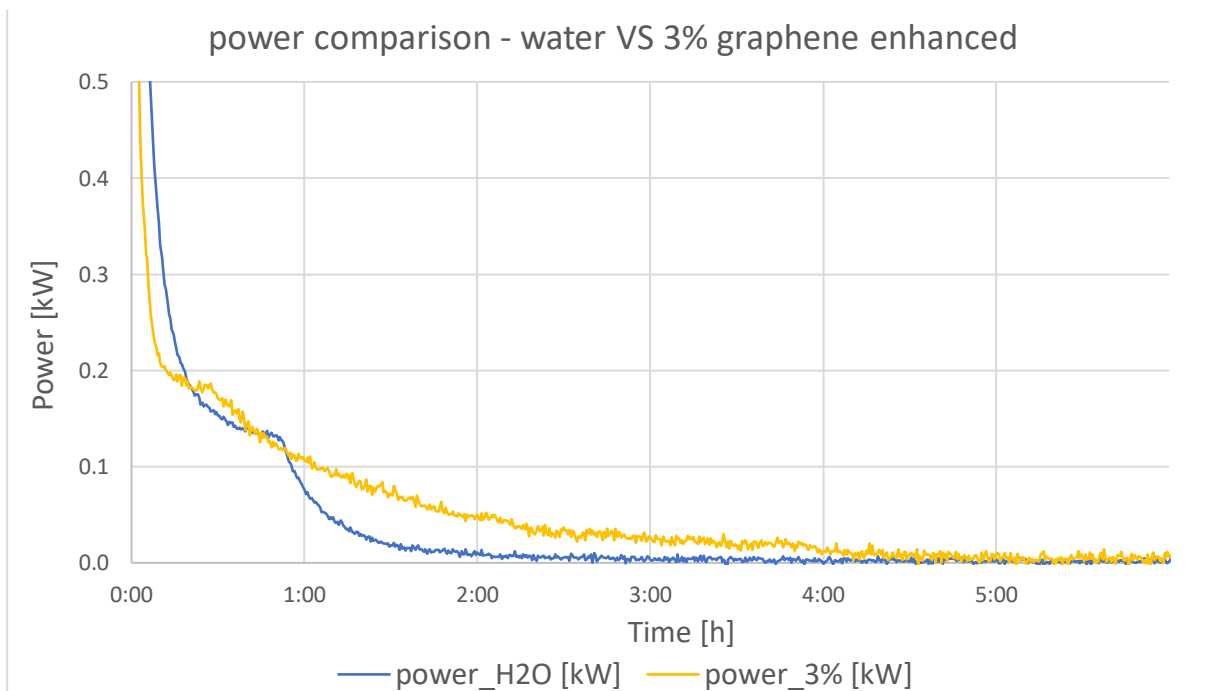


Fig 10.1.1 – power comparison, water VS 3% graphene paraffin

It's possible to see that basically from minute 20 to the end, the power of the graphene enhanced PCM remain higher that the water case.

It is possible to see that the *knee* is present also in the PCM curve although it is less evident. It is almost at minute 27 which is, as in the water case, the moment when the bath becomes able to maintain the fixed temperature of 11 °C (and so its power becomes greater than the system itself).

We can see this difference in the bath temperature in the figure below:

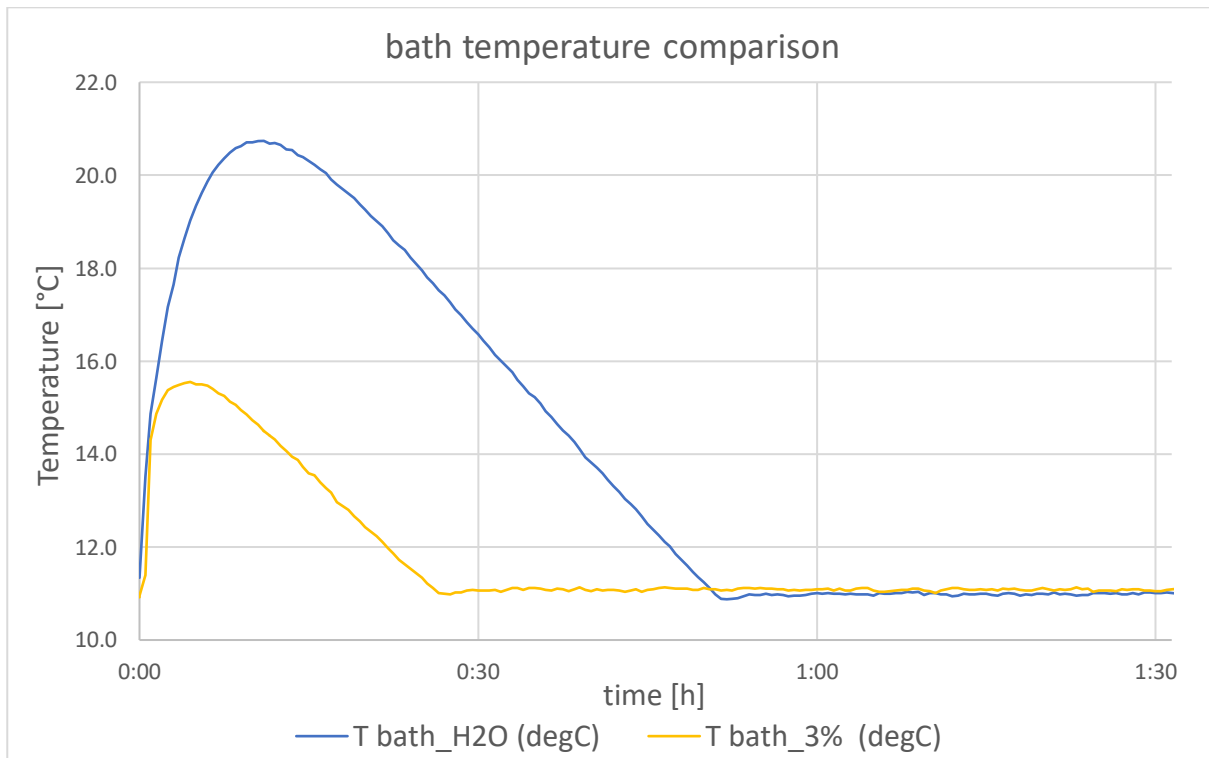
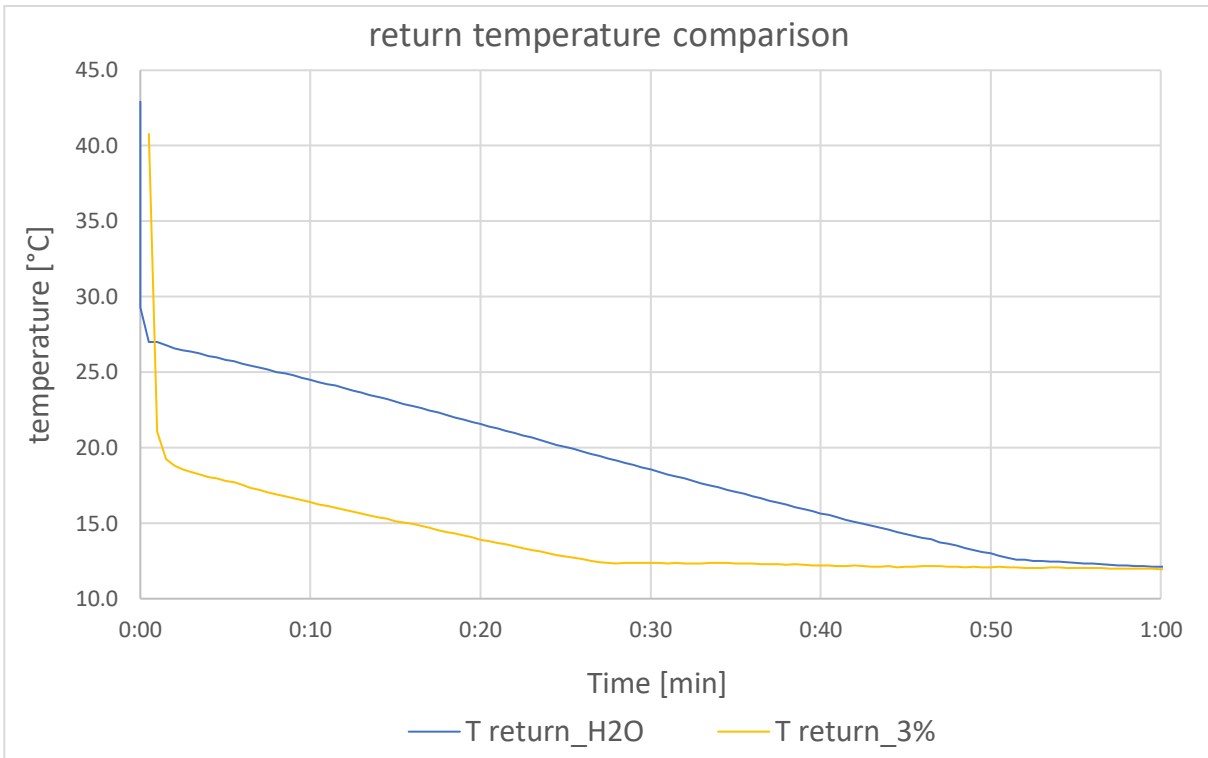


Fig 10.1.2 – bath temperature comparison

In the case with water, as already seen, the bath takes 52 minutes to reach and maintain the fixed temperature of 11 °C while with the PCM it takes 26 minutes. But, the power is almost the same or even lower because also the return temperature is higher and so at the end the ΔT is more or less the same or lower:



Regarding the energy, the two cases are compared in the figure below:

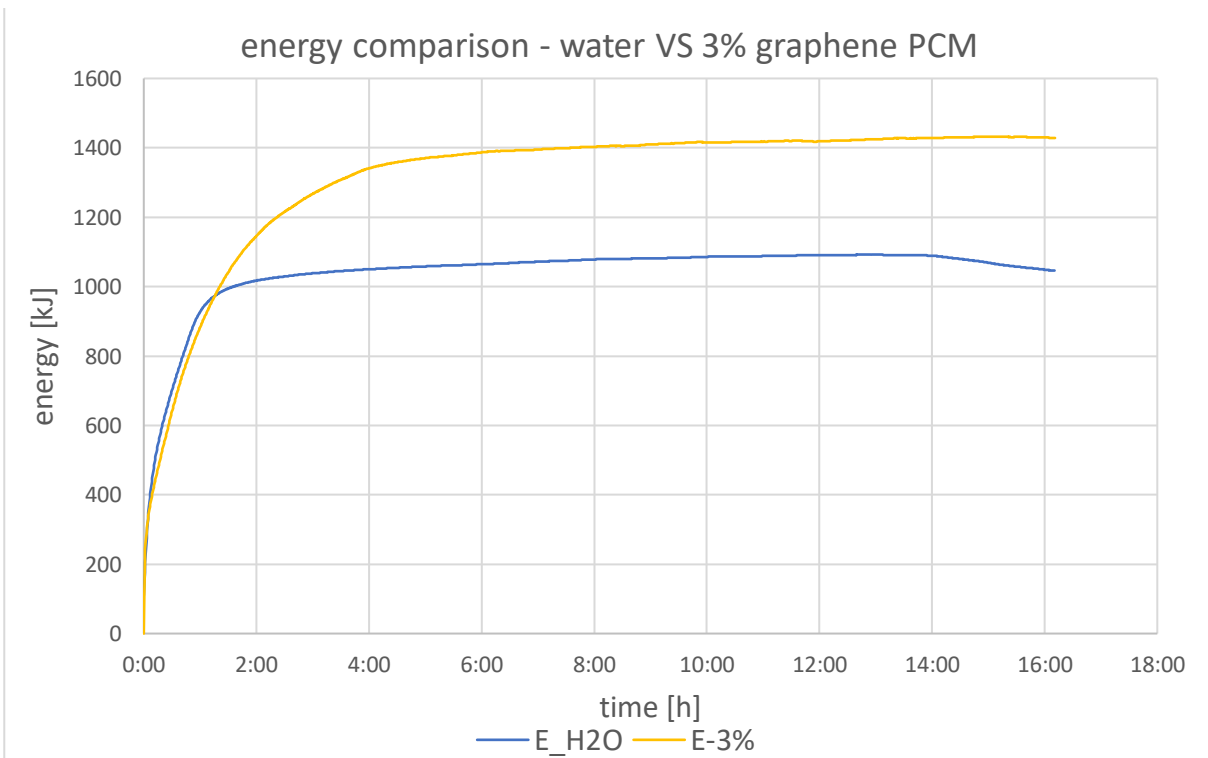


Fig 10.1.3 – energy comparison 3% graphene VS water

It's possible to notice that, in the first hour, the two systems behave basically identical. Then, for the same mass, the system with PCM manages to store almost 33.7% more energy.

This is not an amazing result, but the main reason is that the PCM does not have the expected properties declared by the manufacturer.

If the value declared by the manufacturer, i.e 250 [kJ/kg] of heat storage capacity was true, the system would be able to storage up 70% more energy that the one obtained in this experiment.

10.2 Melting:

The behaviour is almost the same as in solidification. Let's see the power comparison:

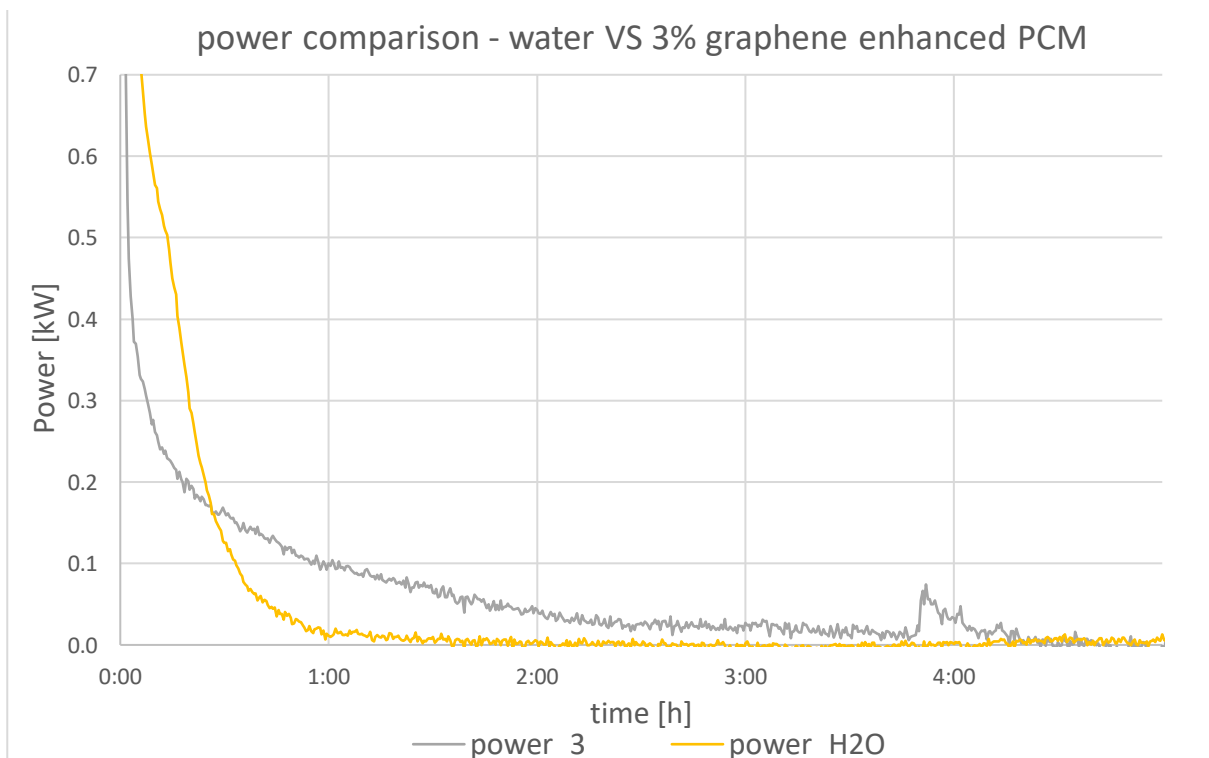


Fig 10.2.1 power comparison

At the beginning since in both cases the heat exchanged is only sensible and the specific heat of the water is more than double respect to the one of PCM (4.2 [kJ/(kg K)] for the water and 2 [kJ/(kg K)] for the PCM), the power exchanged in the water case is higher than the PCM one due to the higher ΔT between the supply and return water from the coil.

Then, from the minute 30 for the rest of the process, the PCM system exchange a higher power thanks to the involvement of the latent heat.

One can see for example also the difference in the ΔT supply–return that justify the higher power in the water case:

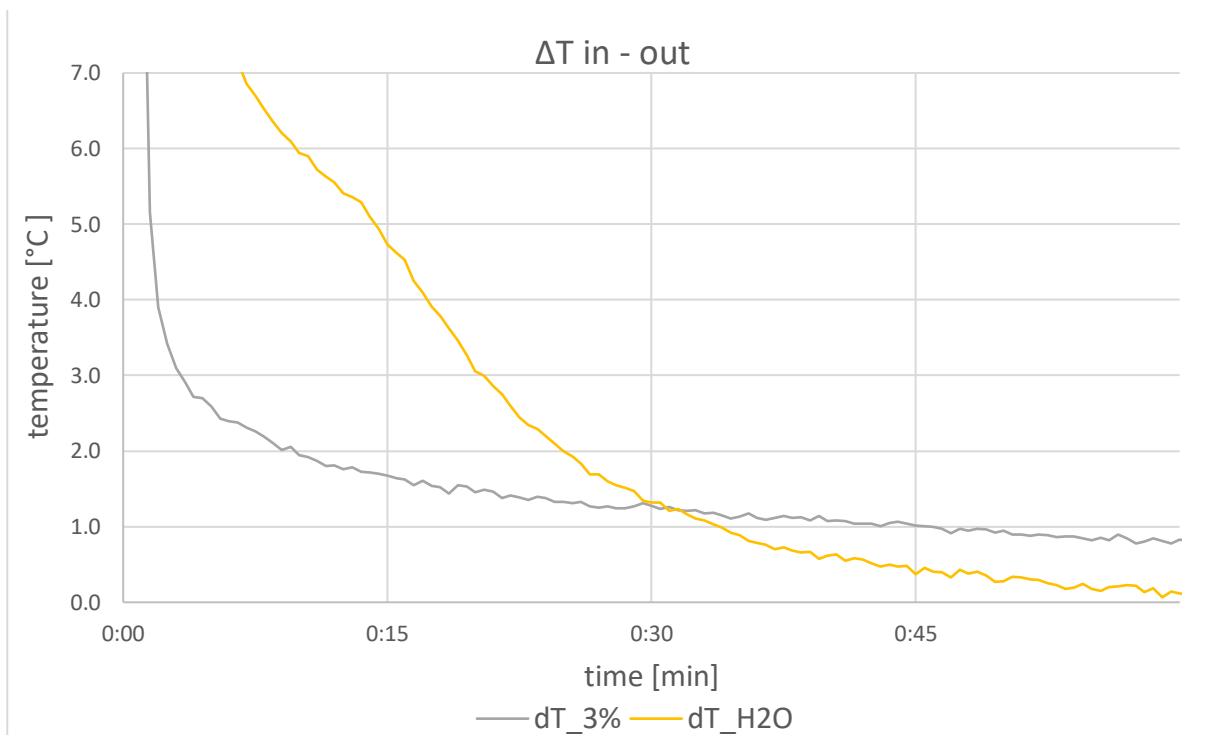


Fig. 10.2.2 - ΔT in – out comparison

It is clear that if the ΔT is higher, for the same c_p and mass flow rate, the power will be higher and so the energy.

In fact:

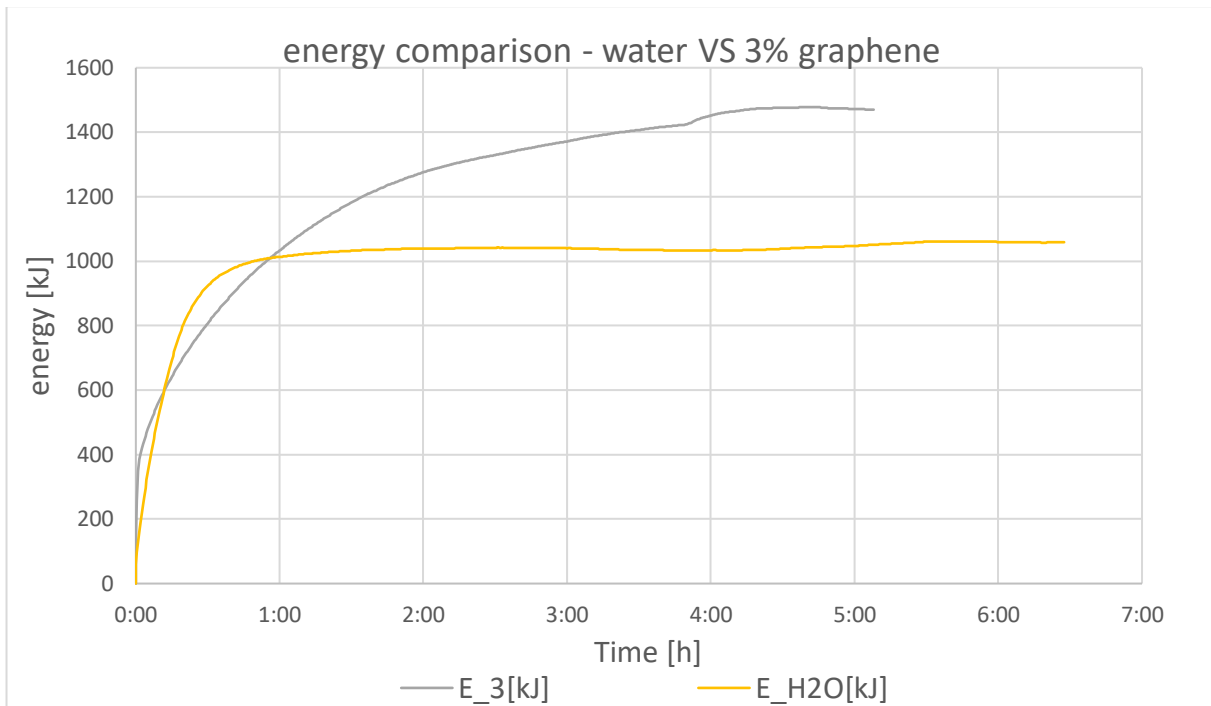


Fig. 10.2.3 – energy comparison between water and 3% graphene PCM enhanced

Note that during melting in the case with PCM there is also the problem of the voids that forms during the solidification and worsen a little bit the process. Clearly with water this problem doesn't exist.

This is why in melting the system with PCM enhanced with graphene behave slightly different from the water case especially at the beginning. The improving is evident after one hour because the PCM continue to accumulate energy while the water has already exploited all its capability (as we have seen also in solidification).

Appendix - COMSOL simulation

At the end of this work, in cooperation with the team a simulation was developed with the software *COMSOL Multiphysics* to see if the experimental results obtained are supported also by the numerical simulation.

COMSOL is a very powerful software which is based on finite element analysis and allows users to study a huge amount of scientific and engineering problems including those of heat transfer, electromagnetics, fluid dynamics and many others.

It has a graphical user interface which allows users to build their geometry defining the properties of the model, the physics, the boundary conditions, and all other inputs that the software require.

In the model we used in particular two physics:

- *Heat Transfer In Solid And Fluids* to simulate the heat transfer between the pipe and the PCM and the heat transfer within the top and the bottom of the heat exchanger through the ambient.
- *Heat Transfer In Pipes* to study what happens inside the coil and so the heat transfer by conduction and convection in pipes and channels

The purpose was only to compare the results from a global point of view, so to see if the simulation supports our experiment in terms of global temperature, power, and energy.

Note that the simulation and the experimental data have two different timestep, so to be able to compare them in the same graph, experimental data were imported into the COMSOL model which interpolate them giving a value of the experimental data in the same time interval as the one adopted into the simulation.

Let's start comparing the power and the energy in the first 5 minutes, when there is the higher power and the highest heat exchange:

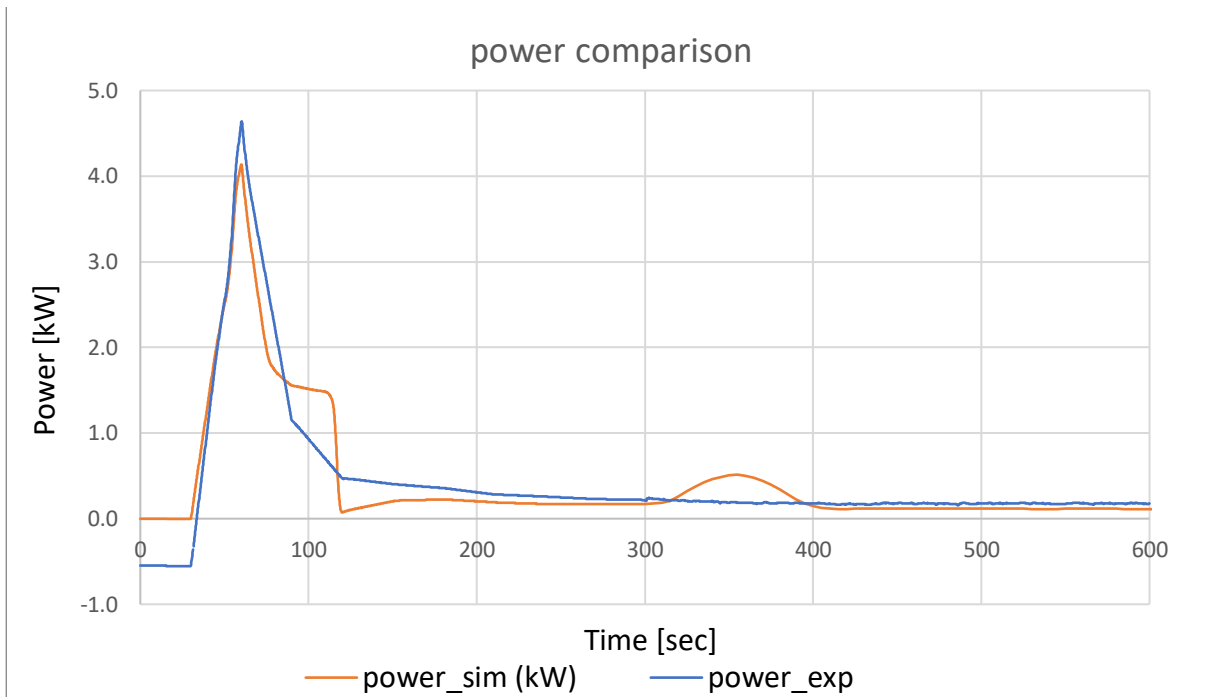


Fig. 11.1 - power comparison simulation VS experimental data

To be a rough simulation one can say that the result is not bad at all, and the two trends are similar. It means that the experiment was pretty accurate and also that the COMSOL model is well representative of the real system.

One could say that the power trends shown before were only descending and different from these, whereas these show an increase to the peak and then descend normally.

The reason is computable to the COMSOL simulation, which consider at the initial moment that the inlet temperature is 11 °C, while the experimental data consider as inlet the temperature of the bath, and so already 45 °C.

In order to make them comparable, the first 30 seconds of the experimental data of the inlet are substituted with 11 °C.

In this way the experimental data and the simulation are comparable and is possible to see that there is a match between the two.

The same comparison can be done regarding the energies:

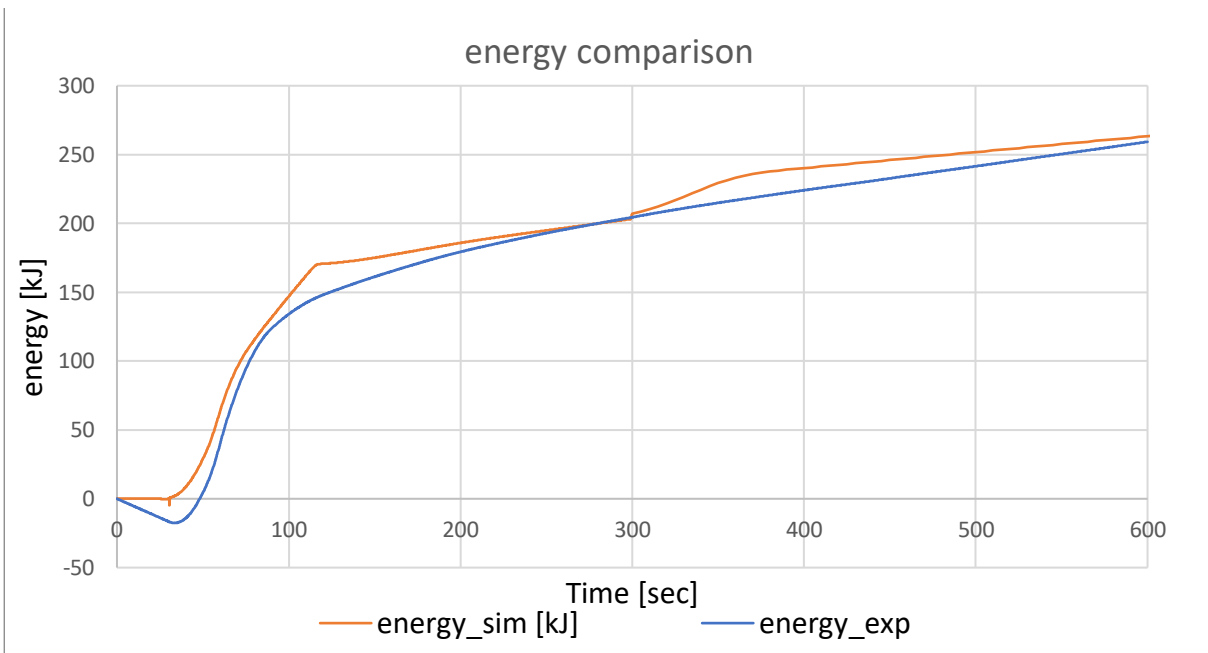


Fig. 11.2 – energy comparison between simulation and experimental data

Also, the simulated energy in the same time interval is pretty accurate compared with the experimental ones.

If one wants to see a temperature comparison between the simulation and the experimental data, is possible to show for example the temperature trend of the TC 5.6:

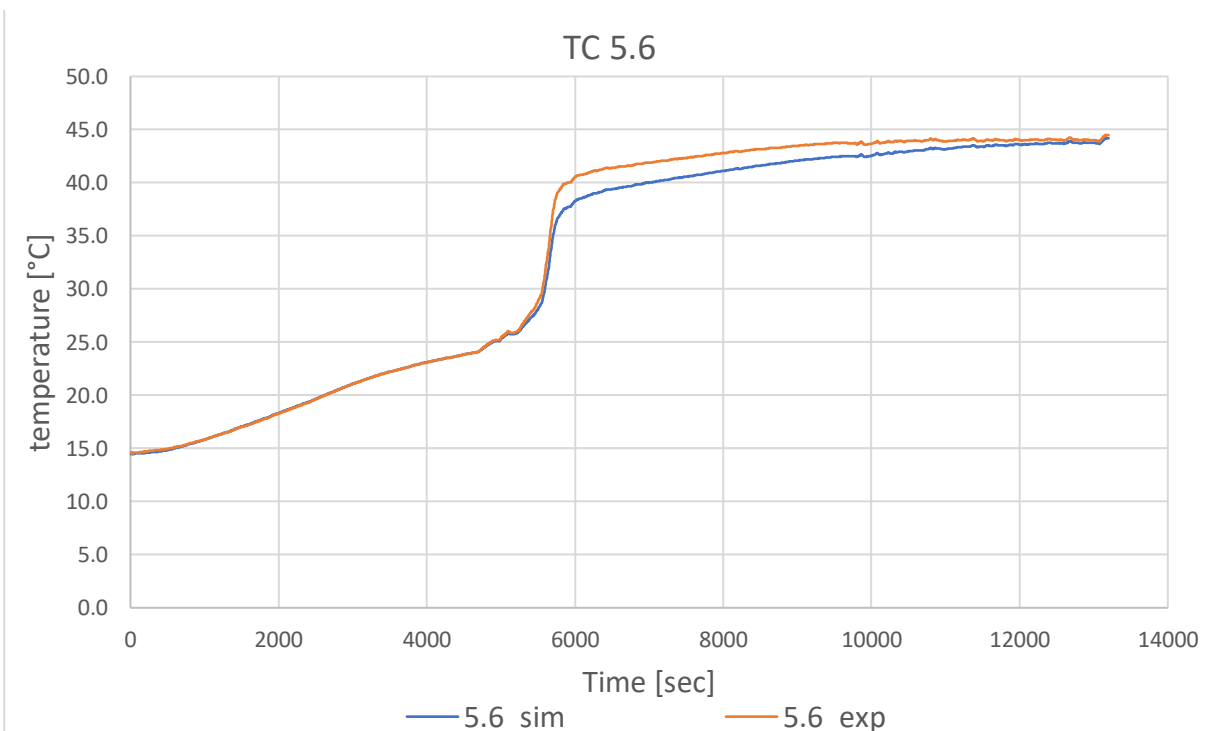


Fig. 11.3 – TC 5.6 comparison between simulation and experimental data

It could be interesting also to see graphically what COMSOL returns regarding the temperature inside the system:

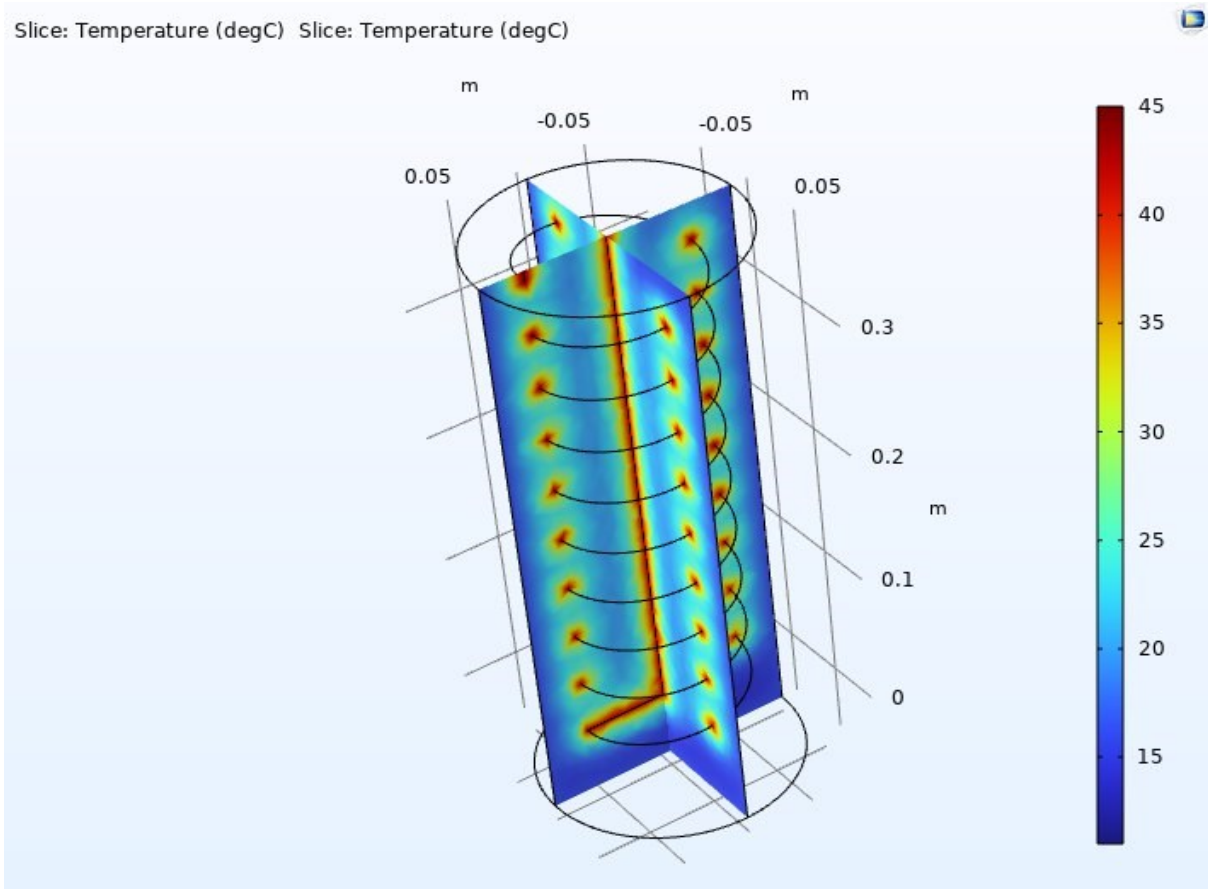


Fig. 11.4 – temperature inside the cylinder after 600 seconds

Conclusions

Adding highly conductive material (in this case graphene oxide) inside phase-change materials is an effective way to improve the thermal performance of PCMs themselves and of storage systems that utilise such materials.

In fact, in addition to exploiting the material's great latent heat, its conductivity and thus its performance are greatly improved.

The aim of this thesis was put into operation a heat exchanger that exploits the latent heat of PCMs to store and release energy.

After that, the thermal behaviour of the system was studied monitoring and collecting all the measurements that are needed to quantify the performance of the system in terms of temperatures, flow rate, power, energies and efficiency.

After studied the behaviour of the system with the pure paraffin, graphene oxide was gradually added first at 1.5% by mass and then at 3%.

The results showed that by switching from pure PCM to PCM with 3% in mass of graphene, the performance improves, and the system behaves even better than water-based systems, which today can still be considered the benchmark for thermal storage systems.

In the solidification case, comparing the pure PCM and the 3 % of graphene case:

- In the first hour the power increase as average by the 32%
- The instant average energy increase is 7.5 %
- The maximum instant increase in energy is 23.6 %
- The average time needed to exchange the same amount of energy is reduced by 65%. To reach the maximum energy of 1400 kJ the time required becomes 80.5% less.

In melting:

- The energy instant average increase is 14.6 %
- The maximum instant increase in energy is 62 %
- The average time needed to exchange the same amount of energy is reduced by 138%. To reach the maximum energy of 1400 kJ the time required becomes 7% more.

Considering that it was put 255 grams of graphene oxide and we paid it 150 €/kg, the cost of the graphene used is: 38 €

In other words, for each kilogram of PCM the graphene costs 4.5 €

To make some conclusions regarding the costs-benefits of the improvement with graphene is possible to say that,

- Adding the graphene, the total cost of the material (PCM + graphene) increases by 55% passing from 68 € to 106 €
- Each percentage point increase in velocity of the system cost 0.6 €
- each additional watt of power in the first hour costs 1.3 €

It is possible to conclude that the operation of adding the graphene oxide to the PCM is cost-effective because even though the overall cost of the materials (PCM + graphene) increases by the 55%, the reduction in operational time (charging and discharging) improves by more than 55 % and this was the final goal of the experiment because one of the weak points of PCMs is the slow phase change due to low conductivity.

A future test could be to use in this same system a hydrated salt, which is well known to have a higher thermal conductivity than paraffins.

Thus, by further increasing the conductivity, it will be possible to achieve even better heat exchange in terms of celerity. But since the hydrated salt is cheaper than the paraffins, the impact of the graphene addition on the total cost would be bigger and the cost-benefit ratio will be completely different, so it is not obvious that the addition of graphene will be cost-effective in those case.

All this while paying attention to the well-known problems of hydrated salts, such as their corrosiveness and tendency to sediment.

Another interesting tests could be trying a system that have a larger exchange surface, for example a finned one because the case studied in this thesis has a very limited exchange surface area.

As other work to support and complete the following thesis could be the development of a COMSOL model that is much more precise and calibrated than the rough one presented.

Acknowledgements

My heartfelt thanks go to my supervisor, Professor Angelo Zarrella for his willingness to follow me in this thesis, and to my assistant supervisors, Professors Michele Bottarelli and Giuseppe Emmi for their passion and kindness in accompanying me in the laboratory activities during these months.

I would like to offer my special thanks also to Eleonora Baccega for her constant willingness to help me and to Silvia Cesari for always being there for any need.

I wish to extend my special thanks also to Dott. Laura Fedele from the CNR laboratory in Padua for her support in the study of material samples providing us DSC results in short time.

Finally, a special thanks goes to my family and my girlfriend for believing in me and supporting me since the beginning of these studies and to my friends and fellow students for sharing these intense years together.

BIBLIOGRAFY

- [1] Prashant Saini, Atul Dhar, Satvasheel Powar, Parametric optimization of a cesaro fins employed latent heat storage system for melting performance enhancement, *Journal of Energy Storage* 51 (2022) 104534
- [2] Mehling, Cabeza, *Heat and cold storage with PCM an up to date introduction into basics and applications*, 2008
- [3] Harald Mehling, Michael Brütting, Thomas Haussmann, PCM products and their fields of application - An overview of the state in 2020/2021, *Journal of Energy Storage* 51 (2022) 104354
- [4] Mohammed Farid, Amar Auckaili, Gohar Gholamibozanjani, *Thermal energy storage with phase change materials*, © 2021 Taylor & Francis Group, LLC
- [5] S.M Hasnain, Review on sustainable thermal energy storage technologies, Part 1: Heat storage materials and techniques, *Energy Convers. Mgmt Vol. 39, No. 11*, pp. 1127-1138, 1998 © 1998 Elsevier Science Ltd
- [6] Amy S. Fleischer, *Thermal Energy Storage Using Phase Change Materials Fundamentals and Applications*, Springer, 2015
- [7] Paulina Rolka , Tomasz Przybylinski, Roman Kwidzinski, Lackowski Marcin, Thermal properties of RT22 HC and RT28 HC phase change materials proposed to reduce energy consumption in heating and cooling systems, *renewable Energy* 197 (2022) 462-471
- [8] PCM (alliance-pcm.com)
- [9] Manish K. Rathod, *Thermal Stability of Phase Change Material*, IntechOpen, 2018
- [10] A. Castell, M. Belusko, F. Bruno, L.F. Cabeza, Maximisation of heat transfer in a coil in tank PCM cold storage system, *Applied Energy* 88 (2011) 4120 - 4127